Energy, Mines and Resources Canada
Earth Physics Branch
1 Observatory Crescent
Ottawa Canada
K1A 0Y3

Énergie, Mines et Ressources Canada
Direction de la physique du globe
1 Place de l'Observatoire
Ottawa Canada
K1A 0Y3

Geothermal Service of Canada

Service géothermique du Canada

NUMERICAL MODELLING OF FLOW IN FRACTURED ROCK MASSES - DISCONTINUOUS VERSUS CONTINUUM APPROACHES

J.-C. Roegiers, J.H. Curran and W.F. Bawden
Department of Civil Engineering, University of Toronto

Earth Physics Branch Open File Number 79-8

Ottawa, Canada, 1979

119 p.

Price/Prix: $29.00

Energy, Mines and Resources Canada
Énergie, Mines et Ressources Canada

Earth Physics Branch
Direction de la physique du globe

1 Observatory Crescent
Ottawa Canada
K1A 0Y3

1 Place de l'Observatoire
Ottawa Canada
K1A 0Y3

Geothermal Service of Canada

Service géothermique du Canada

NUMERICAL MODELLING OF FLOW IN FRACTURED ROCK MASSES - DISCONTINUOUS VERSUS CONTINUUM APPROACHES

J.-C. Roegiers, J.H. Curran and W.F. Bawden
Department of Civil Engineering, University of Toronto

Earth Physics Branch Open File Number 79-8

Ottawa, Canada, 1979

119 p.

Price/Prix: $29.00

ABSTRACT

This report summarizes the state-of-the-art of fluid flow through fractured media. Various existing technical approaches have been brought together to study fracture deformation and its effect on fluid conductivity.

Overall, the report comprises three independent entities which could be considered independently. The first part is a critical literature review of previous work, in which special emphasis has been placed to explain apparent discrepancies. The second part outlines the numerical technique which was selected as well as its limitations. Finally, the third part provides the reader with an in-depth discussion on the engineering implications.

RESUME

Ce rapport résume le niveau de développement de l'écoulement fluide à travers les zones fracturées. Plusieurs méthodes techniques ont été assemblées afin d'étudier la déformation de fracture et son effet sur la conductivité fluide.

Le rapport comprend trois éléments qui peuvent être considérés séparément. La première section est une revue critique de la litérature des recherches antérieures dont une concentration spéciale a été faite pour expliquer les désaccords apparents. La deuxième section présente une esquisse de la technique numérique choisi avec un exposé de sa restriction. Finalement, la troisième section présente au lecteur une discussion profonde sur les implications de l'ingénierie.

UNIVERSITY OF TORONTO GEOTECHNICAL REPORT

A report prepared for

Energy, Mines & Resources, Canada
Earth Physics Branch
Ottawa, Ontario

by

J.C. Roegiers

J.H. Curran

W.F. Bawden

Department of Civil Engineering
University of Toronto
Galbraith Building
35 St. George St.
Toronto, Ontario. M5S 1A4

Contract Number: 2239-3-240-77

April, 1979.

FOREWORD

This report summarizes the state-of-the-art of fluid flow through fractured media. Various existing technical approaches have been brought together to study fracture deformation and its effect on fluid conductivity.

Overall, the report comprises three independent entities which could be considered independently. The first part is a critical literature review of previous work, in which special emphasis has been placed to explain apparent discrepancies. The second part outlines the numerical technique which was selected as well as its limitations. Finally, the third part provides the reader with an in-depth discussion on the engineering implications.

Any opinions expressed in this report are those of the authors and the Earth Physics Branch takes no responsibility neither does it endorse the findings.

J.-C. Roegiers
J.H. Curran
W.F. Bawden

April, 1979.

TABLE OF CONTENTS

NOMENCLATURE

			Dimensions
q_i	=	flow rate	L^3T^{-1}
K_{ij}	=	intrinsic equivalent permeability	LT^{-1}
A	=	area	L
J_j	=	field pressure head gradient	
L_g	=	"smallest" dimension of "specimen" being studied	L
L_c	=	order of magnitude of rock mass heterogeneity	L
e	=	mean fracture aperture	L
ν	=	kinematic viscosity	L^2T^{-1}
Re	=	Reynolds number	
V_m	=	mean flow velocity	LT^{-1}
D_h	=	hydraulic diameter	L
λ	=	friction factor	
ρ	=	fluid density	ML^{-3}
η	=	dynamic viscosity	$ML^{-1}T^{-1}$
ζ	=	hydraulic length	L
P	=	fluid pressure	$ML^{-1}T^{-2}$
Q_t	=	total flow volume	L^3
Q	=	flow per unit width	L^2
g	=	acceleration due to gravity	LT^{-2}
$\overline{\gamma}$	=	fluid acceleration	LT^{-2}
V	=	volume	L^3
k	=	micro roughness	L

K	=	macro roughness	L
K_j	=	fracture conductivity	LT^{-1}
σ	=	normal stress	$M.L^{-1}T^{-2}$
ξ	=	seating load for fracture	$M.L^{-1}T^{-2}$
V_{mc}	=	maximum fracture closure	L
Δv	=	normal fracture displacement	L
$F_{n,o}$	=	initial external force at a nodal point	$M.L.T^{-2}$
F_n	=	external force at some later increment	$M.L.T^{-2}$
ℓ'	=	half length of joint element	L
KN_o	=	initial normal stiffness	$M.L.^{-1}T^{-2}$
KN	=	normal stiffness at some later increment	$M.L^{-1}T^{-2}$
τ_p	=	peak shear strength	$M.L^{-1}T^{-2}$
a_s	=	proportion of joint area sheared through the asperities	
$\dot{v}$	=	dilation rate at the peak shear stress (secant dilatancy rate) $\Delta v(\tau_p)/\Delta u(\tau_p)$	
S_R	=	shear strength of the rock composing the asperities	$M.L^{-1}T^{-2}$
n	=	ratio of compressive to tensile strength	
Q_u	=	unconfined compressive strength of the asperities	$M.L^{-1}T^{-2}$
τ_r	=	residual shear strength	$M.L^{-1}T^{-2}$
$\Delta\bar{g}$	=	fracture shear displacement	L
u_p	=	peak shear displacement	L
u_r	=	residual shear displacement	L
B_o	=	ratio of residual to peak shear strength	

CHAPTER I

GENERAL INTRODUCTION

Theoretical and laboratory studies over the past twenty years have provided considerable insight into the hydrogeologic properties of fissured rock. The development of fracture-flow models has followed two distinct approaches:

i) the discrete model

ii) the statistical model.

In the discrete model each discontinuity is modelled individually. For rock masses with a high fracture density, in order to simplify the problem, several discontinuities may be incorporated and replaced by a single equivalent discontinuity. The main advantage of this approach is that it is then possible to examine the influence of individual joint parameters on the flow through jointed rock.

For laminar flow in a fracture, Wilson (1970) found that fracture aperture is by far the most important parameter governing the flow rate. Fracture orientation was found to have little effect upon the seepage rate beneath dams, but it did significantly influence the water pressure distribution and hence the stability of the structure.

In contrast to the discrete model, the statistical approach treats the heterogeneous fractured rock mass as a continuum-type equivalent porous medium in which the systems of geologic discontinuities are assumed to impart an anisotropic permeability character. The properties of each family are statistically averaged to develop the equivalent anisotropic permeability tensor relating flow and hydraulic gradient.

The power of this method resides in the fact that no detailed knowledge of the fracture geometry is necessary to obtain a quantitative statement of the seepage characteristics. However, as discussed later, the use of the statistical approach can, under certain circumstances, lead to invalid results.

The choice between these two models mainly depends on the volume of the rock mass being investigated relative to its degree of heterogeneity, but also on the relevant geologic information available.

Consider a representative volume of a rock mass subjected to groundwater flow with a hydraulic potential ϕ and gradient $J_i = -\phi_{,i}$. Due to anisotropy introduced by the joints the mean velocity vector $\bar{V}_i$ is in general not parallel to J_i*. The general form of the equation relating V_i and J_i is

$$q_i = -K_{ij} \cdot A \cdot J_i \qquad (2.1)$$

where
- q_i = flow rate in = $V_i \cdot A$ $[L^3T^{-1}]$
- K_{ij} = intrinsic equivalent permeability $[L\ T^{-1}]$
- A = area $[L^2]$
- J_i = field pressure head gradient .

Snow (1965) used a statistical interpretation of borehole injection test results to determine fracture aperture distribution. The remaining parameters are determined from core logs and down-hole techniques. A basic assumption in Snow's work is that the fracture systems form a cubic network.

Rocha and Franciss (1977) give a detailed development of the equivalent porous medium permeability tensor K_{ij}. They determine all properties of the fracture system using a technique called integral sampling. Correction factors are then applied to make the calculated permeability tensor match field pump tests. The correction factors are supposed to correct primarily for the assumption of in-plane fracture continuity.

---

* indicial notation (i = 1,2,3) is used throughout this report and repeated indicies indicate the summation convention.

Considerable work in statistical modelling has also been done by the petroleum industry. However such high pressures are used that the fluid compressibility leads to unsteady state flow, making the results of limited value for civil engineering work. Wilson (1970) provides a good review of petroleum research.

2.2 Discussion

2.2.1 Scale Effect:

Snow (1968) stated that "*fractured crystalline rocks are a media whose permeability is attributable to a large number of intersecting planar conduits with dispersed orientations. Since, in most cases it is impossible to measure the orientation of every fracture the problem must be solved statistically by random sampling of the orientations.*"

In order to idealize a rock mass as a continuum, fractures whose properties are important for permeability considerations must be sufficiently numerous inside volumes which can be deemed small with respect to the problem concerned. If this holds the discontinuous rock mass can then be replaced by a continuous medium, the characteristics of which may be nonhomogeneous.

The applicability of the previous idealization depends on what is generally known as *scale effect*. The fundamental question is what dimensions must a sample have to be representative of the rock mass, notably as regards its permeability. Thus for a rock mass with a single family of continuous fractures, assumed to have the same properties throughout, there must be adequate fractures that the sample permeability is representative of the permeability of the rock mass. This means

that in samples with increasing volumes, V_1, V_2, V_3, ..., the corresponding permeabilities K_{ij} along the plane of the fracture will initially fluctuate but will then tend to a constant value (Fig. 2.2). Thus a sample will be representative if its volume exceeds V_r, the value of which will depend on the accuracy with which the permeability is to be determined, (Rocha and Franciss, 1977).

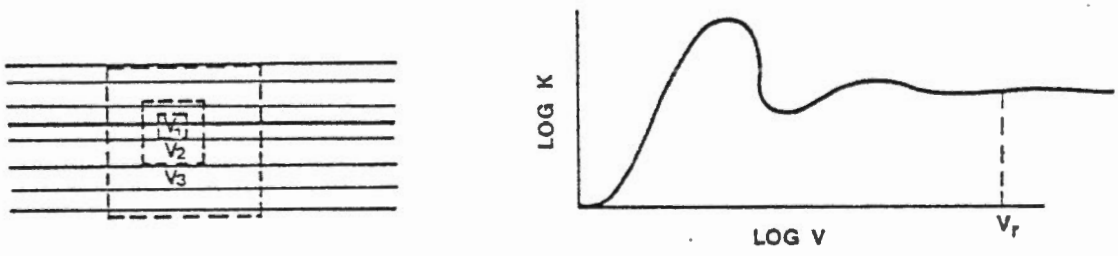

Figure 2.2 Scale effect (adapted from Rocha & Franciss, 1977)

Thus a representative sample must contain a large number of fractures. For this reason Rocha and Franciss (1977) state that it often is necessary to accept samples that are poorly representative.

The concept of scale effect, although intuitively correct, is site dependent and can only be determined through costly field testing.

Statistical models for one- or two-phase flow developed by various researchers in the petroleum field are reviewed by Wilson (1970). This work generally deals with complete reservoirs and hence scale effect should not pose any difficulty. A comparison of these models with appropriate production and field data confirm that at least some reservoirs are adequately modelled as equivalent porous media. Discrepancies between model and field results are more easily appreciated if one considers Baker's (1955) calculation that a single fissure of

2.5 mm aperture is equivalent to 140 metres of unfissured formation having a uniform permeability of 10 millidarcys. Parsons (1972) concludes that for regional flow, where the field hydraulic gradient could not be expected to change abruptly in magnitude or direction, the behaviour of a fractured rock mass can be approximated as an equivalent anisotropic porous medium. This depends, however, on the amount of dispersion present in the aperture population and holds exactly only when the dispersion is zero.

A few authors have attempted to quantify the scale effect factor.

Rats and Chernyashov (1965) used a statistical approach to relate joint parameters and permeability. The author distinguished three types of heterogeneities: (i) microscopic, (ii) aquifer or hydrostratigraphic and, (iii) regional tectonic.

They differentiated homogeneous from heterogeneous structures (Figure 2.3) based on various statistical distributions. The authors conditionally gave the first approximation to this boundary as $L_g/L_c = 10$, i.e. an equivalent homogeneous medium may be assumed if $L_g/L_c < 10$

where L_g is the smallest dimension of structure or volume or rock being studied and [L]

L_c is the order of magnitude or rock mass heterogenity (i.e. fracture spacing). [L]

They concluded that permeability variation decreased as the fracture density increased.

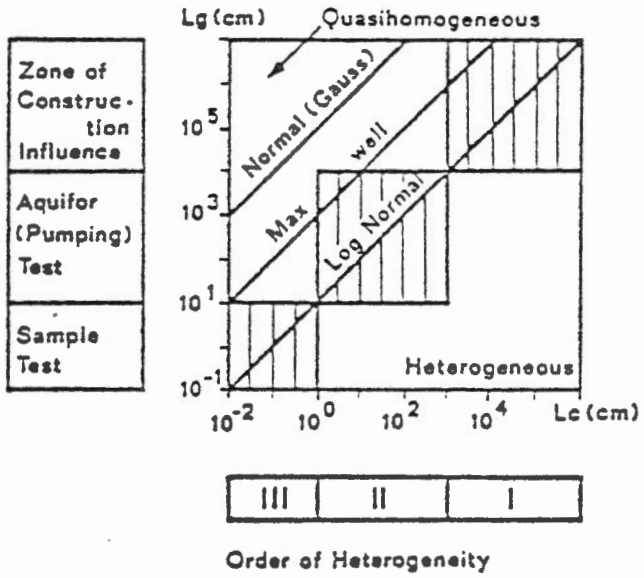

Figure 2.3 Types of heterogeneities (from Rats and Chernyashov)

Maini's (1971) results for scale effect in an injection test are shown in figure 2.4. However there appears to be some question of the data and assumptions used, as will be discussed in detail in chapter IV.

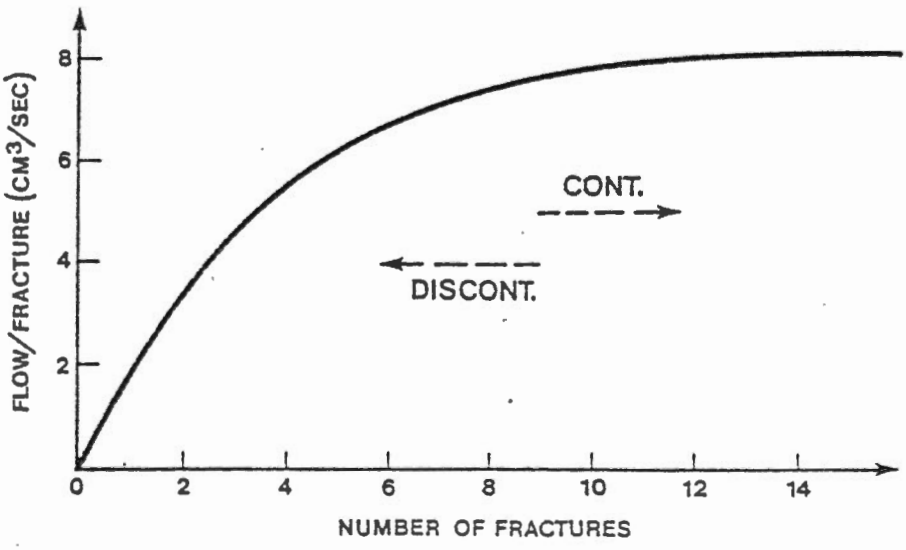

Figure 2.4 Scale Effect in an Injection Test (after Maini, 1971)

Wilson (1970) concludes from numerical tests that in general when the smallest dimension of the engineering structure is 50 times as long as the longest dimension of the larger rock matrix blocks, a discrete approach need not be used.

Barton (1972), used Snow's statistical method to interpret pump tests in Norway. He relaxed the assumption that all fractures conduct water. This was confirmed by the packer test results which showed fractured sections with zero water acceptance. Barton found that the equivalent spacing of water conducting joints was four to fifteen times the observed fracture spacing. It would appear that at greater depths there may be even fewer conductors. Barton states that in such cases the equivalent porous medium analogy is not valid.

2.2.2 Stress-dependent permeability

For a single smooth fracture the quantity of flow q_i can be shown to be proportional to the cube of the mean fracture aperture e (Navier-Stokes equation)

$$Q_t \alpha e^3$$

Therefore, correlation with Darcy's Law (i.e. $V_i = K_{ij} J_j$) shows that the joint conductivity is porportional to e^2. Hence a small change in fracture aperture may lead to a major variation in permeability, especially for the very small aperture ranges encountered in fractured rock. Numerous researchers, e.g. Goodman (1976), Gale (1975), Iwai (1977) have shown that fracture aperture is dependent on existing stress conditions and previous stress history. Snow (1968) measured surface strains at up to 100 m from a well for a drawdown of 10 m. Gale (1975), using a specially designed apparatus, measured fracture deformation in

one well during injection and withdrawal in a second well. Bernaix (1961), in studying the Malpasset gneiss, found the permeability of fractured samples to be much higher for divergent flow where the sample is submitted to a stress field where tension predominates than for convergent flow where compression predominates. Therefore, in many cases it is necessary to account for permeability changes under load.

Most researchers dealing with statistical flow models have neglected loading effects on permeability. This assumes that fracture apertures measured either directly in the field or else determined indirectly from packer tests will remain constant both during construction and after completion of the engineering structure.

Sarafim and del Campo (1965) developed a mathematical model for steady state flow in a network of three orthogonal joints including a term to account for the change in aperture under load. The authors relate their stress dependent term to the sum of the principal stresses, hence assuming that the deviatoric component does not affect fracture aperture.. While this may be true of very smooth joints and or rough joints at very high normal stress levels, for general civil engineering projects dilatation associated with shear stresses may have considerable effect on permeability, as discussed in more detail later. Furthermore, an assumption in the model of Serafim and del Campo is that each fracture may be considered to operate independently from flow in any other fracture. Wilson (1970) points out, however, that this type of model is allowed only in regions where the field hydraulic gradient maintains a constant orientation in space so that component of gradient is the same within each portion of each fracture in a given parallel set.

Snow (1968) developed a permeability tensor including stress dependent terms. He assumes the fractures deform in a linear elastic manner to account for the deformability of the fractured intact rock. As discussed later, experimental evidence indicates that joint closure in highly non-linear and non-recoverable, especially in the intial load cycles.

Rocha and Franciss (1977) provide a very detailed methodology for determining the complete permeability tensor for fractured rock based on integral sampling. Although the authors do not directly account for stress dependency, they do use correction factors to make the permeability results, based on integral sampling, correlate with values determined from packer tests in the boreholes. They claim that these correction factors are needed to compensate for the assumed continuity of the fractures plus deviations due to roughness and head losses at joint intersections. It would seem at least as probable, depending on how the packer tests are performed, that the correction factors may be needed to account for aperture changes during pressure testing as have been measured by Gale (1975). If so, the correction factors would only be applicable for the effective stress conditions during that test.

CHAPTER III

THE DISCRETE MODEL

3.1 Introduction

The theoretical and experimental basis for the discrete model is the Hele-Shaw or parallel plate model. In the case of viscous laminar flow between smooth parallel plates it is possible to obtain a 'closed form' solution for the flow rate q_i as a function of joint aperture, viscosity and pressure gradient.

The influence of parameters such as tortuosity, roughness, etc., is determined experimentally.

3.2 Experimental Investigations

The first systematic studies on flow through fractured media were conducted in the Soviet Union. The studies by Lomize (1951) are especially important in that he was the first to systematically examine the influence of parameters such as spatial distribution and aperture as well as shape and structure of the wall roughness. He conducted laboratory experiments using a relatively small (about 20 cm long) joint model. The roughness was varied by gluing individual sand grains on both surfaces. In addition, Lomize conducted a number of experiments changing the wall shape (Figure 3.1). Both laminar and turbulent regimes were investigated.

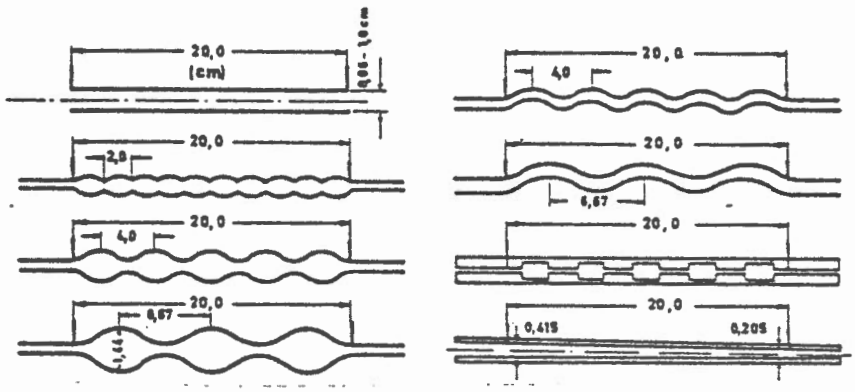

Figure 3.1 Different shapes of the joint walls investigated by Lomize

Louis (1969) independently developed similar ideas and performed similar tests using a substantially larger model (70 x 200 cm) formed from two slabs of washed concrete. He studied parallel as well as non-parallel flow through both the laminar and turbulent regimes. The parallel flow studies were carried out, mainly to verify the applicability of the pipe flow laws of non-circular cross sections to flow in rock discontinuities.

Louis differentiated between a micro-roughness "k" and macro-roughness "K" as shown in Figure 3.2.

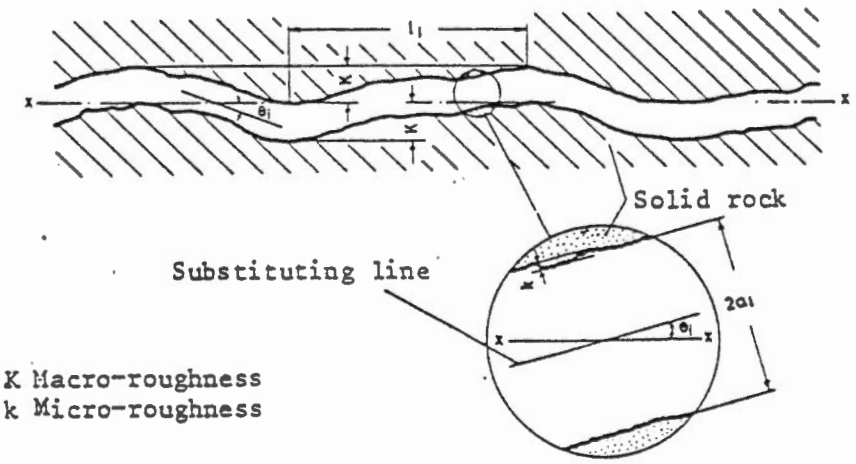

Figure 3.2 Illustration of a fracture surface in rock (After C. Louis, 1969)

If the centre line of the fracture is approximated by the straight line 'x - x' then the 'macro-roughness', or waviness can be described mathematically by the angle θ_i. The deviation of the joint wall from this 'substituting line', is then defined by

$$\tan \theta_i = \frac{K}{\ell_i/2} \tag{3.1}$$

where K is the macro-roughness of the fracture.

As K increases, the flow path length increases, introducing curvature losses which result in a decrease in the hydraulic gradient in the joint. The author concluded that macro-roughness can be ignored unless K is nearly equal to the fracture aperture. The local joint wall roughness is described in terms of the micro-roughness.

Defining V_m as the mean flow velocity and υ as the kinetic viscosity, Louis defined a Reynolds number similar to pipe flow:

$$Re = \frac{D_h V_m}{\upsilon} \tag{3.2}$$

where D_h = the hydraulic diameter and is equal to 2e. $[L]$

B_m = mean fluid velocity. $[LT^{-1}]$

υ = kinematic viscosity. $[L^2T^{-1}]$

Sharp (1970), based on laboratory flow experiments on a single natural rock fracture, questioned the cubic relationship between flow rate and aperture. The author noted that although Darcy's law held for most porous media, it could not necessarily be assumed for fissured rocks where much higher velocities may exist. In addition, he suggested that inertial forces due to irregularities are the reason for the existence of a considerable transitional period occurring between linear and fully turbulent regimes.

Turbulent flow is influenced by the following parameters:

(a) roughness,

(b) channel curvature: sharp changes initiate turbulence,

(c) change in cross-section: divergence induces instability,

(d) contact points and surrounding deadwater areas which lead to non-linear flowlines.

The flow boundaries between laminar and turbulent regimes for both parallel and non-parallel flows are defined on the basis of friction factor λ and a Reynolds number "Re" with the relative roughness "k/D_h" as a parameter. A compilation of the different flow laws and their range are shown in Figure 3.3

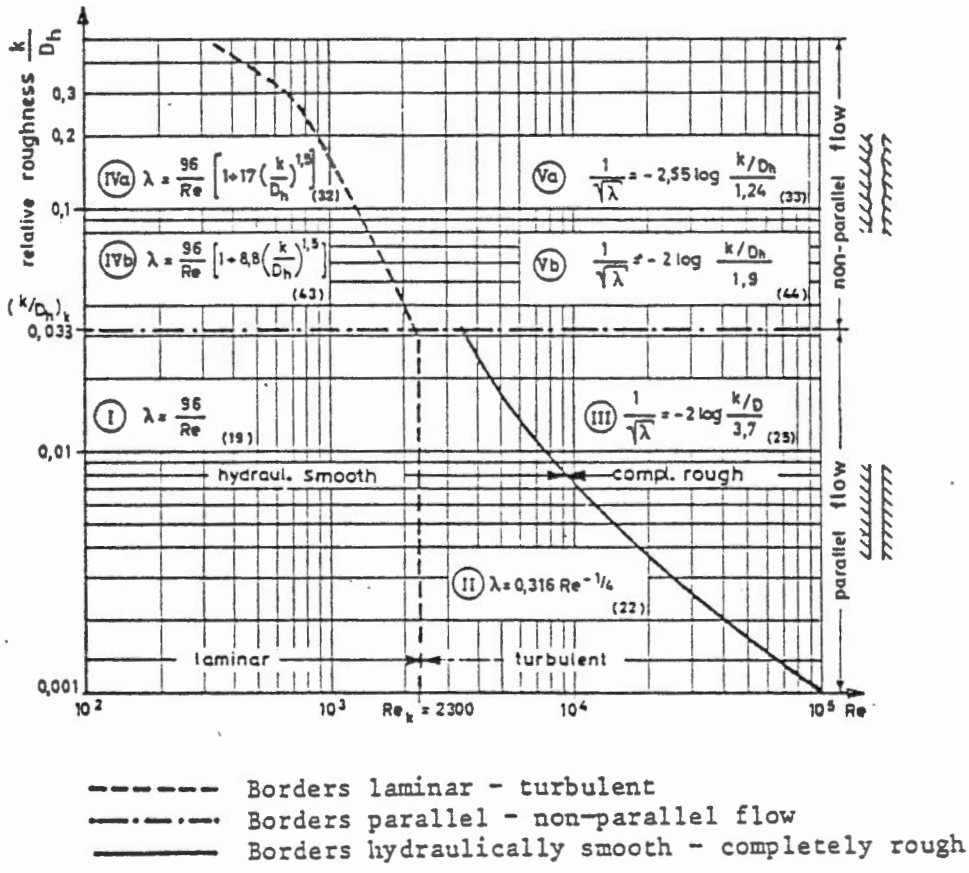

Figure 3.3 Compilation of the different flow laws and their range of validity. (After C. Louis 1969).

Figure 3.4 shows the same laws plotted on a graph of the friction factor "λ" versus R_e for various values of k/D_h.

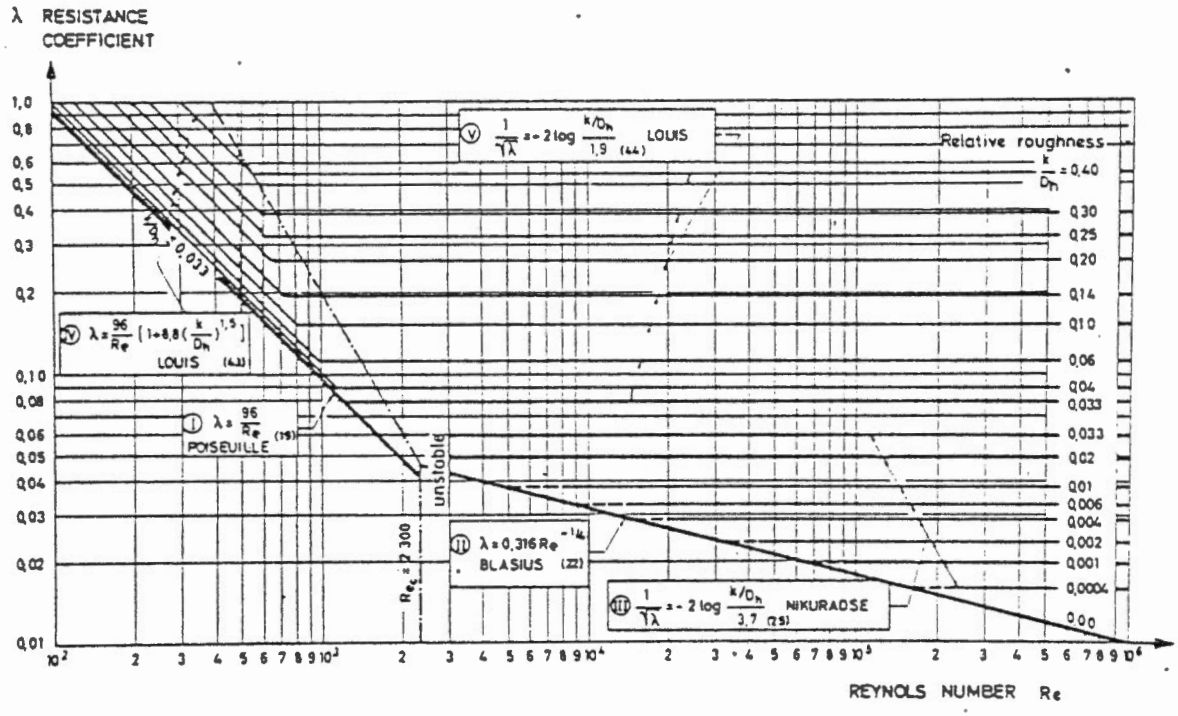

Figure 3.4 Diagram of the proposed laws of resistance for flow in a joint. (After Louis, 1969)

Finally Figure 3.5 summarizes the laws governing friction factor and flow rate developed by various authors.

	Reg.	FLOW LAW	FLOW RATE (per unit width)
Parallel flow $k/D_h \leq 0{,}033$	lam.	(I) $\lambda = \frac{96}{Re}$ (19) (Poiseuille)	$q_i = \frac{g}{12\nu}(2a_i)^3 J_i$
	turbulent	(II) $\lambda = 0{,}316\, Re^{-1/4}$ (22) (Blasius)	$q_i = \left[\frac{g}{0{,}079}\left(\frac{2}{\nu}\right)^{1/4}(2a_i)^3 J_i\right]^{4/7}$
		(III) $\frac{1}{\sqrt{\lambda}} = -2\log\frac{k/D_h}{3{,}7}$ (25) (Nikuradse)	$q_i = 4\sqrt{g}\left(\log\frac{3{,}7}{k/D_h}\right)(2a_i)^{1{,}5}\sqrt{J_i}$
Non-parallel flow $k/D_h > 0{,}033$	laminar	(IVa) $\lambda = \frac{96}{Re}\left[1+17\left(\frac{k}{D_h}\right)^{1{,}5}\right]$ (32) (Lomize)	$q_i = \frac{g}{12\nu\left[1+17(k/D_h)^{1{,}5}\right]}(2a_i)^3 J_i$
		(IVb) $\lambda = \frac{96}{Re}\left[1+8{,}8\left(\frac{k}{D_h}\right)^{1{,}5}\right]$ (43) (Louis)	$q_i = \frac{g}{12\nu\left[1+8{,}8(k/D_h)^{1{,}5}\right]}(2a_i)^3 J_i$
	turbulent	(Va) $\frac{1}{\sqrt{\lambda}} = -2{,}55\log\frac{k/D_h}{1{,}24}$ (33) (Lomize)	$q_i = 5{,}11\sqrt{g}\left(\log\frac{1{,}24}{k/D_h}\right)(2a_i)^{1{,}5}\sqrt{J_i}$
		(Vb) $\frac{1}{\sqrt{\lambda}} = -2\log\frac{k/D_h}{1{,}9}$ (44) (Louis)	$q_i = 4\sqrt{g}\left(\log\frac{1{,}9}{k/D_h}\right)(2a_i)^{1{,}5}\sqrt{J_i}$
	lam.	Filled joints (see section 4.5)	$q_i = 2a_i\, k_s\, J_i$ (45)

Note in this table $2a_i$ = e = fracture aperture

Figure 3.5 Compilation of the different laws of resistance and the corresponding flow rates. (After Louis)

The major criticisms of both Lomize's and Louis' work are:

(i) It is very difficult if not impossible to obtain a meaningful value of the fracture aperture in the field.

(ii) It is very difficult to define a Reynolds number for very rough discontinuities since the true cross-sectional area cannot readily be measured.

(iii) The models are for constant aperture with no contact points between the fracture walls.

(iv) Both models neglect the effect of stress on aperture and hence on permeability.

Sharp stated that representing fracture flow by a Reynolds number/friction factor criterion was not realistic. His expressions for the Reynolds number and friction factor are given respectively by:

$$Re = \frac{\rho V_m \zeta}{\mu} \quad , \quad \lambda = \frac{2\zeta \ \text{grad}P}{V_m^2 \ \rho} \quad , \tag{3.3}$$

where
- ρ = density of fluid, $[ML^{-3}]$
- μ = dynamic viscosity of fluid, $[ML^{-1}T^{-1}]$
- ζ = the hydraulic length of the system, $[L]$
- V_m = average velocity of fluid, $[LT^{-1}]$
- grad P = gradient of pressure = $\frac{\Delta P}{\Delta X}$
- P = fluid pressure. $[ML^{-1}T^{-2}]$

For small values of roughness, ζ is simply proportional to the discontinuity openings ($\zeta = 2e$). In rough discontinuities, however, the very irregular nature of the fracture walls plus the existence of dead water areas surrounding points of contact where no flow occurs, make the measurement of the true cross-sectional area of flow impossible. Hence the (λ, Re) flow criterion may be impractical. Also the hydraulic radius does not account for channel curvature, transitional flow or high velocity flow.

Sharp assumed that the fracture was closed when three or more contact points were present even though a measurable flow rate was still present. He referred to this condition by introducing the concept of "effective zero" aperture. Based on this analysis Sharp obtained the following empirical equation relating the quantity of flow per unit width Q to the joint aperture e:

$$Q = A\, e^{n} \tag{3.4}$$

where { A is a constant depending on the gradient, and
n is a parameter dependent on the flow domain

Flow Domain	n
Linear Laminar	2
Transitional	1.2 to 2
Fully turbulent	1.2

Sharp concluded that linear flow was restricted to very small gradients and that a long transitional zone usually occurred between the linear and the fully turbulent regimes.

However, Gale (1975) reviewed Sharp's experimental data and suggested that the cubic relation between Q and e was still valid, provided one took the flow rate corresponding to Sharp's effective zero opening into account. He suggested that the reduced flow rates obtained in discontinuities with significant wall roughness can be accounted for by either altering the aperture size or adding a compatible term to compensate for the deviation.

Maini (1971), also rejected the use of a Reynolds number/friction factor criterion for fracture flow and stressed the importance of non-linear pressure flow rate relations and large transition zones. Using a transparent model he was able to clearly demonstrate the discontinuous nature of the flow field within the fracture. He found this to be primarily attributable to dead water areas due to contact points and surrounding boundary layers and/or tortuosity of streamlines.

Maini suggested that one of the main differences between the continuum and discrete models resulted from head losses at joint intersections due to mixing of several flow paths, these losses being minimum when the discharges are equal. However he found that the intersection losses are negligible for small values (<100) of the Reynolds number.

Maini derived the following flow equations for radial flow between parallel plates:

$$P = A^*Q_j + B^*Q^2 \qquad (3.5)$$

where

Q = quantity of flow per unit width $[L^2]$

$$A^* = \frac{\ell n\ (r/r_o)}{2\pi k_j\ n\ e}\ , \qquad [L^{-2}T] \qquad (3.6)$$

k_j = hydraulic conducitivity of the fracture $[LT^{-1}]$

$$B^* = \frac{3}{20\pi^2\ e^2\ g}\left(\frac{1}{r^2} - \frac{1}{r_o^2}\right), \qquad [L^{-5}T^2] \qquad (3.7)$$

r_o is the well radius and $[L]$

P is the pressure at a radial distance r from the centre of the well. $[ML^{-1}T^{-2}]$

n is the number of fractures

The last term in equation (3.5) accounts for kinetic energy losses at joint intersections.

From field tests he found this term to be generally negligible but maintained that if the pressure flow curve is non-linear the kinetic energy term should be evaluated before proceeding to a non-linear law.

Using the laws of Miesbach, Maini obtained the following law for non-linear radial flow:

$$Q^n = C \left[2\pi r\ (e) \right]^n \left(\frac{r^{n-1}\ r_o^{n-1}}{r^{n-1} - r_o^{n-1}} \right) (P_o - P)\ (n-1) \qquad (3.8)$$

$$\text{or} \quad EQ^n = (P_o - P) \qquad (3.9)$$

where the subscript 'o' refers to the wellbore.

The intercept of this equation (i.e. for Q = 0) gives what is referred to as the *permeability function.*

$$C_e = \frac{1}{C \left[2\pi r\ (2e) \right]^n} \left(\frac{r^{n-1} \cdot r^{n-1}}{r^{n-1} - r_o^{n-1}} \right) \qquad (3.10)$$

The author also stated that the kinetic energy term is negligible in the case of non-linear flow.

Using the equation for linear radial flow developed above, a 58.5% pressure drop occurred at $r = 2r_o$, whereas the continuum model would predict virtually no pressure drop at that distance. Based on this, Maini concluded that, in the case of radial flow, the permeability characteristics near the borehole mainly control the pressure/flow relationship.

He also suggested that equation (3.5) could be used to determine whether the fracture opens or closes. A negative slope in the diagram $(\frac{P}{Q})$ versus Q indicates decreasing kinetic energy losses and hence increasing aperture.

Maini noted that the form of the pressure-flow rate relation implies that additional observation wells are necessary to evaluate borehole injection tests. The standard Lugeon test using the *radius of influence* concept ignores the effect of barrier and/or recharge boundaries making it a nonsteady state problem. He concluded that one observation well is necessary if a discontinuity is suspected while two wells are necessary if anisotropic conditions prevail.

Jouanna (1972) performed both laboratory and field tests on flow through a finely fissured micaschist. However, due to the very intensely fissured nature of this particular rock, measurement of individual parameters was impossible and the author had to choose a global approach.

The study concentrated largely on the effect of stress on permeability. Laboratory samples were subjected to biaxial loading while field data was obtained for various loading conditions. In both situations, irreversible changes in flow rate occurred when cycling the applied stress, the most profound variation being associated with the first cycle.

These laboratory studies indicated that linear flow did not exist for this rock type except at very low gradients near unity. The study was extended to very high gradients by using air as the fluid. The results indicated that some rocks have a unique flow law relating velocity and gradient which is independent of the viscosity.

The field testing on the same rock lead to a pressure-flow rate relationship which remained nearly linear throughout the test range. It should be noted however that in the laboratory test planar flow prevailed while in the field the flow was radial.

For analytical purposes Jouanna idealized the fissured medium as an equivalent, homogeneous continuum. He also assumed linear elastic behaviour and laminar flow conditions. The in-situ results show that this idealization is far from reality.

Rayneau (1972), studied radial flow in a single artificial fracture made of duraluminum, subjected to various loading conditions. This author also used a Reynolds number/relative roughness criterion to separate the different flow domains. In his numerical approach he assumed an elastic, isotropic, impermeable matrix with rock bridges to carry the stress transfer across the discontinuity.

In the case of radial flow, Rayneau showed that for constant flow rate the Reynolds number is independent of the aperture. In addition, for a relative roughness less than 0.033 the onset of turbulence becomes independent of the roughness. As the relative roughness increases however, the onset of turbulence occurs at lower flow rates.

Finally, Rayneau's study indicated that several different flow domains may occur within one single discontinuity especially within the vicinity of a borehole.

Goodman et al (1972) performed fundamental experimental research on the strength - deformability - water pressure relationships for fractures subjected to direct shear. Both rough and smooth fractures were investigated.

In his textbook, Goodman (1976) gave a comprehensive review of the factors affecting the mechanical behaviour of geological discontinuities based on field and laboratory tests on natural and artificial joints. Empirical laws developed by several investigators to describe joint

behaviour are critically reviewed. The author also described in detail his 'joint element' which can be used to model the behaviour of fractured rock masses.

In performing in-situ tests, Gale (1975) found that aperture changes were indicated by changes in the shape of the fluid pressure profile. Using a fracture deformation gage he concluded that aperture changes constitute a significant percentage of the initial aperture. He also found that when a number of fractures intersect a well, perferential opening of certain fractures occurs.

Although there seemed to be good agreement between field and numerical data, the author found that the assumed linear joint stiffness did not accurately model the non-linear behaviour of the fracture deformation, especially when the change in effective stress was a significant percentage of the initial effective stress.

His laboratory studies on large cores showed that the fluid pressure profile within the fracture plane is very sensitive to changes in aperture and thus may provide an indirect means of detecting fracture deformation in field situations.

Iwai (1976) studied the fundamental hydraulic characteristics of laminar flow through natural fractures and the effect of inherent geometric characteristics, i.e. small scale roughness and contact areas.

Laboratory permeability tests were done to examine how actual flow characteristics are influenced by aperture changes (up to $2.5 \cdot 10^{-2}$ cm), stress changes and geometry.

From measurement of the flow rate, pressure gradient and vertical displacement, Iwai was able to confirm the applicability of the cubic law to flow in rock discontinuities. Most tests utilized radial flow although one linear flow test was performed.

The author concluded that small scale relative roughness does not greatly influence the flow characteristics provided the aperture is larger than about 20×10^{-4} cm. He also found that nonuniform apertures may be treated as equivalent uniform apertures without inordinate error if a wedge shaped fracture is assumed. The study also indicated that the contact areas significantly influence the flow rate. This conclusion was reached from numerical data using a model based on randomly distributed contact points but was not substantiated in the laboratory tests.

A rather interesting feature was that the stress-deformation behaviour of the laboratory models was non-linear throughout the testing range, (up to 20 MPa), and cyclic loading produced hysteresis and permanent deformation. Moreover, small residual flow persisted even at very high normal stress (30 Mpa).

Under cyclic loading the flow rate was analogous to the deformation behaviour. The dependency of flow on stress history can however be avoided if the flow rates are taken as a function of the fracture aperture.

Iwai found that with the exception of highly non-uniform fractures the cubic law is applicable provided that the Reynolds number is less than 100 and a correction is introduced to take care of the residual flow.

The author suggested the following expressions:

(a) For radial flow

$$Q = \alpha \frac{\pi\gamma}{6\mu} (b_d + \Delta b_a)^3 \frac{\Delta h}{\ln(r_o/r_i)} \qquad (3.11)$$

where r_o = well radius [L]

r_i = distance remote from well [L]

Δh = change in head between r_o and r_i [L]

γ = specific weight of water $[ML^{-2}T^{-2}]$

μ = dynamic viscosity of fluid $[ML^{-1}T^{-1}]$

α = flow rate reduction factor

α_r = α for $b_d = 0$,

$b_d = V_m - \Delta V$ [L]

Δb_a = fracture aperture at $b_d = 0$, expressed as

$$\Delta b_a = \frac{\Delta b}{\sqrt[3]{\alpha_r}} \qquad [L] \qquad (3.12)$$

V_m = maximum closure

(b) For planar flow

$$Q = \alpha \frac{\gamma}{12\mu} (b_d + \Delta b_a)^3 \frac{\Delta h}{L} \qquad (3.13)$$

where Δh = head difference over length L [L]

L = flow distance, [L]

$\alpha = 1.0$ for $b_d > 15 \times 10^{-4}$ cm

$\alpha \leq 1.0$ for $b_d \leq 15 \times 10^{-4}$ cm

Although Gale (1975) and Wilson (1970) stated that turbulent flow was not important for practical considerations Iwai (1977) recommended extension of the tests to include the turbulent regime in order to see if the proposed flow equations remain valid. It is interesting to note that his test data began to deviate significantly (about 20%) from the

cubic law for Reynolds numbers greater than 100, even though the apertures tested are very small ($<250 \times 10^{-4}$ cm).

3.3 Numerical Investigations

The previous section of this report reviewed the experimental models using either an artificial or a natural joint. In order to study problems of practical interest the aforementioned data has to be applied to a rock mass containing a large number of intersecting fractures, necessitating the use of a numerical technique.

Louis (1969) examined the effect of flow on the stability of rock slopes by numerically solving a system of linear equations. The numerical model of Sharp (1970) and Maini (1971) was based on the finite difference technique.

The relatively recent and rapid advancements in the finite element method have provided a further powerful and versatile tool for the solution of complex boundary value problems.

Wilson and Witherspoon (1970), developed a finite element program to analyse steady state flow in jointed rock, assuming the rock mass to be rigid. They were able to simulate flow from a porous matrix into the fractures along with the effect of varying aperture and interference at fracture intersections.

Noorishad (1971), investigated two-dimensional, steady state flow behaviour within a fractured rock mass subject to fluid forces, body forces and boundary loads. The analysis was performed by coupling two finite element programs, one for stress analysis and the other for fluid flow. In comparing this technique with the rigid fractures

approach the author found that the interaction between fluid pressures and rock stresses is rather important. For example, less discharge and higher uplift pressures are encountered.

Witherspoon et al (1974), devised a numerical technique to analyse stress flow problems in complex rock systems containing deformable features. The method again couples two finite element programmes in a manner similar to Norrishad. Their analysis showed that fracture orientation strongly affects the extent of pressurization for both injection and withdrawal tests. Also an increase in the fracture stiffness causes the pressure to affect a larger region around the injection point. The authors concluded that the assumption of rigid fractures cannot be used to predict the behaviour of a fractured rock mass.

Gale (1975) presented a thorough study of flow in deformable fractured systems. He extended the work of Noorishad to include axi-symmetric conditions. The rock matrix was idealized as a linear elastic continuum while the fracture deformability was modelled using the "joint element" of Goodman (1976).

Gale found considerable difference in the pressure - flow rate distribution for injection versus withdrawal. The greater the deformability of the fracture the larger the difference. His numerical study indicated the existence of a considerable difference in the pressure - flow rate distribution when non-uniform versus uniform fractures were considered.

CHAPTER IV

COUPLED DEFORMABLE FRACTURE FLOW

4.1 Introduction

The previous chapter has shown that prior to the recent work by Witherspoon, Norrishad, Gale and Iwai, researchers in fracture flow had regarded fractures as rigid networks. However recent work has demonstrated that the effect of fracture deformation on flow behaviour as well as the role of fluid pressures as deformation agents must be taken into account. These effects may alter the hydrologic response of the entire system.

In order to solve this problem any mathematical model should account for:

(i) the deformability of the fractures,

(ii) the coupling between fluid pressures and stresses in the intact rock.

With respect to the latter factor, the pressure distribution through the fractured rock mass must be compatible with the state of stress of the system.

Several assumptions concerning rock and fracture behaviour are necessary to make the method tractable yet realistic:

(i) the geometry of the system is known (i.e. fracture density, aperture distribution, etc.)

(ii) the permeability of the fractured rock mass is essentially due to flow through the fractures, i.e. the primary permeability is negligible.

(iii) the intact rock blocks behave elastically.

(iv) the fracture deformations are non-elastic.

The finite element technique was used to model coupled deformable fracture flow. The linear fracture flow element developed by Wilson (1970) was coupled using an iterative process with Goodman's (1976) joint element model. The model was then used for parametric studies of the principal factors controlling fracture flow. The results of these studies are discussed in the remainder of this section.

4.2 Fracture Deformation

4.2.1 Generalities

Goodman (1976) describes a discontinuity as a 'special link' between block faces - one that parts in response to tensile forces, slides in response to shear forces, and transmits any force in response to compression forces. Each of these modes of deformation contributes primarly non-elastic displacements to the rock mass. The *Goodman joint element* is an elastic linkage element constrained through an iterative solution procedure to obey the non-elastic, non-linear deformation laws observed experimentally with rock fractures.

Figure 4-1 shows a four nodal point joint element as an idealization of an actual discontinuity. It has a small aperture 'e' to simulate the irregular and variable region between the joint walls. For simplicity it will be considered as a linear feature.

The finite element model is based on the displacement method. In order to solve for the displacements and stresses resulting from an imposed load, the rock mass is divided into two parts.

(i) a homogeneous continuum idealized as a linear elastic solid represented by orthotropic constant strain triangular elements.

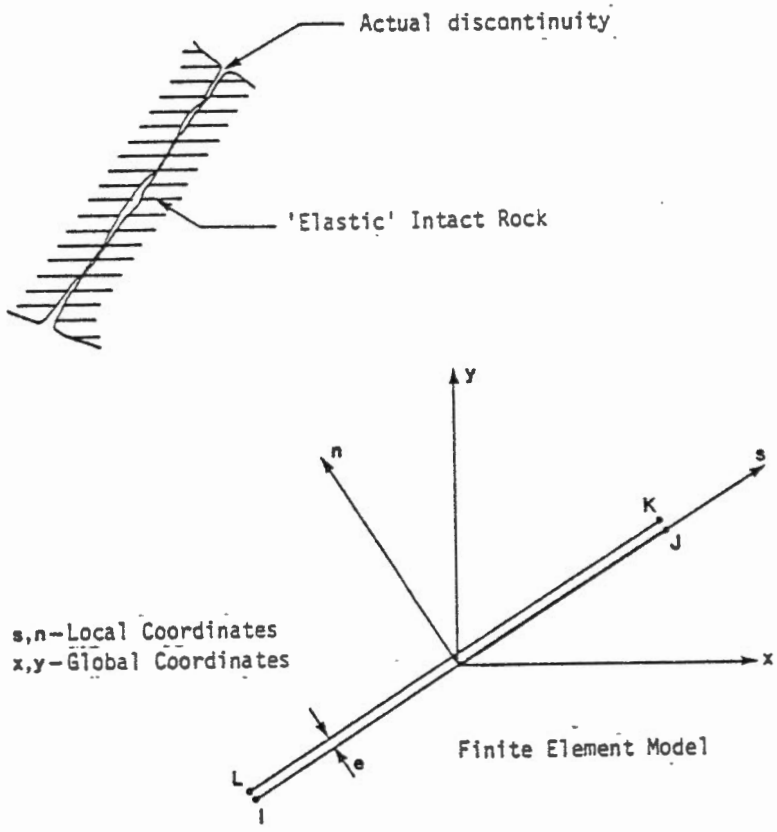

Figure 4.1 Actual and Idealized Discontinuity (after Goodman, 1976)

(ii) joints behaving elasto-plastically and represented by linear linkage elements.

Details of the formulations for the above elements are given by Goodman (1976).

4.2.2 Fracture Behaviour Under Normal Load

An empirical relation between normal deformations and increasing normal load on a fracture as developed by Goodman (1974) was used in the present model. Two conditions must be satisfied:

(i) an open fracture exhibits no tensile strength,

(ii) there is a limit to the maximum allowable compression, defined by the maximum closure, (V_{mc}), which must be less than or equal to the mean joint aperture (See Fig. 4-2).

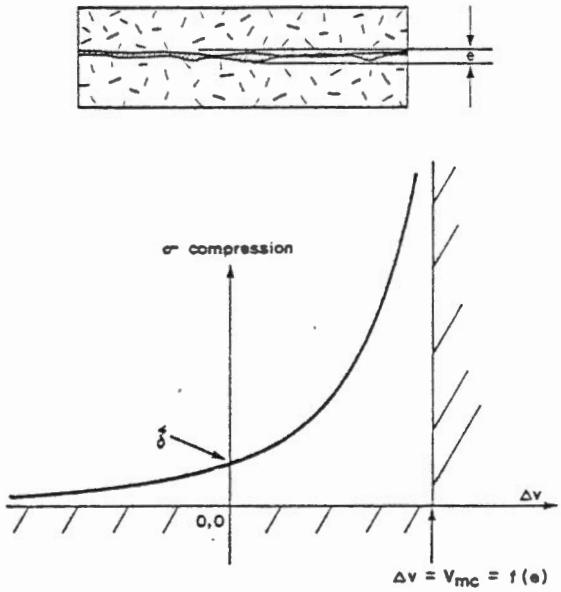

Figure 4.2 Fracture behaviour in compression (after Goodman, 1976)

A relation between normal stress (σ) and normal displacement (Δv) which accounts for the above constraints is represented by the hyperbolic equation:

$$\frac{\sigma - \xi}{\xi} = A \left(\frac{\Delta v}{V_{mc} - \Delta v}\right)^{t} \quad (*) \quad (\Delta v < V_{mc}) \qquad (4.1)$$

where { ξ is the seating pressure $[ML^{-1}T^{-2}]$
{ A and t are empirical coefficients.

The highly non-linear load deformation character evidenced in Figure 4.2 leads to similar non-linearities in other parameters related to fracture aperture (e.g. fluid permeability).

Following the example of Goodman (1976) the parameters A and t have been taken as 1 and 0 respectively for all examples in the present research. Furthermore, if one substitutes:

$$\xi = F_{n,0}/\ell' \quad \text{and} \quad \xi = F_n/\ell'$$

where { $F_{n,o}$ = initial external force at a nodal point $[MLT^{-2}]$
{ F_n = external force at some later increment $[MLT^{-2}]$
{ ℓ' = half-length of the joint $[L]$

---

* tensile forces are taken as positive.

in equation 4.1 it can be shown that:

$$F_n = \left(\frac{\Delta v}{V_m - \Delta_v} + 1\right) \quad F_{n,0} \tag{4.2}$$

Using this last equation, the normal load-deformation curve can be drawn for any fracture, the initial normal stiffness being obtained by differentiating the equation with respect to Δv, i.e.

$$KN_o = \frac{-\sigma_o^2}{\xi V_{mc}} \tag{4.3}$$

This expression is used to initiate the iterative computation process.

Two examples of normal closure behaviour are presented on figures 4-3 and 4-4. The first example is from Goodman (1976) and was used to test the program. In this case a block under an initial stress of 5 MPa compression is next to a fracture with an initial compression of 1 MPa, held by a constraint. Removal of the constraint distresses the block and compresses the joint to restore equilibrium. Goodman uses this example to show that the rate of convergence is dependent on the initial stress in the fracture and that very low initial stresses may lead to excessively slow rates of convergence.

The very large maximum closure (5 cm) used in this example leads to a very low normal stiffness for the fracture. Similarly a low stiffness was used for the rock. Although this is instructive for observing how the load transfer method reaches convergence it has very little meaning from the viewpoint of practical rock engineering. Hence a second more realistic example, shown on Figure 4-4, was used. The rock matrix was assigned typical properties for an average granite while the fracture

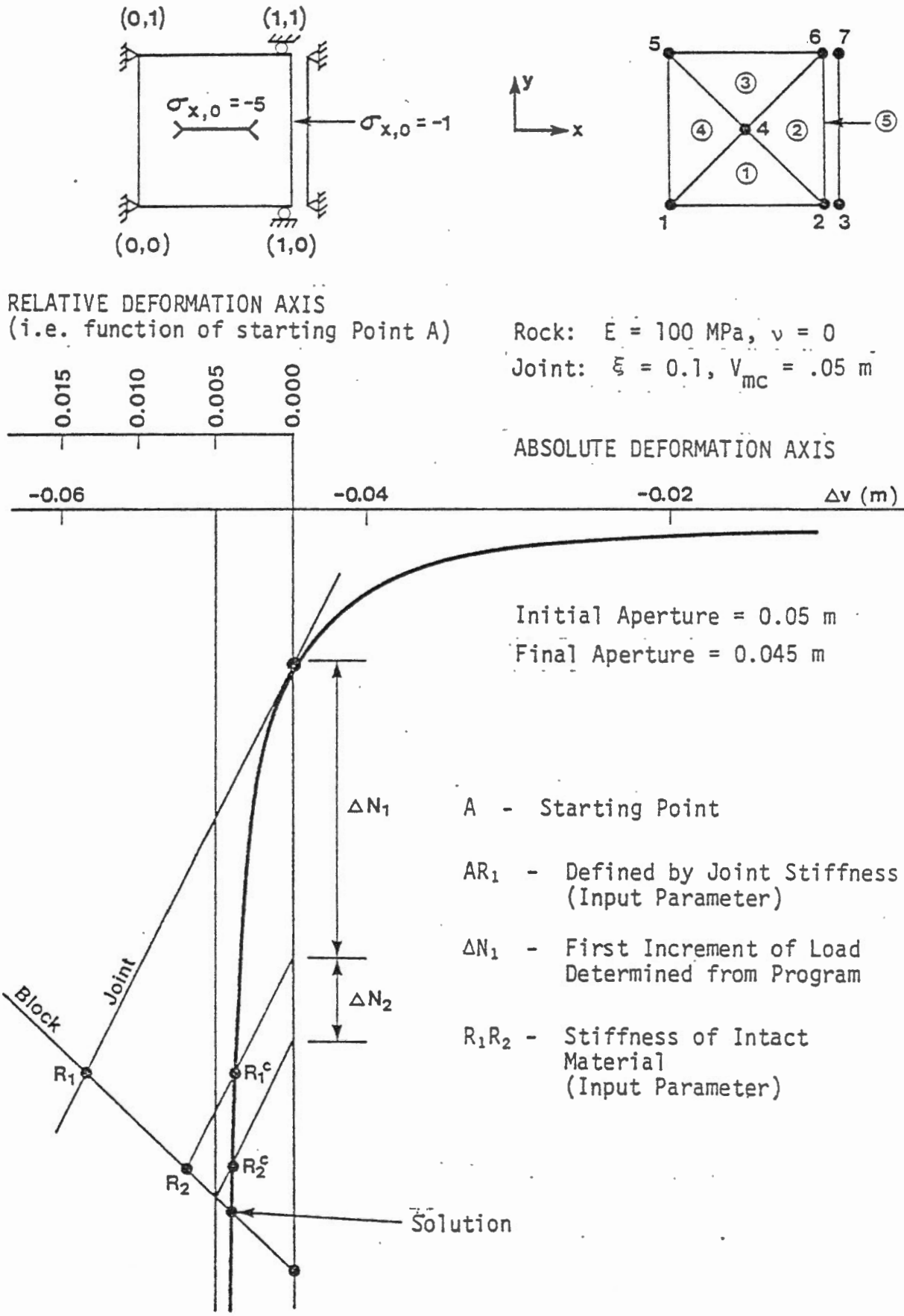

Figure 4-3 Normal load versus deformation diagram for soft fracture. (Goodman, 1976)

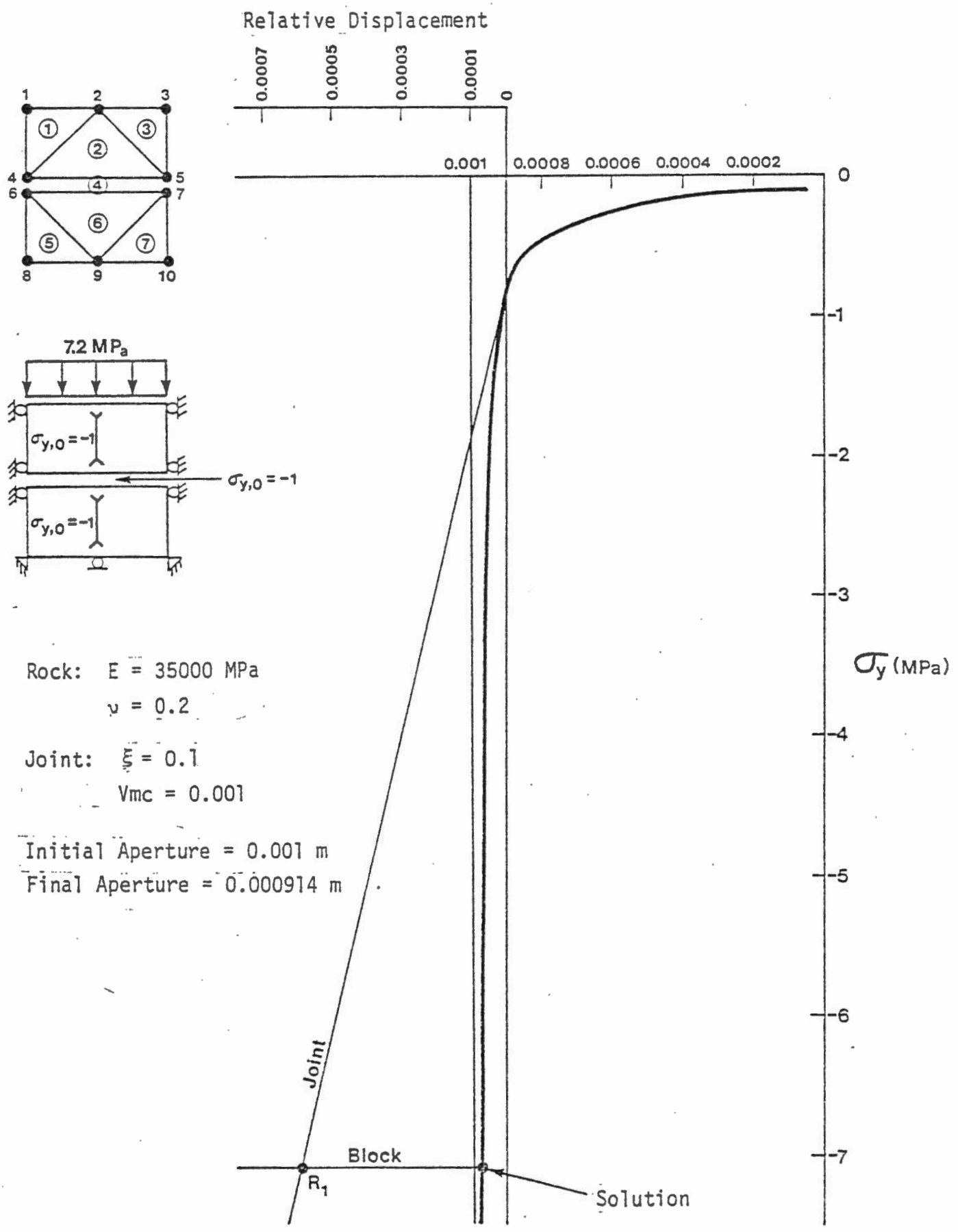

Figure 4.4 Normal load versus deformation diagram for stiff fracture.

aperture was set at 1 mm. In this and all remaining examples the following assumptions were made:

(i) the maximum closure (V_{mc}) was set equal to the initial aperture (e_o)

(ii) The initial stress in both the matrix and fractures was set at -1 and the seating load for the fracture at 0.1.

As may be seen from comparing the two figures, the narrower and hence stiffer fracture converges much more rapidly and although the normal load is almost twice that on the soft fracture the percent change in aperture remains about the same. The table below shows typical initial normal stiffnesses for various maximum closures, assuming in all cases $\sigma_o = -1$ and $\xi = 0.1$..

NORMAL STIFFNESS FOR VARIOUS MAXIMUM CLOSURES

V_{mc} (meters)	KN_o (force/length)
.05	200
.01	1,000
.005	2,000
.001	10,000
.0001	100,000

From the viewpoint of practical rock engineering it is generally only those apertures 1 mm and less that are of interest.

4.2.3 Fracture Behaviour Under Shear Load

In recent years considerable research has been conducted on the shear stress - shear deformation behaviour of individual rock fractures and fractured rock masses. Barton (1978), Goodman (1976), and Hoek (1977) give comprehensive reviews of existing shear strength theories and present extensive available data.

For the joint element program Goodman chose to use the mechanistic model proposed by Ladanyi and Archambault (1970) since the equation for peak shear strength is derived from identifiable properties of the joint and wall rock. They combined the friction, dilatancy and interlock contributions to peak shear strength to derive a general strength equation that has proven accurate in model studies (Goodman 1976). Their equation for peak strength is:

$$\tau_p = \frac{\sigma\,(1-a_s)\,(\dot{v} + \tan\phi_u) + a_s\,S_R}{1 - (1-a_s)\,\dot{v}\tan\phi_u} \qquad (4.4)$$

where
- a_s is the proportion of joint area sheared through the asperities
- $\dot{v}$ is the dilation rate at the peak shear stress (secant dilatancy rate) $\Delta v\,(\tau_p)/\Delta u\,(\tau_p)$
- S_R is the shear strength of the rock composing the asperities. $[ML^{-2}]$

Ladanyi suggested substituting Fairhurst's parabolic criterion for S_R:

$$S_R = Q_u \frac{(1+n)^{\frac{1}{2}} - 1}{n}\,(1+n\,\sigma/Q_u)^{\frac{1}{2}} \qquad (4.5)$$

where $\begin{cases} Q_u \text{ is the unconfined compressive strength of the asperities} & [ML^{-2}] \\ n \text{ is the ratio of compressive to tensile strength of the asperities.} \end{cases}$

Ladanyi and Archambault also suggested power laws for $\dot{v}$ and a_s:

for $\sigma < Q_u$

$$a_s = 1 - (1 - \sigma/Q_u)^{K_1} \tag{4.6}$$

$$\dot{v} = (1 - \sigma/Q_u)^{K_2} \tan i_o \tag{4.7}$$

and suggested exponents $K_1 = 1.5$ and $K_2 = 4$. The values of a_s and $\dot{v}$ then vary between the limits

$$a_s = \begin{cases} 0 \ @ \ \sigma=0 \\ 1 \ @ \ \sigma= Q_u \end{cases} \tag{4.8}$$

$$\dot{v} = \begin{cases} \tan i_o \ @ \ \sigma=0 \\ 0 \quad @ \ \sigma= Q_u \end{cases}$$

With the above conditions equation (4.5) defines a curved peak stress criterion as shown on Figure 4.5.

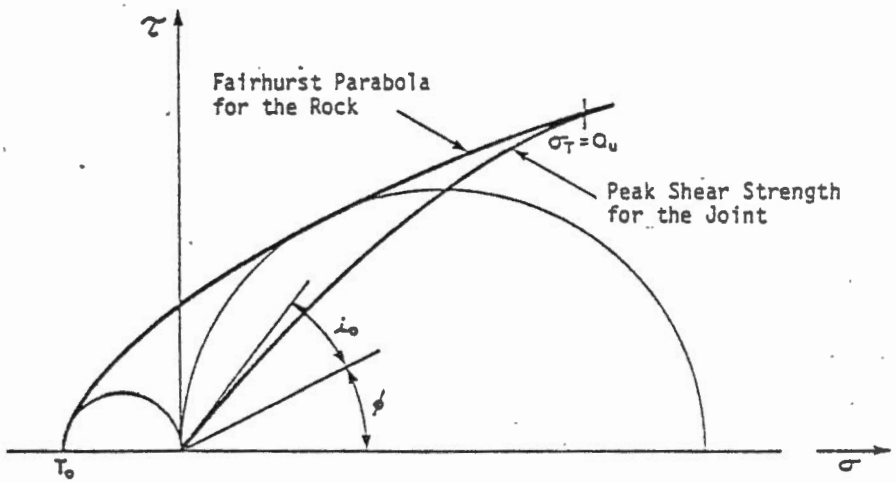

Figure 4.5 Ladanyi and Archambault's Shear Strength Relationship for Rough Joints.

Note σ_T = transition pressure where joints are no longer weaker than rock matrix.

Goodman treats the shear stress/shear deformation behaviour in a similar manner to fracture opening with the limiting shear stress criterion being analogous to the *no tension criterion* imposed on the normal stress/normal displacement curve. Lacking a universal model for shear stress-shear deformation of fractures, he assumes the simple constitutive law shown in Figure 4-6. The initial stress, τ_o, and initial shear stiffness, KS, define the elastic region. The joint is assumed to behave elastically up to the peak stress τ_p, which is a function of the normal stress , i.e.

$$\tau_p = f_1 (\sigma) . \tag{4.9}$$

If τ_p is exceeded the shear strength falls attaining a residual value, τ_r, when the displacement u_r has been attained.

$$\tau_r = f_2 (\sigma) \tag{4.10}$$

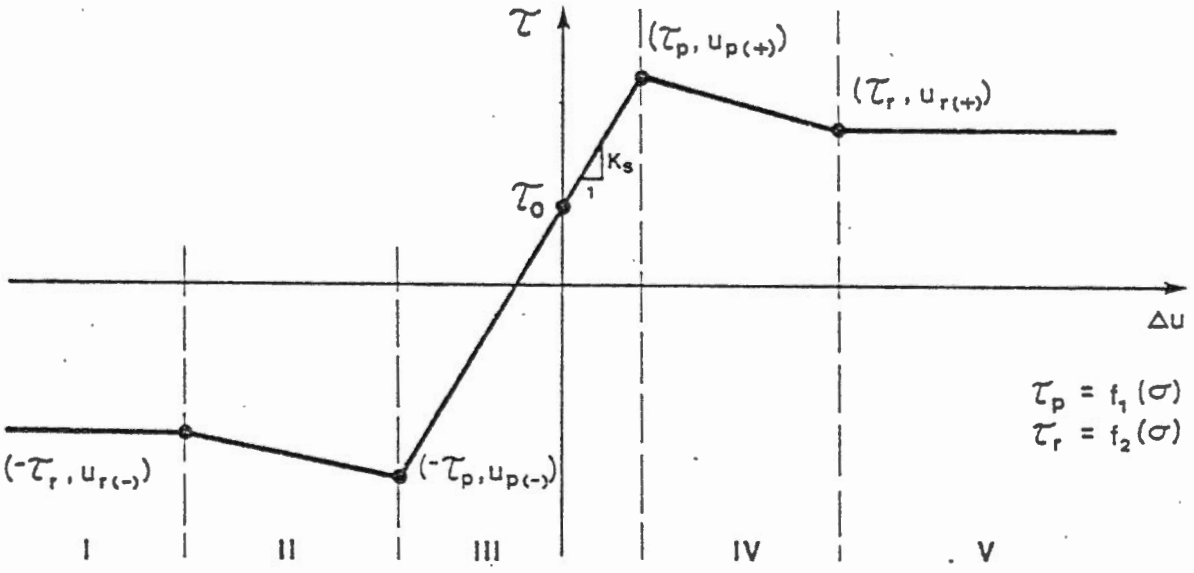

Note: I, II, etc. represent separate regions

Figure 4.6 Goodman's Constitutive Law for Shear Deformation

Details of the formulation for the constitutive law are given by Goodman (1976). Any consistent experimental or empirical results can be used to define (f_1) and (f_2). Goodman has used the results from Ladanyi and Archambault and these same laws were used to obtain the results presented in this report.

Little is known of the variation of residual shear strength, τ_r, with σ. Goodman inputs f_2 in a consistent manner as follows:

$$\tau_r/\tau_p = B_o \tag{4.11}$$

where

$$B_o = \begin{cases} \geqslant 0 \\ \leqslant 1 \end{cases} \quad @ \quad \sigma = 0$$

$$= 1 \quad @ \quad \sigma = Q_u$$

The parameter B_o is then left as an input parameter such that both brittle and plastic behaviour may be studied.

Figure 4-7 shows a computer simulation of a simple direct shear test on a smooth fracture. In this case the applied shear stress (τ) exceeds the peak shear strength (τ_p). The load transfer process is able to follow the deformation into the post-failure range. The increasing values of ΔS indicate divergence and in this case shear failure of the fracture.

Natural fractures are seldom perfectly smooth and planar. Rather they generally exhibit a varying degree of roughness. A shear test conducted under restricted normal displacement conditions, (Figure 4-8 curves B), generally show much higher shear strengths than those with constant normal load as in curve A. This effect is related to a

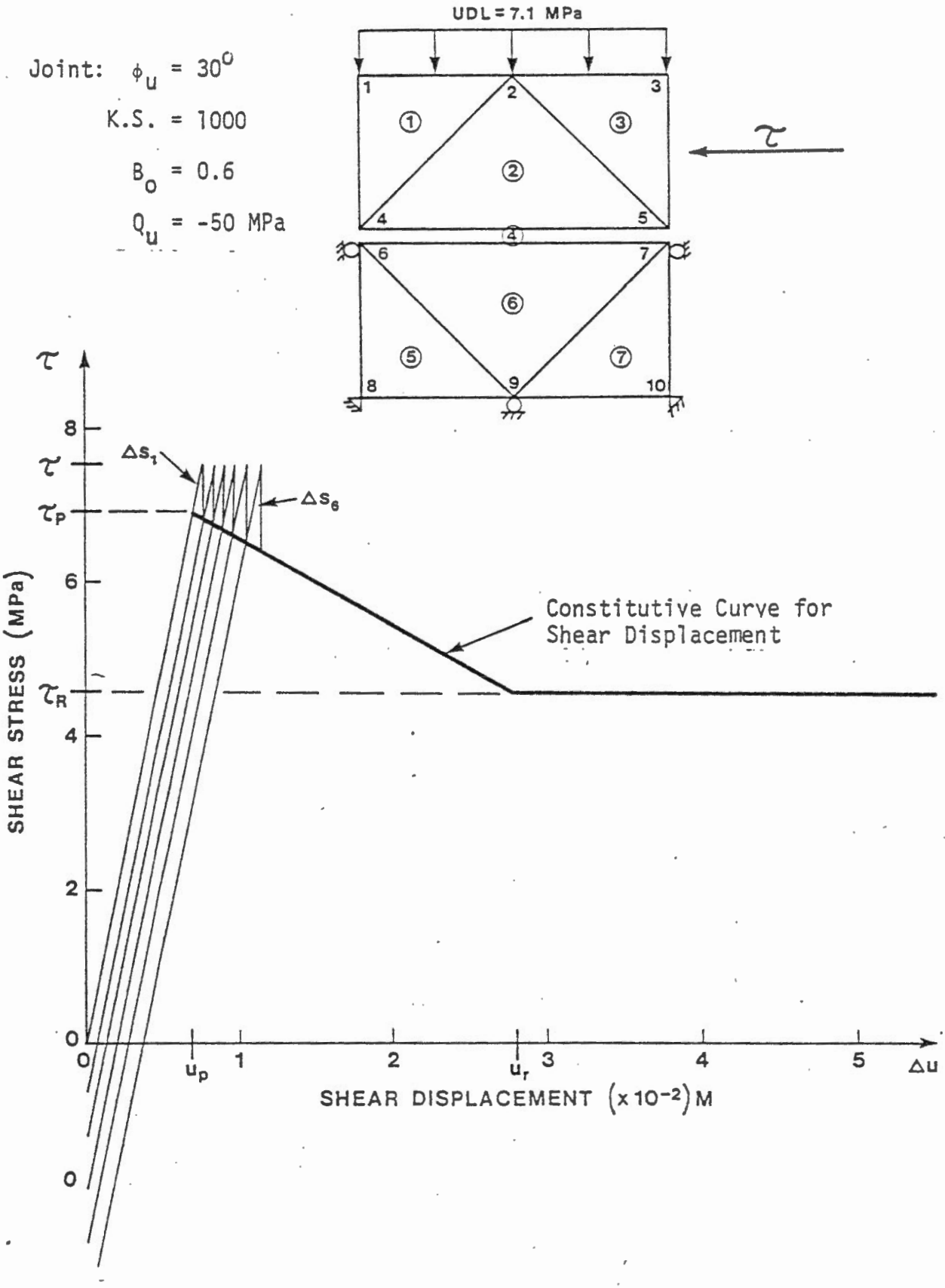

Figure 4-7 Shear stress versus shear deformation diagram for smooth joint.

phenomenon known as dilatancy. Perfectly mating rough blocks can be forced to slide past one another only if they are free to move apart or dilate. If the normal movement is restricted, the shear may only occur if the asperities themselves are sheared through. Hence dilatancy may have two important effects:

(i) if normal movement is restricted it may considerably increase the shear strength of a fracture.

(ii) if normal movement is allowed dilatancy may lead to significant changes in fracture aperture.

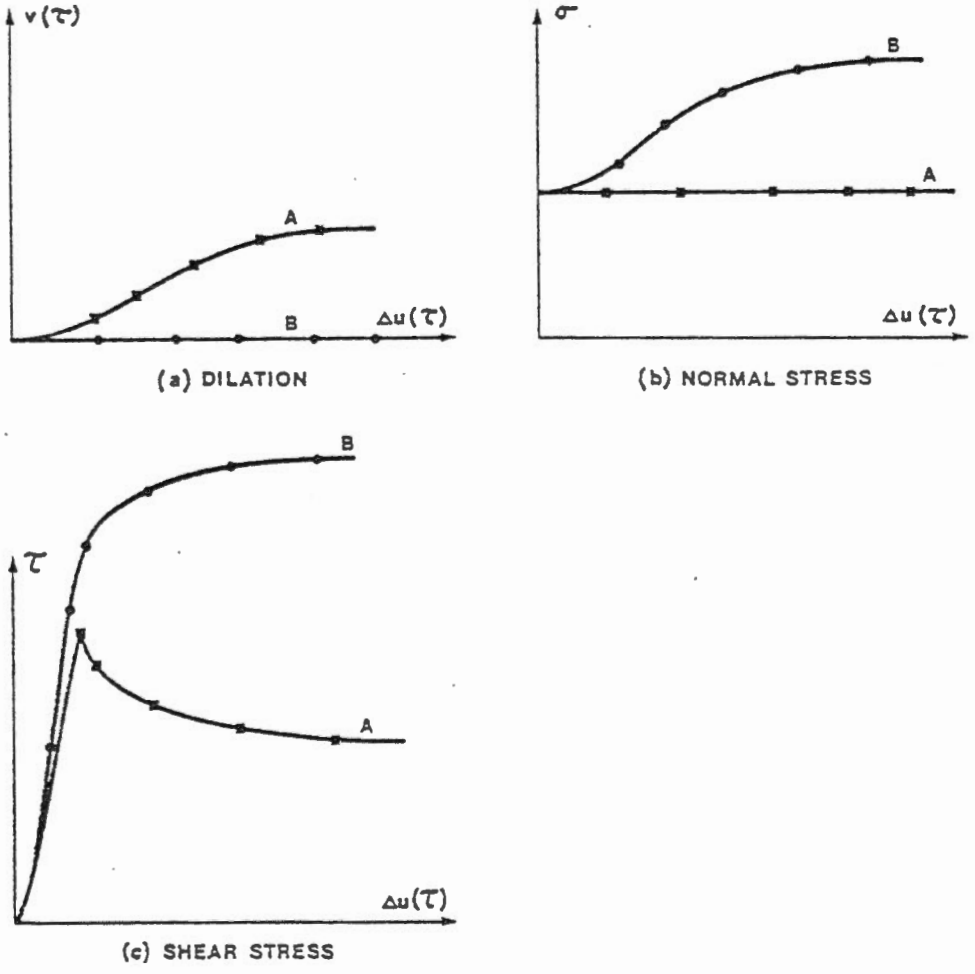

Figure 4.8 Effect of Test Mode on Shear Deformation Curves for dilatant joints.

{ A: shear at constant normal stress
{ B: shear with condition of no normal displacement

(after Goodman 1976)

The latter point is discussed in more detail in the next section of this report.

Dilatancy is thus a function of the normal load acting on the fracture, the degree of confinement and the strength of the wall rock. Figure 4-9, (Barton, 1971), shows a plot of peak dilation angle as a function of the ratio of normal stress to wall rock strength. As may be seen with either low normal stress or very high fracture wall strength one may expect much higher peak dilation angles than for higher values of this ratio.

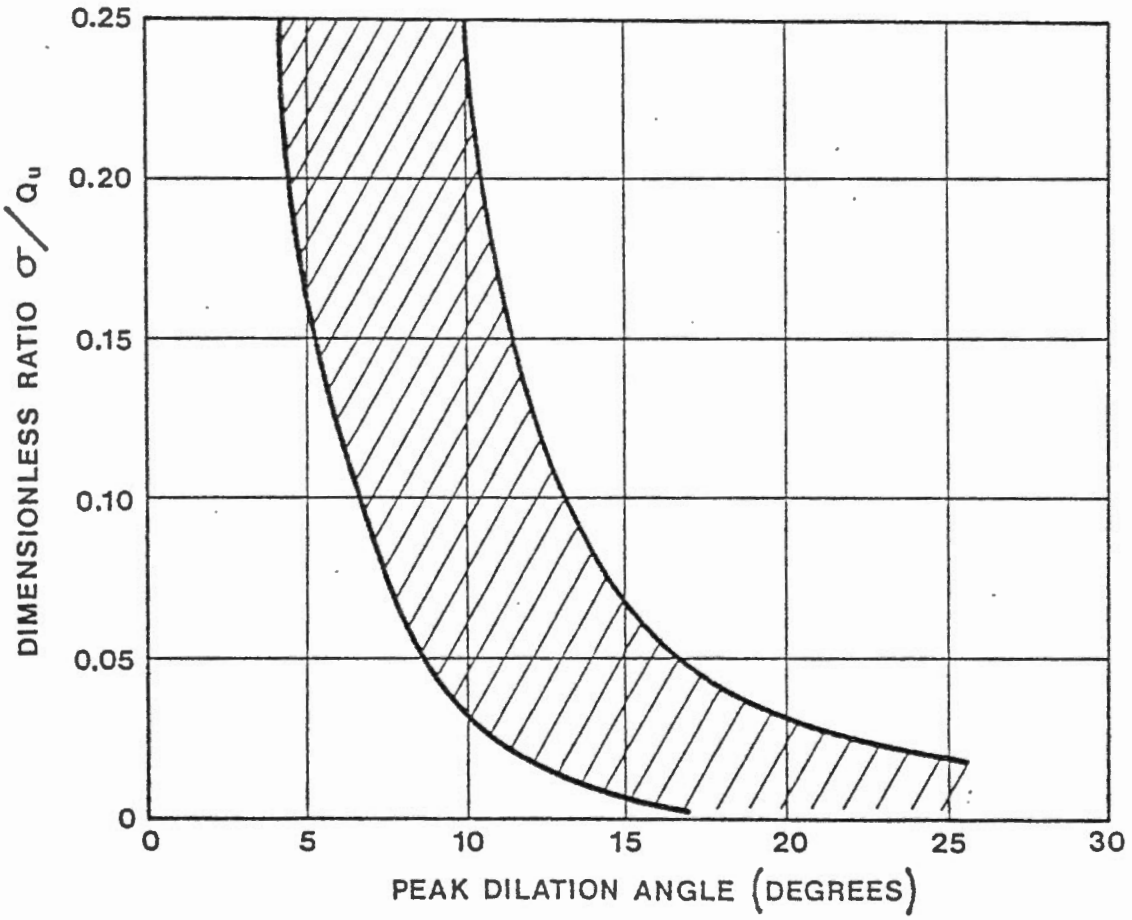

Figure 4.9 Peak Dilatancy Angle as a Function of the Ratio of Normal Stress to Compressive Strength for Model Extension Joints.
(after Barton 1971)

Figure 4-10, based on work by Ladanyi and Archambault, shows that although the effect of dilation on shear strength is significant at low normal stress it rapidly drops to zero as σ approaches the wall rock strength.

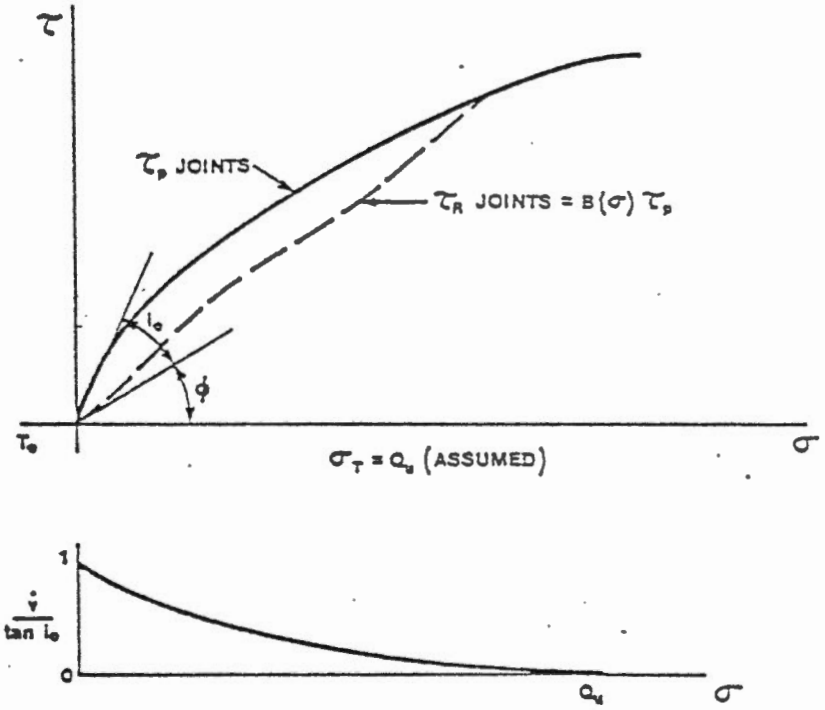

Figure 4.10 Assumed Variation of Peak and Residual Shear Strength and Peak Dilatancy ($\dot{v}$) with Normal Stress (based on Ladanyi and Archambault, 1970)
(After Goodman 1976)

Figure 4-11 shows the effect of increasing the σ/Q_u ratio on peak shear strength for various specific dilatancy angles, using Ladanyi and Archambault's shear criterion. These effects appear most pronounced for σ/Q_u ratios below about 0.2

With the above discussion in mind let us examine the effect of performing the shear box test shown in figure 4.7 on a rough fracture. The σ/Q_u ratio for this fracture is 0.144. Referring to figure 4-9 a dilatancy angle of 10^o was chosen. The test was then rerun including

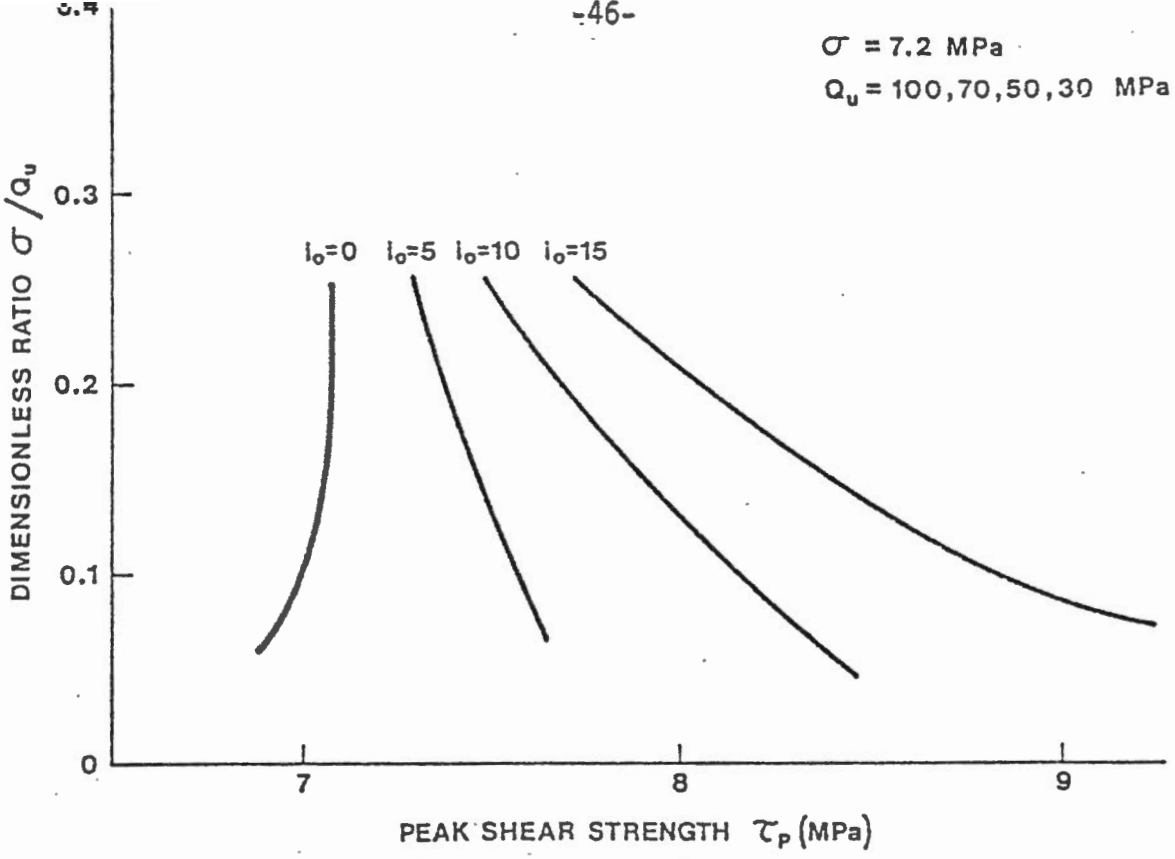

Figure 4.11 Effect of Increasing Normal Stress and Dilatancy on Peak Shear Stress

a 10^o dilatancy and the results are shown on Figure 4-12. As shown the peak shear strength now exceeds the applied shear stress and the shear deformation remains in the elastic range, that is:

$$u = \tau/K.S.$$

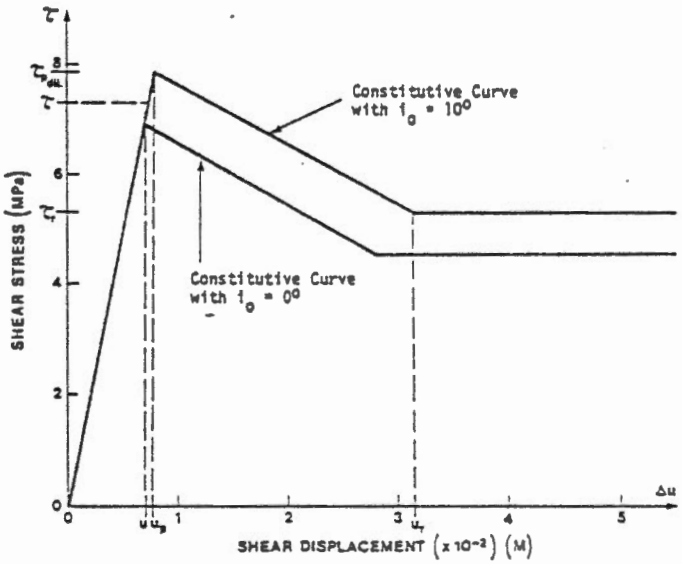

Figure 4.12 Shear Stress Versus Shear Displacement for Dilatant Joint

4.3 Fracture Permeability

4.3.1 Generalities

For numerical studies of fluid flow through rock fractures the discontinuities are idealized as smooth parallel plates as was shown in Figure 4.1. For this model, which is generally known as the Hele-Shaw model, the flow quantities and pressure distribution can be solved in closed form as long as the flow remains laminar (see Batchelor, 1970).

If the fluid flow between the plates is assumed to be one-dimensional, the velocity varies from zero at each boundary to a maximum in the center with the result that the velocity gradient and hence shear stress, is a maximum at the boundaries and zero in the centre.

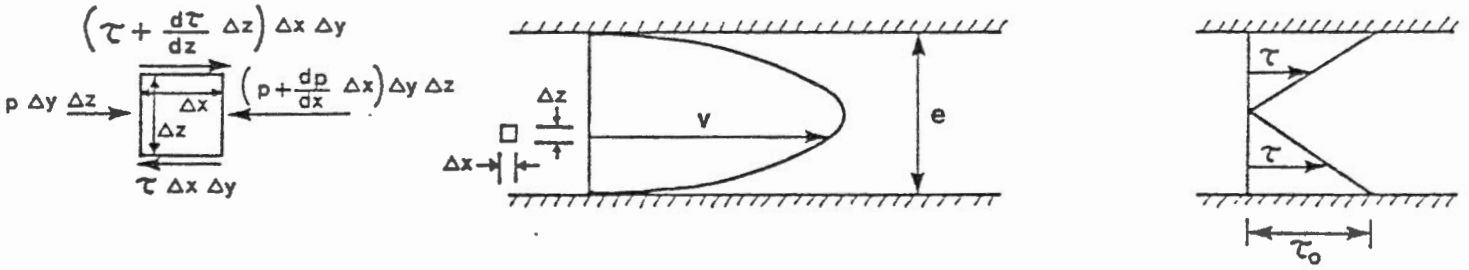

(a) Forces on Fluid Element (b) Velocity Distribution (c) Shear Distributi

Figure 4.13 Hele-Shaw Model

For this case of steady state laminar viscous flow through such a model the general equation of motion (i.e. Navier-Stokes equation) is given by:

$$\bar{\gamma} = -\frac{1}{\rho}\,\overline{\text{grad } p} + \nu\Delta\bar{v} + \bar{F} \qquad (4.12)$$

where
- $\overline{F}$ = external forces — $[M, L, T^{-2}]$
- p = fluid pressure — $[ML^{-1}T^{-2}]$
- ν = kinematic viscosity = μ/ρ — $[L^2T^{-1}]$
- $\overline{\gamma}$ = fluid acceleration — $[LT^{-2}]$
- $\overline{v}$ = fluid velocity — $[LT^{-1}]$

For the case of motion between two parallel plates:

$$u = u(x,y,z);\ v = 0;\quad w = 0 \tag{4.13}$$

The equation of continuity gives

$$\text{div } \overline{v} = 0 \quad \text{or} \quad \frac{\partial u}{\partial x} + \frac{\partial v}{\partial y} + \frac{\partial w}{\partial z} = 0 \tag{4.14}$$

When considering equations (4.13) and (4.14), it can easily be seen that u is a function of y and z only.

Now, assuming an aperture e = 2 a and u = u(z) (Two infinite parallel plates), it can be shown that the final differential equation is:

$$\frac{\partial p^*}{\partial x} = \rho \frac{\partial^2 u}{\partial z^2} \tag{4.15}$$

where p^* is the hydrostatic head $[L]$

Integrating 4.15 twice yields

$$u = \frac{1}{2\rho} \frac{\partial p^*}{\partial x} z^2 + cz + 0 \tag{4.16}$$

Inserting the following boundary conditions

(i) no flow at the boundaries, i.e. $u(+a) = u(-a) = 0$

(ii) maximum flow at the centre

$$\text{i.e. } \left.\frac{\partial u}{\partial z}\right|_{z=0} = 0$$

gives

$$u = \frac{z^2 - a^2}{\partial \rho} \frac{\partial p^*}{\partial x} \tag{4.17}$$

But

$$h = z + \frac{p}{\rho g} + \frac{v^2}{2g} \tag{4.18}$$

$\frac{v^2}{2g} \rightarrow 0$ for laminar flow

which gives the result

$$p^* = p + \rho g z \tag{4.19}$$

and equation (4.17) can be written as

$$\bar{u} = \frac{g\,(2a)^2}{12\,\nu} \frac{dh}{dz}$$

or

$$\bar{u} = \frac{g\,(2a)^2}{12\nu} \bar{J}_z \tag{4.20}$$

where $\bar{J}_z$ is the component of the gradient in the z-direction.

The permeability of a planar joint K_p is then defined as:

$$K_p = \frac{ge^2}{12\nu} \qquad [LT^{-1}] \tag{4.21}$$

If q is the flow rate per unit width, $\overline{q} = e\overline{u}$. One may then define

$$K_p' = \frac{ge^3}{12\nu} \qquad [L^2T^{-1}] \qquad (4.22)$$

as the area permeability.

This derivation shows that for smooth planar fractures, the conductivity is proportional to the square of the aperture. However, as discussed previously with respect to shear deformation, many natural fractures deviate significantly from the above model. Louis (1969) and Lomize (1951) investigated experimentally the effect of fracture geometry and roughness on conductivity and documented a number of empirical laws governing fracture flow. This experimental work and the corresponding flow laws have been reproduced earlier in chapter III. These laws have been plotted using log coordinates (q versus gradient J for varying apertures and roughnesses), for parallel flow (relative roughness $K/D_h \leq 0.033$) and non parallel flow ($K/D_h > 0.033$) assuming a water viscosity of $10^{-6}(m^2s^{-1})$(see figures 4.14 and 4.15). All of the various flow laws vary only by minor numerical factors and can be represented by the general law

$$Q = K_p^* J^{\alpha} \qquad (4.23)$$

where K_p^* is the area permeability.

Further, it should be noted that in Figures 4.14 and 4.15 both laminar flow (lower) and turbulent flow (upper) laws have been plotted. Questions however remain concerning the validity of the turbulent flow equations, (Wilson (1970), Gale (1975), Iwai (1977)), and further laboratory and field experimentation is required to determine if turbulence plays

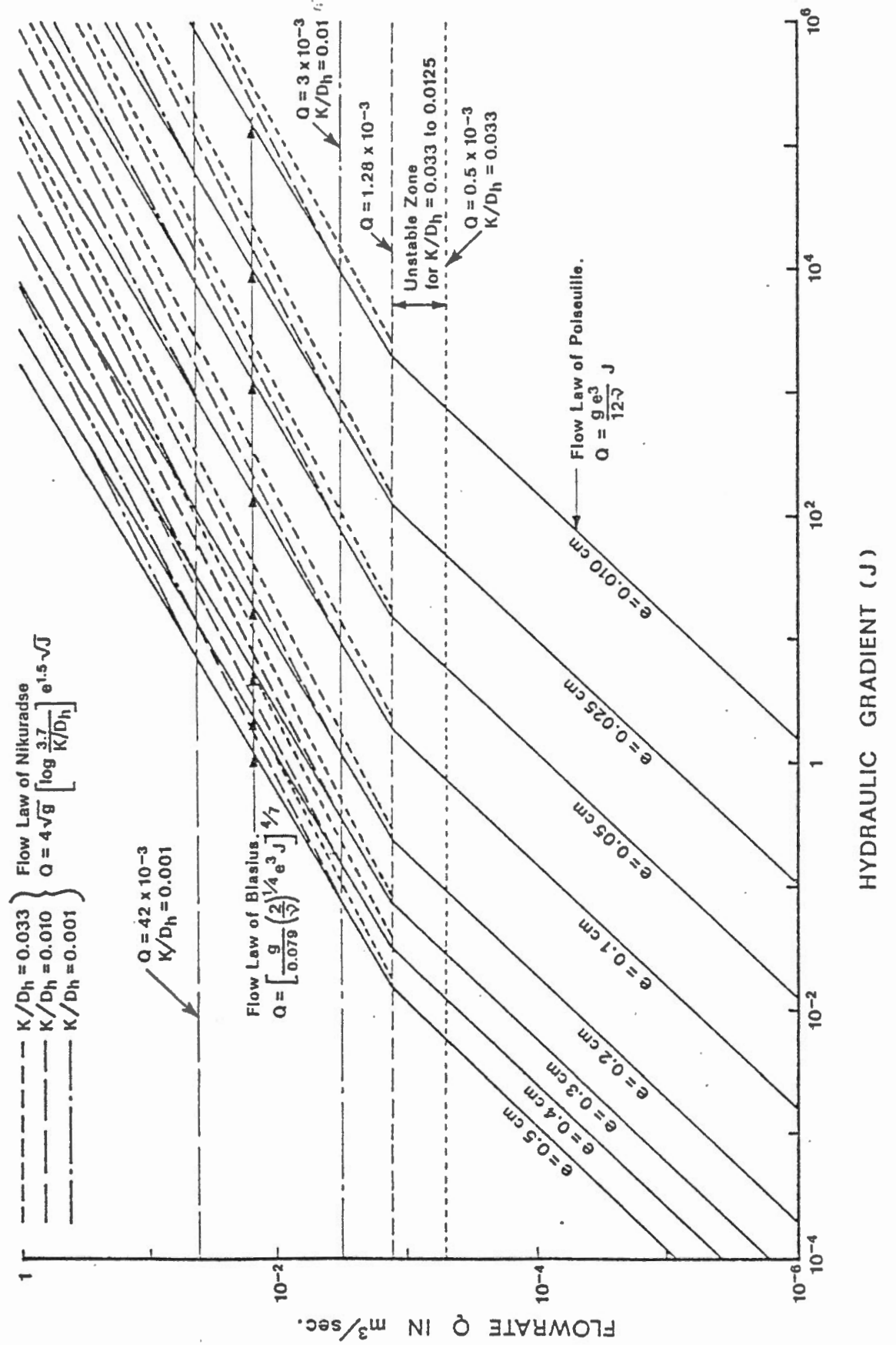

Figure 4.14 Discharge versus gradient for parallel flow.

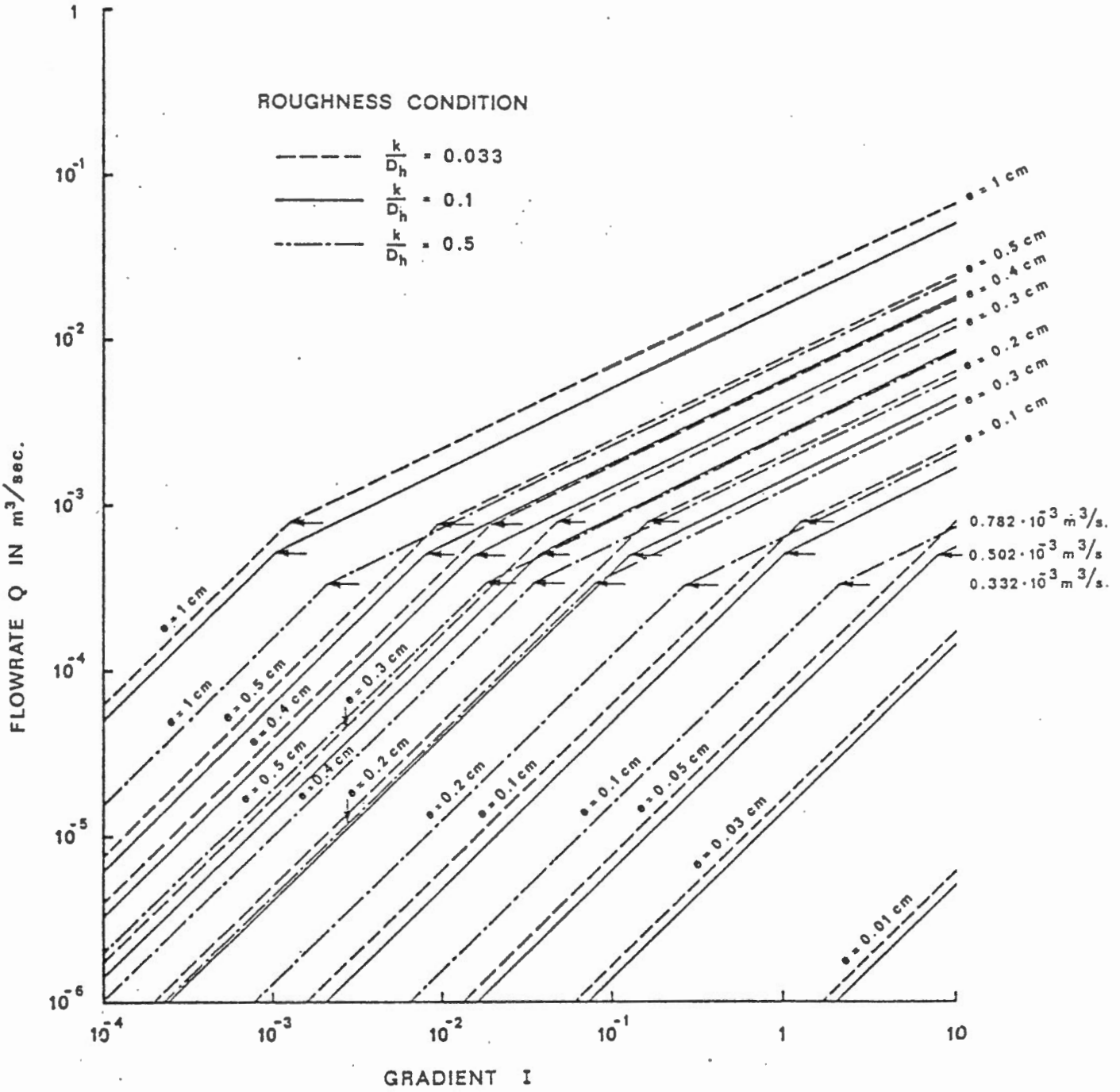

Figure 4.15 Discharge versus gradient for non-parallel flow.

a significant role in fracture flow. This question is beyond the scope of the present study and only laminar flow is considered.

For both parallel and non-parallel laminar flow conditions the relation between joint conductivity and fracture aperture is:

$$K_p \alpha e^2 \tag{4.24}$$

or for area permeability

$$K_p^* \alpha e^3 \tag{4.25}$$

For the remainder of this report we will refer to fracture conductivity.

It can easily be seen that a small change in fracture aperture can make a large difference on fracture conductivity and hence on flow rates and pressures. It is of interest then to consider intuitively what effects the fracture stress-deformation characteristics, discussed in section 4.2, might have on fracture flow. These effects depend on whether the deformation results from normal or shear deformation as:

(i) normal closure decreases the aperture in varying amounts depending on the load, normal stiffness, etc. and hence decreases q and/or increases the pressure magnitude.

(ii) normal tension opens the fracture but is not of practical interest since fractures are assumed not to be able to withstand tension.

(iii) non-dilatant shear should act the same as normal closure, the shearing displacement having no effect on conductivity.

(iv) dilatant shear:

(a) With vertical restraint the fracture may open slightly but will probably have minimal effect on conductivity.

(b) Without restraint the fracture may open by varying amounts depending on dilation angle, shear deformation, shear stiffness etc. This could radically alter the conductivity and hence also flow rates and/or pressures.

Any of the above factors may be beneficial or detrimental, depending on the engineering structure and geologic regions involved. In the remainder of this section we will evaluate the significance of the above factors in detail using simple models and in the next chapter will show the effect of some of these on a simulated full scale structure.

4.3.2 Effect of Normal Deformation on Fracture Conductivity

A typical normal stress-normal deformation curve was shown on Figure 4.3 and was discussed in detail in section 4.2.2. Since the fracture is assumed to show no strength in tension, only normal closure will be discussed with respect to fracture conductivity.

As noted previously the fracture conductivity is directly proportional to the square of the fracture aperture. Hence under normal closure we would expect a considerable decrease in permeability. Furthermore since the constitutive law for normal stress-normal deformation is highly non-linear we expect the conductivity to show at least as pronounced a non-linearity.

Several factors which affect the amount of closure and consequent change in conductivity are:

(i) magnitude of applied normal load .

(ii) stress history of fracture.

(iii) normal stiffness of fracture.

The effect of an increase in the applied normal load is to cause the fracture aperture to decrease. The actual amount of closure is dependent on both the previous stress history of the fracture and its initial normal stiffness. This may be more easily understood by referring to figure 4.3. The stress history dictates what level of initial stress is acting on the fracture. This in turn governs the starting point on the normal closure curve. If the fracture has only been subjected to low normal stress then the starting point will be on the upper flat or "soft" portion of the curve whereas if the insitu stresses are high the starting point will be on the steep "stiff" part of the curve. Larger deformations would be expected in the former than the latter case for the same applied load.

For any given fracture having a particular insitu stress and normal stiffness, increased load will lead to increased deformation. The increase in deformation will be non-linear and will have a maximum, being the maximum closure of the fracture. The load also has a limit, the compressive strength of the rock. As the fracture closes the fracture conductivity also decreases. An example of this for one particular fracture is shown on Figure 4.16.

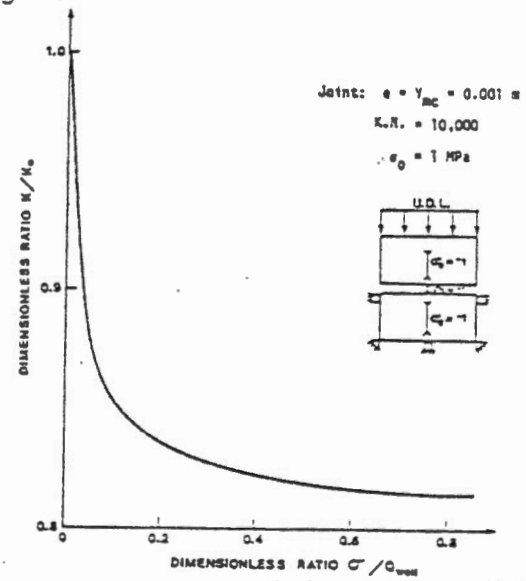

Figure 4.16 Change in Conductivity versus Normal Load

As can be seen, for this particular case, once the normal load reaches about 40% of the wall rock strength further changes in conductivity become negligible. Other fractures having different stress histories will show similar trends but the point at which conductivity changes become negligible and the absolute change in conductivity may vary. The data is plotted as dimensionless ratios showing the change in conductivity relative to the conductivity of the initial "rigid" fracture versus the applied load relative to the wall rock compressive strength.

The stress history of a fracture depends on the geologic processes to which it has been subjected. Laboratory experiments (Goodman (1976), Gale (1975), Iwai (1977) indicate that fractures subjected to cyclic normal loads show a stress hysteresis. Hence once a fracture has been subjected to load (e.g. from overburden) even though this load may be reduced (e.g. by erosion) the fracture stiffness will not decrease appreciably. The initial normal stiffness is dependent on the initial stress:

$$KN_o = \frac{\sigma_o^2}{v_{mc}\,\xi} \tag{4.26}$$

where
- σ_o = Initial stress $[ML^{-1}T^{-2}]$
- v_{mc} = maximum closure $[L]$
- ξ = seating load $[ML^{-1}T^{-2}]$

The variation of normal stiffness with insitu stress for various values of normal closure (assuming ξ = 0.1 in all cases) is shown in figure 4.17. As may be seen the normal stiffness can easily vary over one or two orders of magnitude for a given fracture depending on initial stress

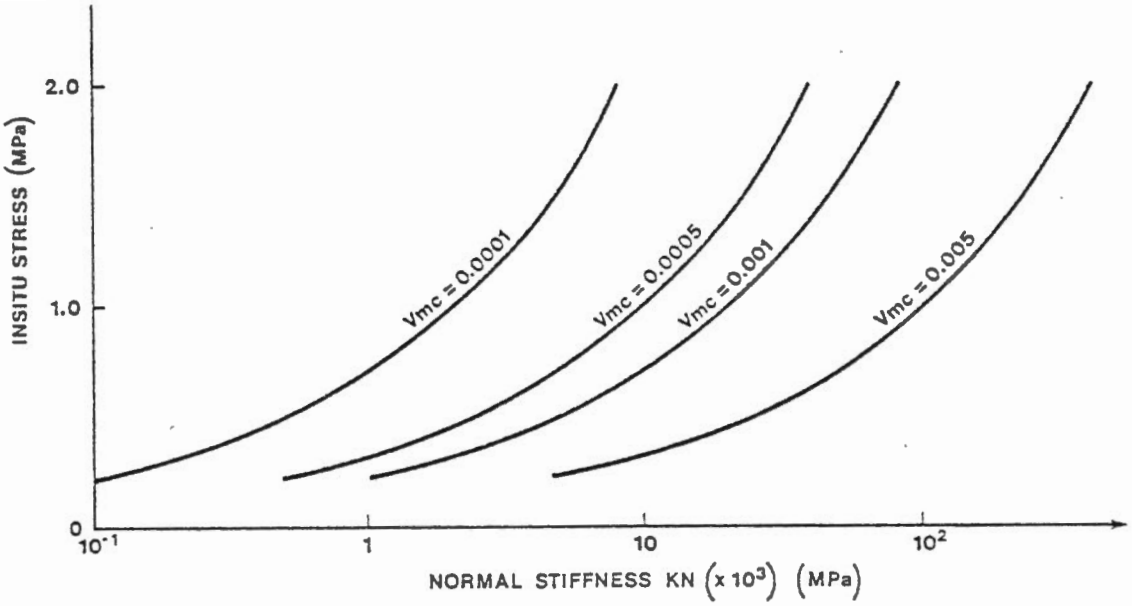

Figure 4.17 Variation of Normal Stiffness with Insitu Stress and Maximum Closure.

or for a given initial stress depending on the maximum closure (V_{mc}). As noted the initial stress depends on the geologic history and because of the loading hysteresis one would only imagine the most near surface and highly stress-relieved fractures to be on the flat portion of the loading curve. The maximum closure however depends mainly on the strength of the wall rock asperities. This depends on the lithology, degree of weathering or chemical alteration and the number of contact points (i.e. stress concentration on the asperities). The variation of conductivity with normal stiffness as V_{mc} is changed for a given fracture and normal load is shown on figure 4.18. As may be seen the change in conductivity for this case becomes negligible for normal stiffness of about 50,000 KN.

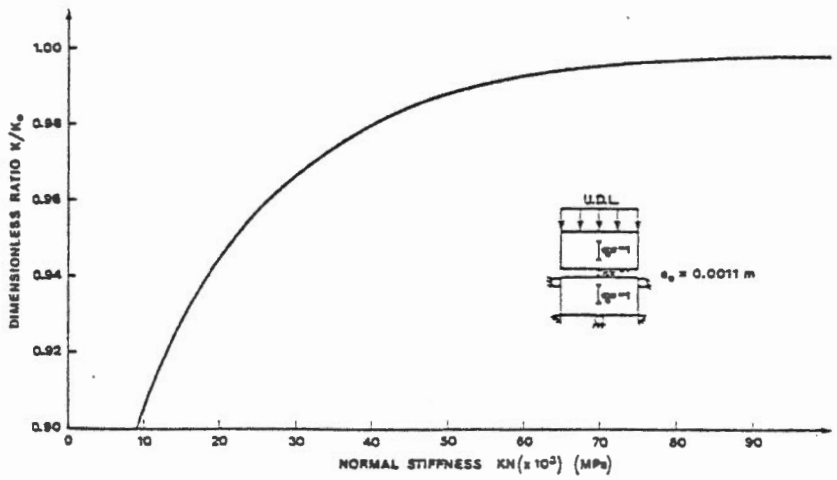

Figure 4.18 Change in Conductivity vs. Normal Stiffness

Normal stiffness is of course different for fractures with different initial apertures (e_o). However it is found that if such fractures are all loaded with the same normal load, the same percent change in conductivity occurs in each case (i.e. K/K_o = constant).

The relationship of normal closure and conductivity discussed above indicates that while normal loads might significantly reduce the conductivity of certain fracture sets below surface structures such as a dam where significant stress relief may have occurred, the effect around underground structures such as tunnels or cavities would be expected to be much less.

4.3.3 Effect of Shear Deformation on Fracture Conductivity

The shear stress - shear deformation characteristics of rock fractures, as discussed in section 4.2.2, are extremely important in practical rock engineering. However, from the viewpoint of fracture flow, since conductivity is proportional to the aperture squared, only those deformations directly affecting the magnitude of the fracture aperture are of interest. In shear stress - shear deformation behaviour two distinct categories must be evaluated: smooth (non-dilatant) and rough (dilatant) fractures.

a) Shear on Non-Dilatant Fractures

When a smooth fracture is sheared the two fracture planes are forced to slide past one another. Neither the shear stresses nor the shear deformations directly affect the magnitude of the fracture aperture.

However, in order to develop shear resistance a normal load is required. For the most simple case of a smooth fracture this may be expressed as:

$$\tau = \sigma \cdot \tan\phi \qquad (4.27)$$

where
- τ = maximum shear strength $[ML^{-1}T^{-2}]$
- σ = normal applied stress $[ML^{-1}T^{-2}]$
- ϕ = friction angle of the material.

Thus for fracture flow on smooth surfaces, the only critical parameter is the normal applied load. Consequently, the conductivity changes will be identical to those discussed in section 4.3.2. of this report.

b) Shear on Dilatant Fractures

The shear stress - shear deformation characteristics of rough (dilatant) fractures differs radically from that of non-dilatant fractures. As discussed previously two separate boundary conditions may occur:

(i) movement normal to the fracture plane is restrained

(ii) movement is not restrained and normal stress is kept constant.

In the first case, deformation normal to the fracture plane (aperture increasing), is restrained, leading to large increases in the normal stress across the fracture and, consequently, in peak shear strength. From the point of view of fracture flow this case differs markedly from the non-dilatant shear case. Even though the aperture does not increase, or increases only slightly such that the fracture conductivity essentially remains unchanged, in non-dilatant shear the aperture would have closed under the normal load, with a consequent decrease in conductivity. In the restrained case then the fracture system tends to act as a "rigid" system.

In the second case where movement normal to the fracture plane is not restrained very signficant changes in conductivity may occur. One of the first researchers to recognize the significance of dilation to conductivity was Maini, (1971). He performed a very simple shear test to determine what order of magnitude the effects might be. Maini used (0.125m x 0.125m) slabs of slate split along the cleavage with the two halves mounted in a plexiglass frame as shown on Figure 4.19. He then first measured the initial conductivity at zero shear displacement and then at 0.2 cm intervals. His results are shown on the same figure.

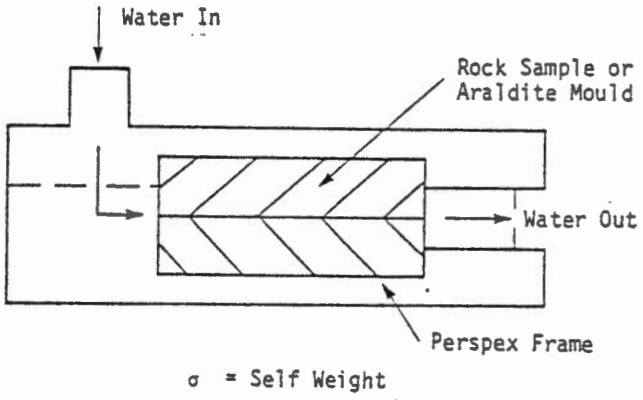

(a) EXPERIMENTAL APPARATUS

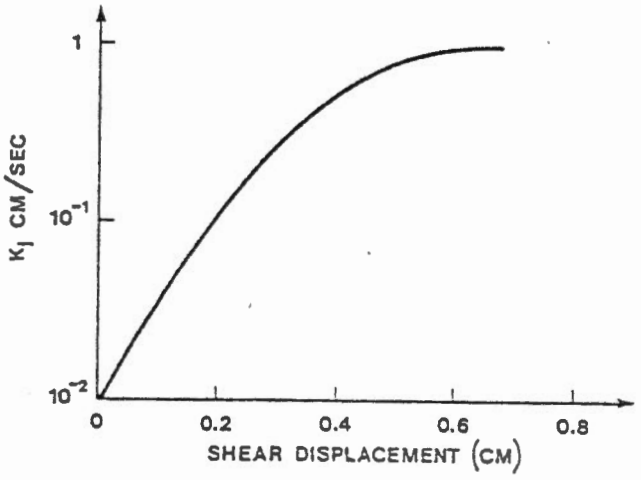

(b) EXPERIMENTAL RESULTS

Figure 4.19 Dilatancy versus fracture conductivity. (After Maini, 1971).

Maini suggests that this may be an important mechanism in fracture flow and that more controlled tests should be done. Concerning his own results he notes the following criticism:

(i) One expects the initial change in conductivity to be less since

(a) even at low σ, dilation will be less than at $\sigma = 0$,

(b) fines (gouge) developed during shearing might block the fissures and reduce the effective aperture.

(ii) higher increases in conductivity may be expected in hard rocks than in soft rocks.

Although the absolute conductivity values from Maini's experiment are not reliable the trends shown are very interesting.

As noted previously (section 4.2.2) the dilatant shear criteria proposed by Ladanyi and Archambault was used in the numerical model for this research. This model then coupled with the fracture flow model, was used to predict conductivity changes associated with dilatant shear.

The model presupposes a rather straightforward coupling of dilatancy and conductivity which has not been reliably tested in the laboratory. However until detailed controlled laboratory testing of the phenomenon has been done this is the only model available. The data presented is in no way meant to be interpreted as exact or final. It is merely presented to demonstrate the trends that might be expected in nature and the relative importance of the various parameters involved.

The model was found to be extremely sensitive to data input and cases with numerical instabilities were quite common. Some of these

could be attributed to incompatible data, however others appear to be related to the dilatancy formulation itself. During the course of the study it became very apparent that a great deal more research into many aspects of the dilatant behaviour of fractures is required.

In order to attempt to obtain compatible data the input parameters were selected based on the work done by Barton (1971). The dilatancy angles were selected from the graph shown on figure 4.9 while shear stiffness values were selected from figure 4.12. The data is presented in the form of dimensionless ratios as much as possible such that relative changes rather than absolute numbers will predominate.

Figures 4.20 through 4.24 present the results of a parametric study of the dilatancy - conductivity relationship. In each graph the ordinate represents a dimensionless ratio of the final permeability after shear displacement to the original conductivity of the undeformed rigid fractures. The abscissa represent dimensionless ratios of various other parameters such as shear stress, normal load, etc. In all cases the shear stress was kept below the shear strength since it is the potential change in fracture flow characteristics prior to failure that are of most interest.

Figures 4.21 and 4.22 show the change in conductivity associated with increasing shear stress. In figure 4.21 the ratio of σ/Q_u is about .07, hence low normal stress. The initial fracture aperture was 0.5 mm. The fracture then represents a very stiff joint with strong unaltered wall rock. At low normal stress one would expect significant dilation. The conductivity changes are plotted for dilatancy angles of 5, 10 and 15 degrees. Relative roughness (k/D_h)

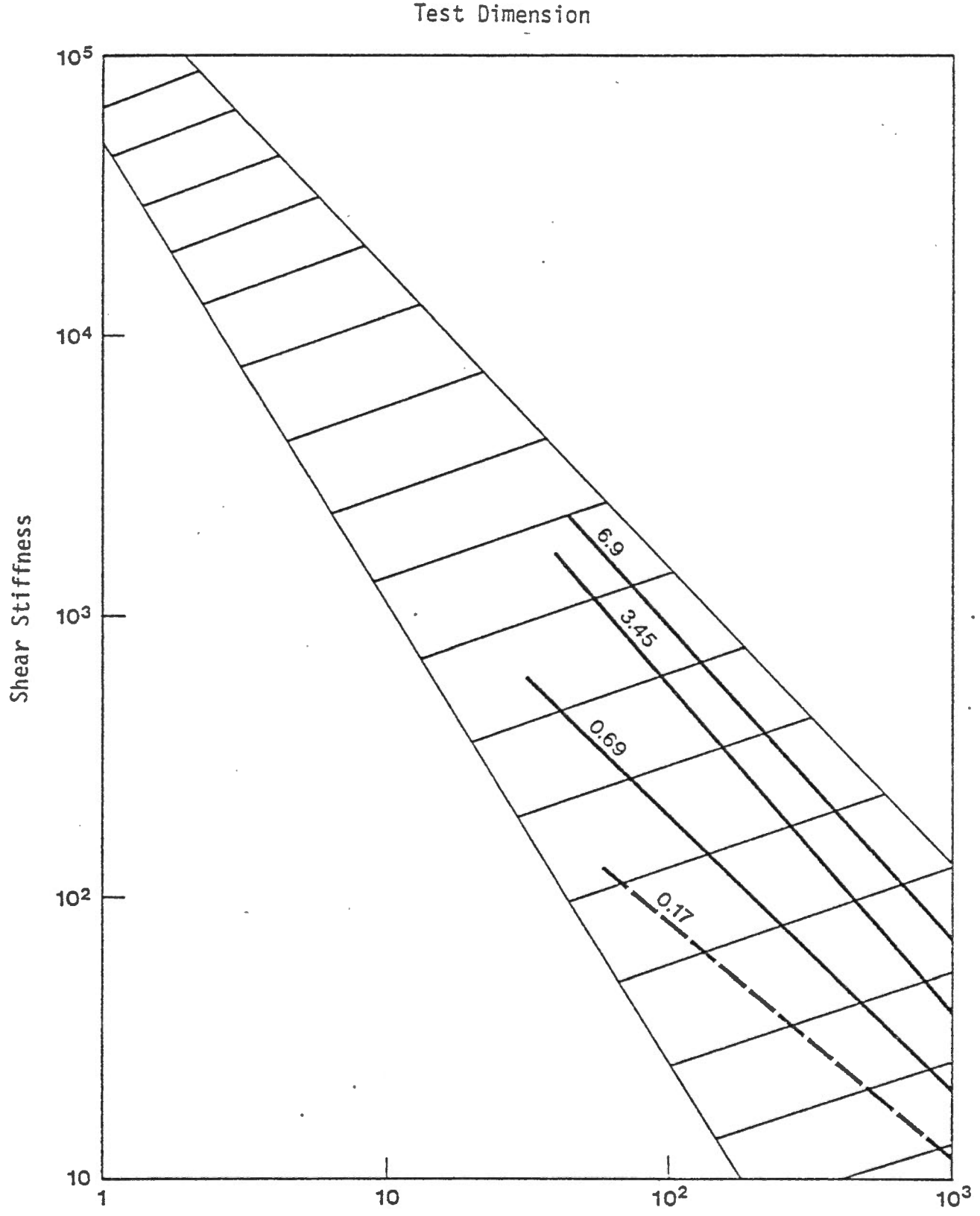

Figure 4.20 Joint Shear Stiffness as a Function of the Square Root of the Loaded Area (L) and the Normal Stress (0.17, 0.69, 3.45 and 6.9 MPa Lines Given) (Barton, 1972)

Figure 4.21 Normalized Dilatant Shear versus Normalized Conductivity

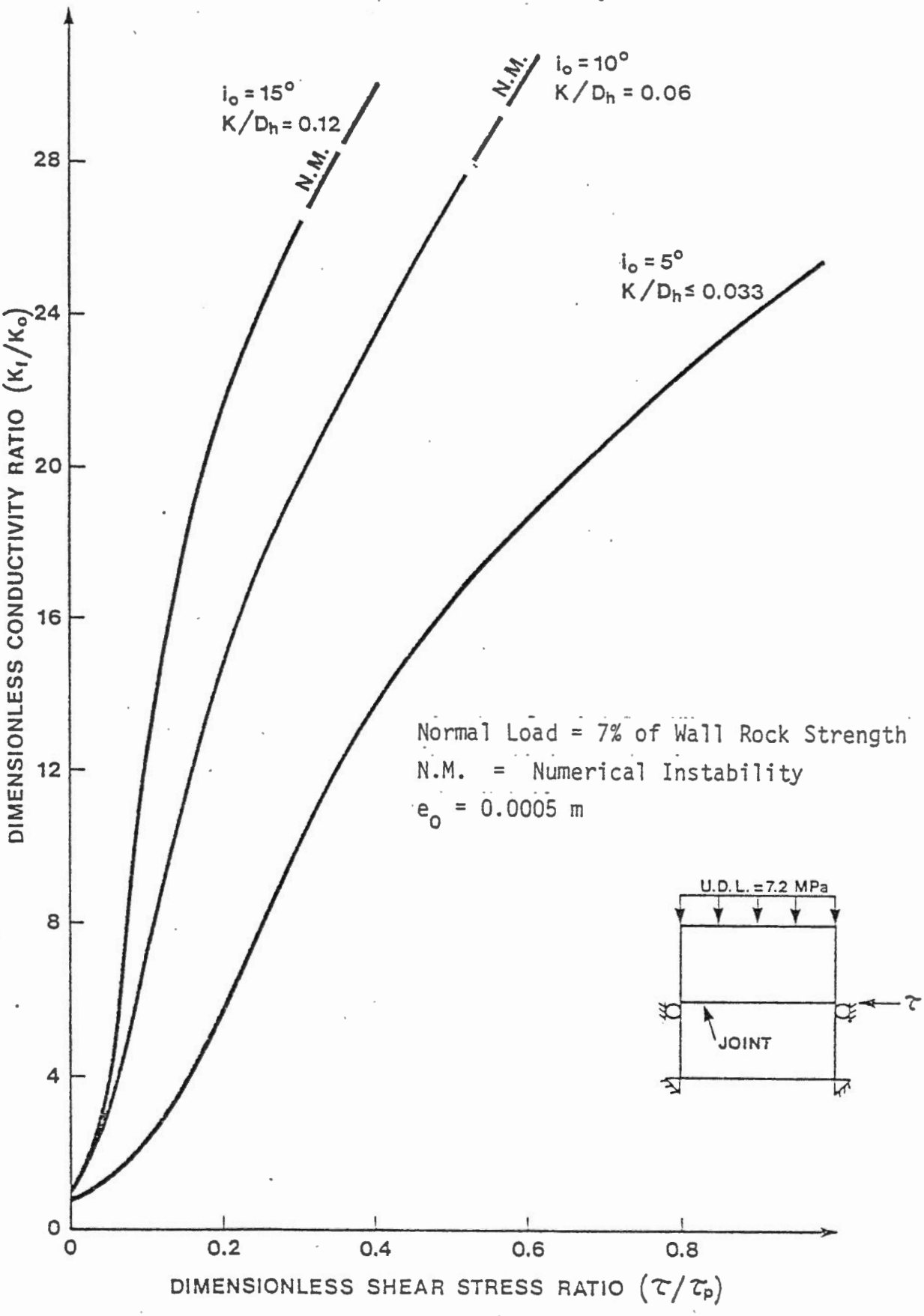

values of .06 and .12 were assigned for 10 and 15 degree dilatancy angles respectively. As may be seen enormous conductivity changes could be expected under these conditions and at the higher values of dilatancy angle (i_o) these changes occur at very low shear stresses.

Figure 4.22 shows the relative conductivity changes associated with shear of a softer fracture under higher normal load (σ/Q_u = .18) for a dilatancy of 5 degrees. Comparison of the two graphs proves that small changes in normal load and fracture stiffness may exhibit a remarkable influence on fracture conductivity; the relative conductivity change at τ/τ_p of 0.5 of the former case being four times as great as in the latter.

Figure 4.23 represents the effect of normal stress on the conductivity ratio for a dilatant ($i_o=5^o$) fracture using the shear stiffness as as parameter. It can easily be seen that increasing normal stress rapidly eliminates conductivity increases associated with dilatancy. From the data there also appears to be a definite limit in the normal stress beyond which dilatancy effects are completely overidden. It should be noted that for higher values of the dilatancy angle, i_o higher normal stress levels would be required to suppress dilatancy.

Figure 4.23 also shows that changing the shear stiffness of the fracture radically alters the relative change in conductivity. This is to be expected. Since, in the elastic range, the shear deformation is given by

$$u = \tau / K.S \qquad (4.28)$$

Figure 4.22 Normalized Conductivity versus Shear Stress

$\sigma/Q_u = 0.18$, $V_{mc} = 0.001$, $i_o = 5^o$

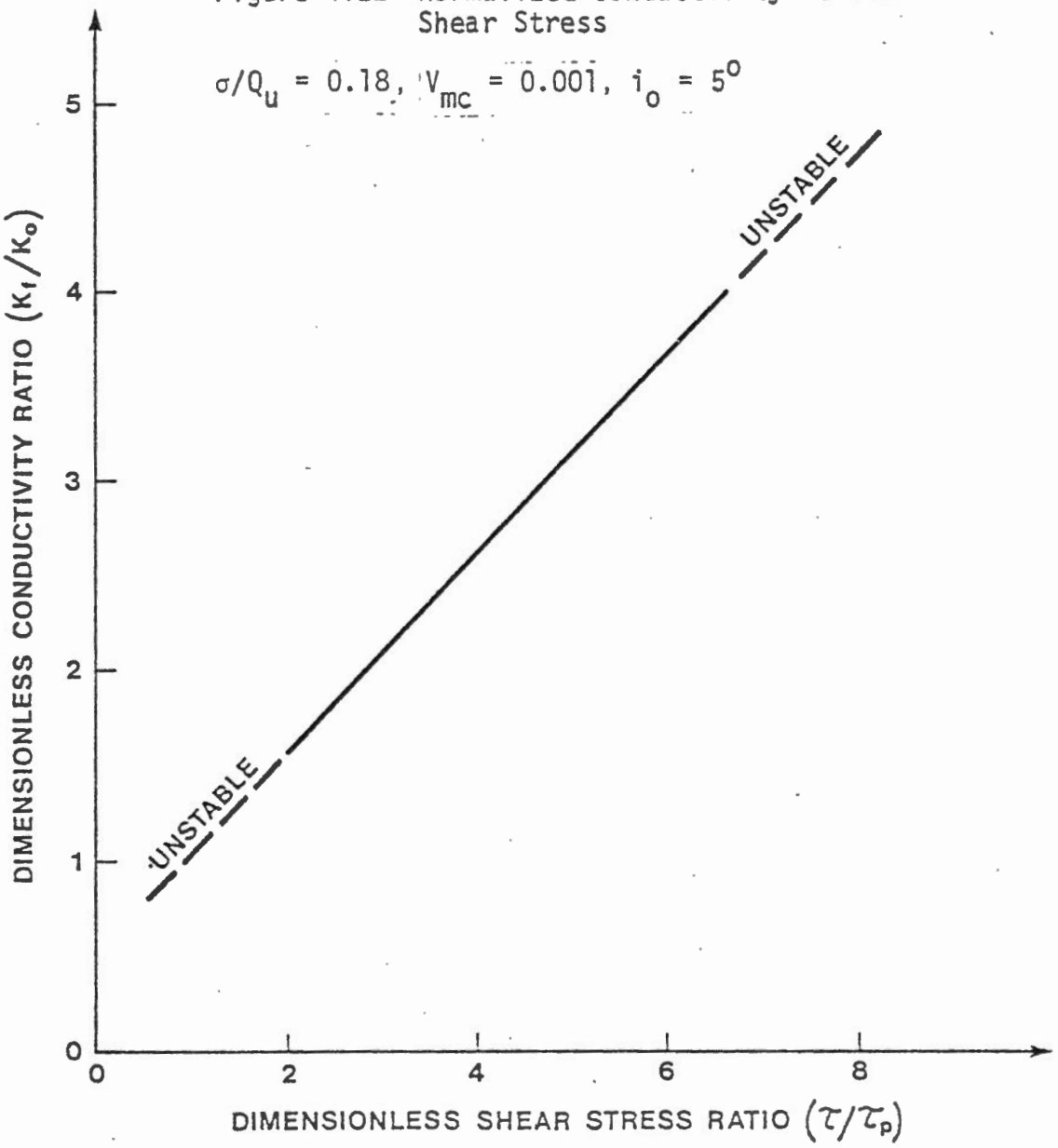

Figure 4.23 Normalized Conductivity versus Normal Stress - Influence of Shear Stiffness

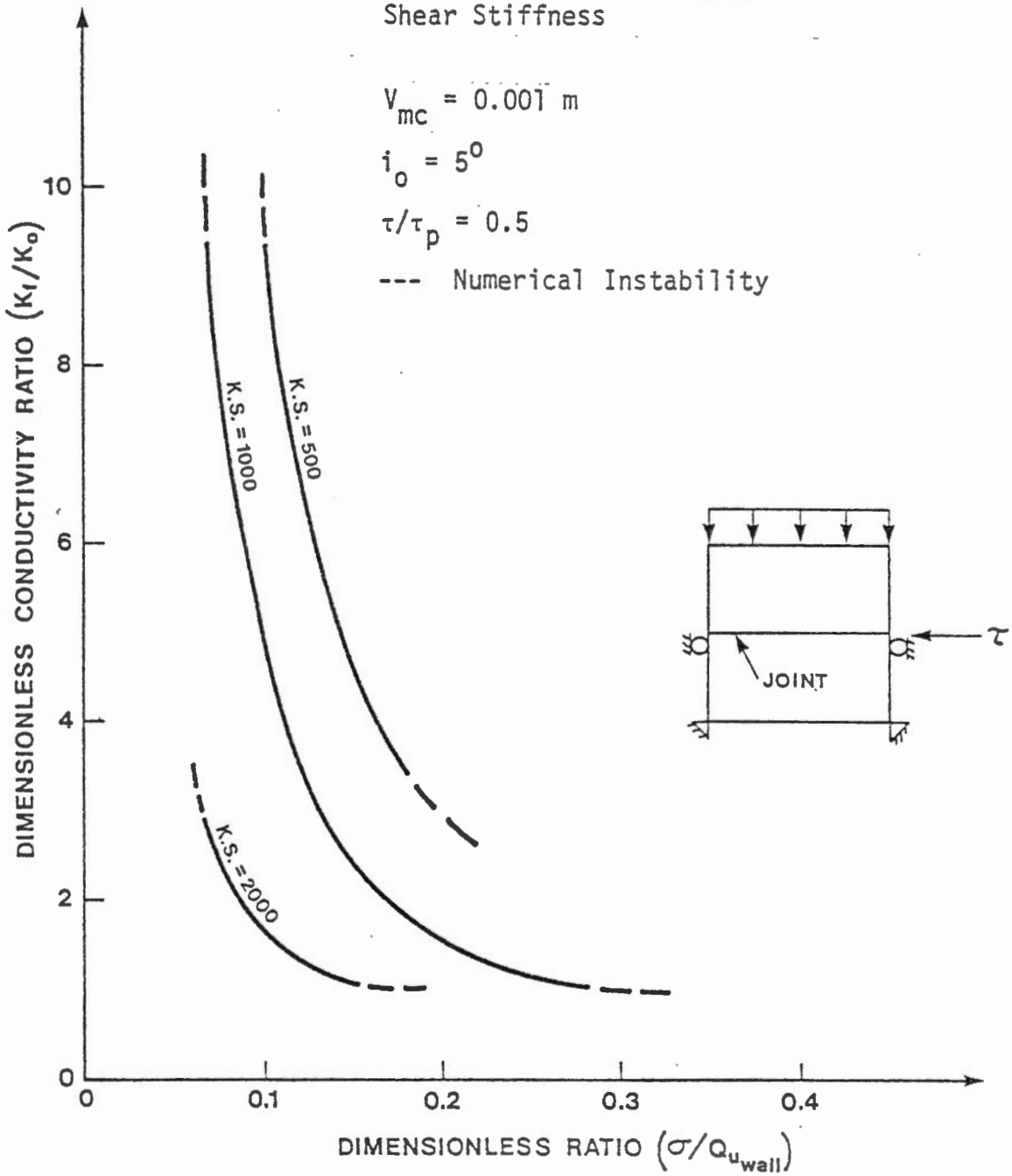

Hence as the shear stiffness increases the shear displacement decreases and, consequently, the associated normal displacement and conductivity decrease.

Figure 4.24 shows a similar plot except for the fact that the normal stiffness of the fracture is used as the parameter. This data indicates that for given normal and shear stresses, increasing the normal stiffness may significantly increase the conductivity ratio. This data is easily understood if one recalls that for a given normal load increasing the normal stiffness will decrease the normal deformation (closure), enabling it to mask the conductivity changes due to dilatancy.

Figure 4.25 shows the conductivity changes associated with changing shear stiffness using the dimensionless ratio σ/Q_u as a parameter. As would be expected from earlier results increasing the shear stiffness decreases the change in conductivity. Interestingly there appears to be a cut-off where, for a particular dilatancy angle and shear stress, the shear stiffness is so great that conductivity changes associated with that shear stress are negligible. As before, for high values the dilatancy angle i_o this cut-off shear stiffness would obviously be larger. The dimensionless parameter σ/Q_u simply indicates that for a given shear stiffness, dilatancy angle and shear stress, increasing the normal load will decrease the associated conductivity change as would be expected from the preceeding data.

In summary,

(i) at low σ, dilatancy may greatly increase K.

(ii) increasing normal load and/or shear stiffness will decrease the associated conductivity change.

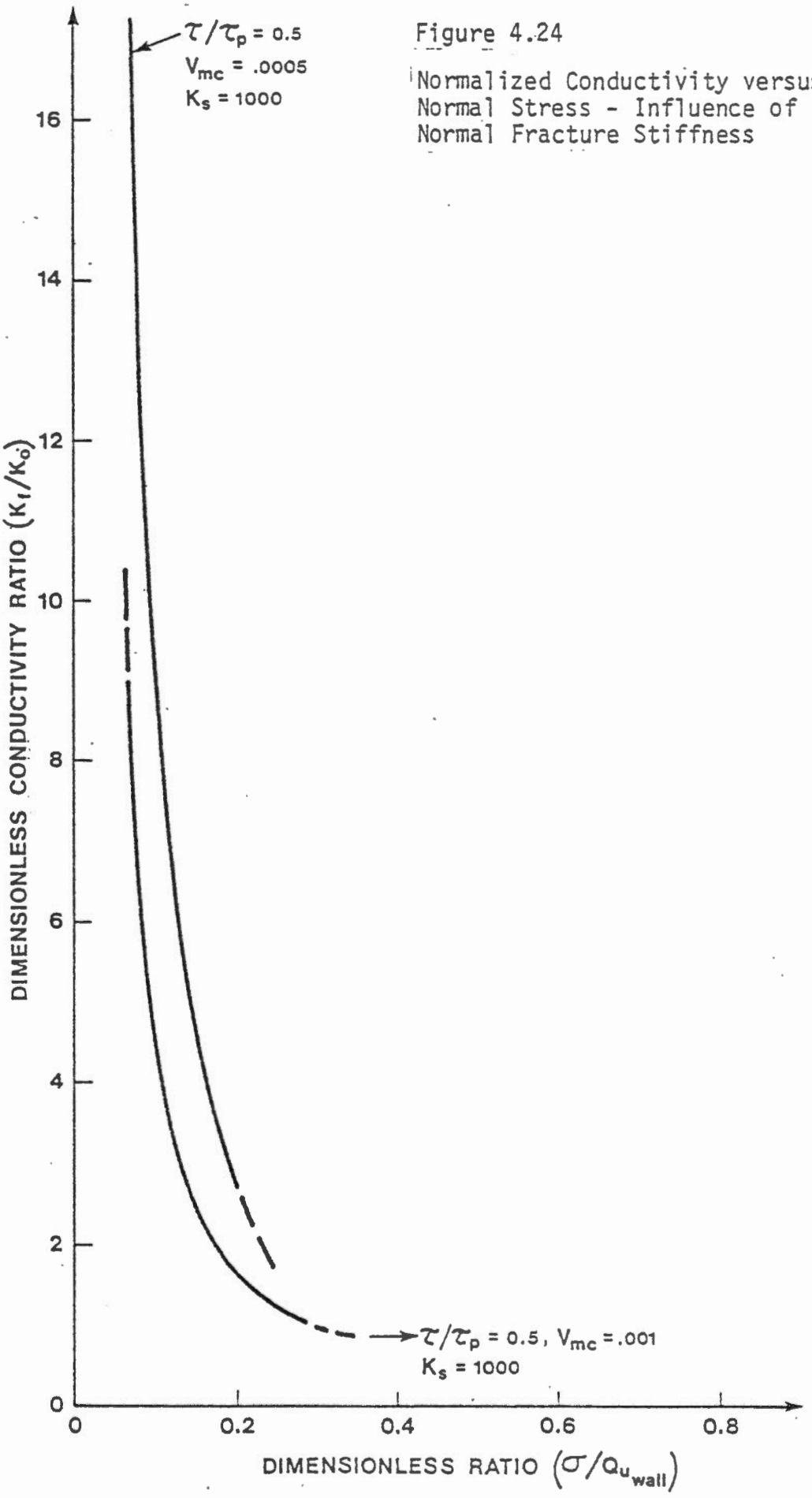

Figure 4.24

Normalized Conductivity versus Normal Stress - Influence of Normal Fracture Stiffness

Figure 4.25 Normalized Conductivity versus Shear Stiffness - Influence of σ/Q_u

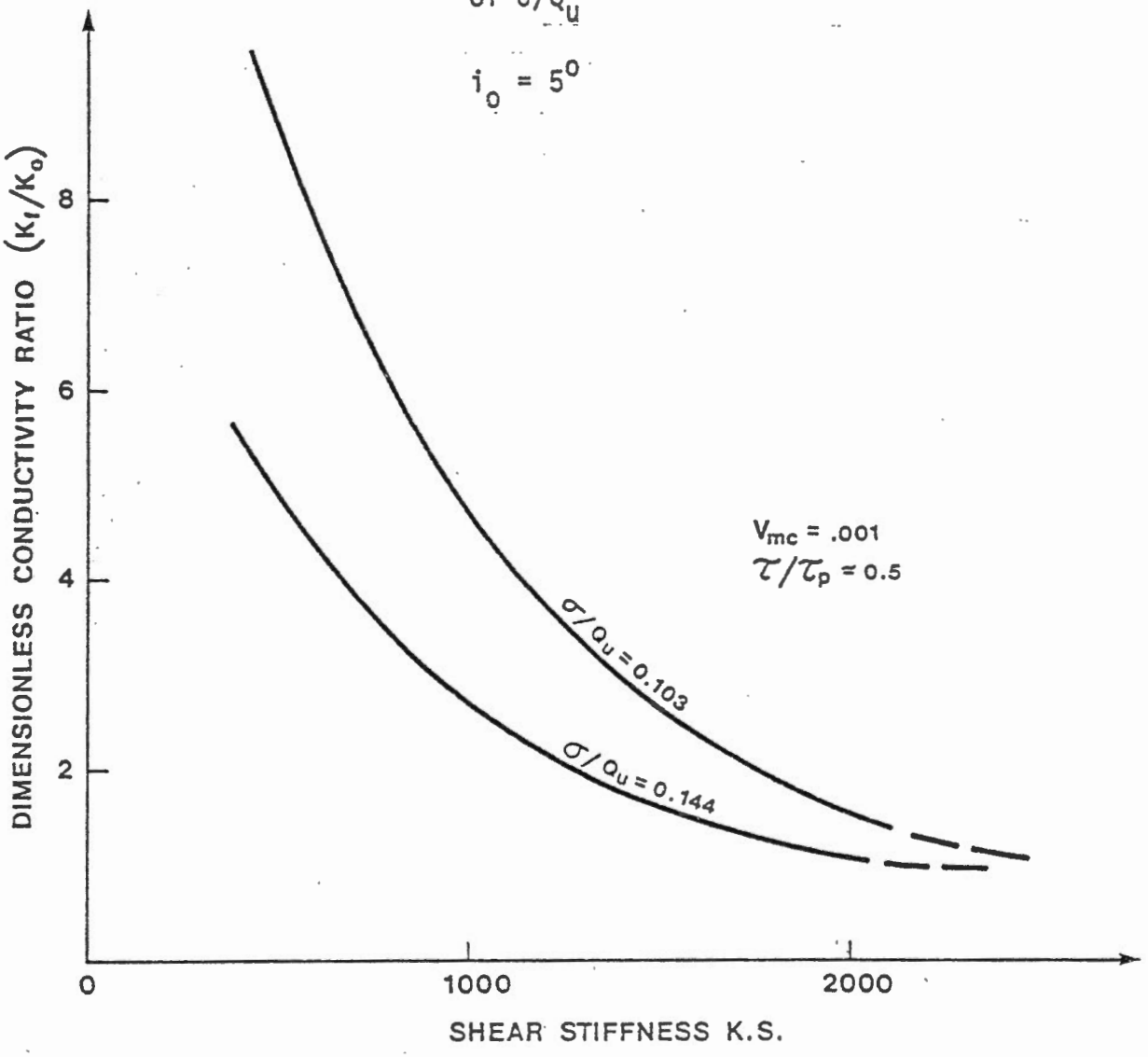

(iii) increasing the fracture normal stiffness will increase the associated conductivity change.

The conductivity changes associated with dilatant shear as described above might be of importance to many rock engineering problems. Fracture conductivity changes for example in rock slopes due to shear movement might be extremely significant to the long term slope stability. Similarly in dam foundations and abutments conditions could be altered from the assumed design condition due to shear loads transmitted from the structure. In underground storage caverns rock movement into the cavern if occurring as shear movement along fracture planes could alter the conductivities around the cavern in such a way as to be detrimental to its storage capability.

As mentioned previously the model used for this research is an extension of existing discrete fracture flow models and has yet to be experimentally verified. Convergence was very slow for most rough fractures. Although some of the convergence problems may be due to incompatible data it is the authors belief that much of the problem lies in the dilatancy formulation itself. Because of the potential significance of this problem to general rock engineering considerable research into dilatancy and the dilatancy-conductivity relationship is warranted in the immediate future.

CHAPTER V

LARGE TEST CASES

5.1 Generalities

The ultimate goal of any numerical modelling is to simulate full scale practical field situations. The present development was used to simulate two different configurations: a dam founded on a rock wedge bounded by two discontinuities and a tunnel intersecting horizontal fractures.

The main problems encountered in testing these examples were numerical instabilities associated with joint dilatancy as well as the rapidly escalating cost and computer storage requirements as additional fractures were considered.

The two large scale examples discussed below were highly idealized, especially with respect to the number of fractures. Therefore, they should be primarily regarded as illustrations of the potential of this technique for sophisticated in situ modelling rather than within the quantitative context.

5.2 Dam Stability

The first example, shown on figure 5.1, models a thin concrete arch dam founded on a bedrock wedge bounded by two intersecting fractures labelled joints 1 and 2 respectively. The fractures forming the wedge are hydraulically connected to the full reservoir head and the wedge is subjected to the full loading from the dam and reservoir.

Figure 5.2 shows a schematic of the fracture deformation around the wedge for the case where the initial apertures of both joints

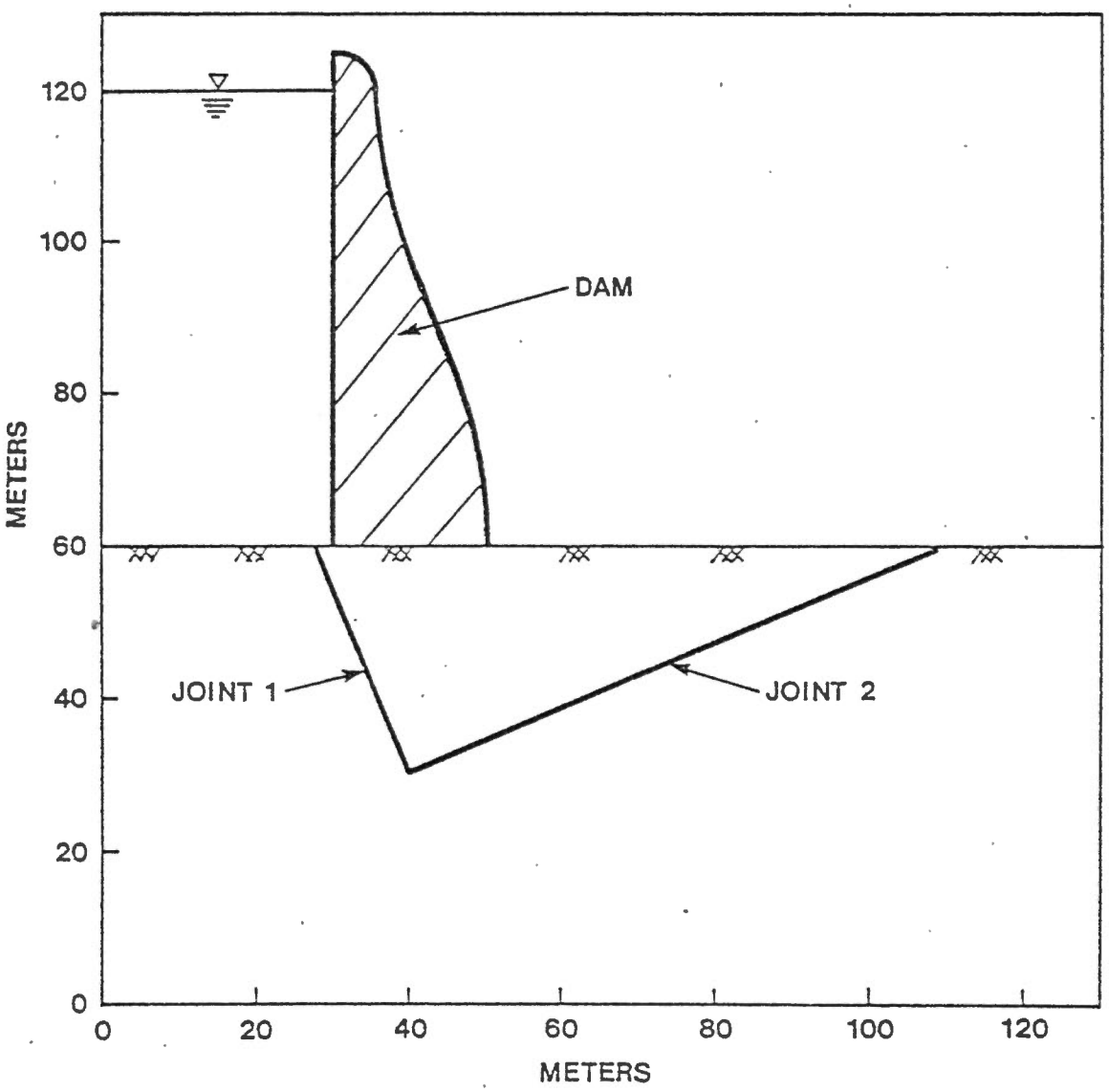

FIGURE 5.1 THIN DAM ON JOINT WEDGE

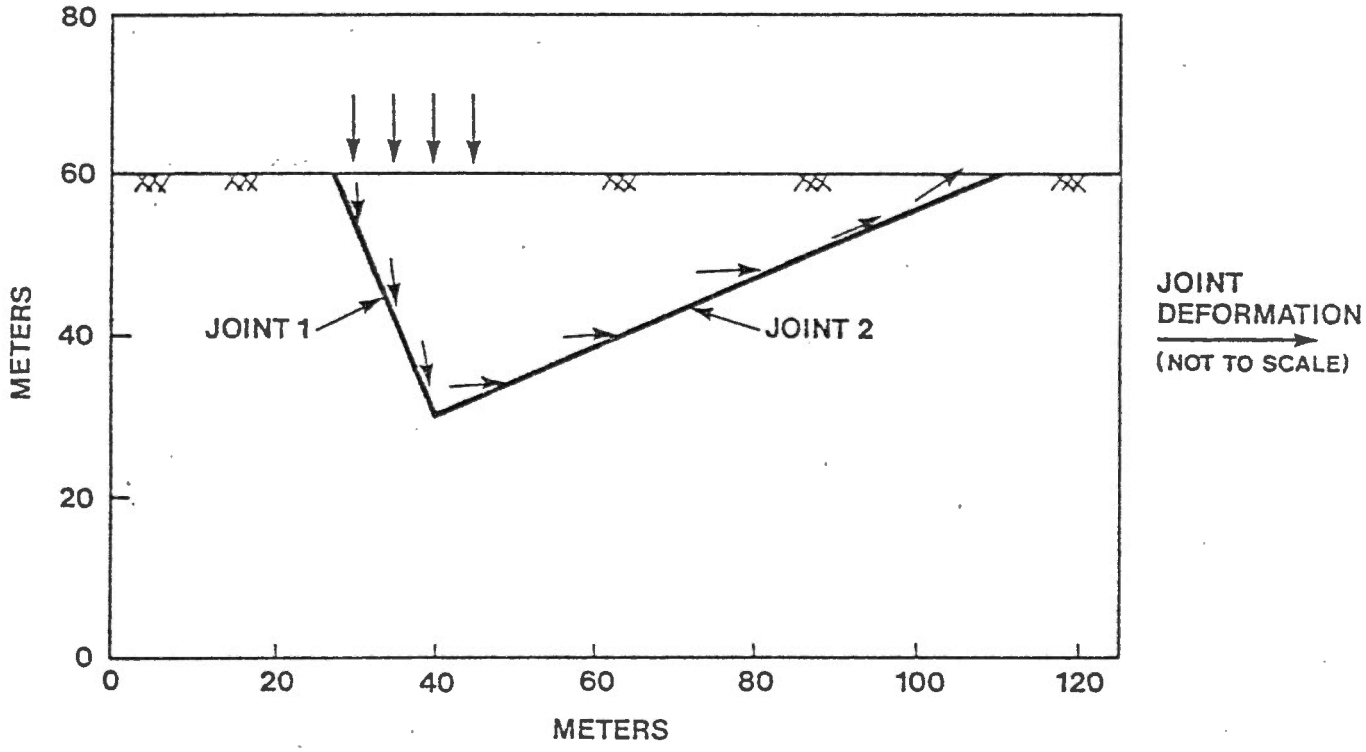

FIGURE 5.2 GENERALIZED DEFORMATION OF JOINT WEDGE UNDER DAM AND HYDRAULIC LOADING

1 and 2 are equal. Similar trends were encountered in all other computer runs. The dam load tends to put joint 1 under a high shear load. This load, with the given fracture configuration, then tends to rotate the complete wedge counter-clockwise. Joint 1 and the lower half of joint 2 close in response to the normal load while the wedge rotation opens the downstream half of joint 2 slightly.

Figures 5.3 and 5.4 show the hydraulic potential along the two fractures below the dam for various initial aperture conditions and the changes in potential due to the particular loading conditions of this example. The boundary head conditions were set at 120 and 60 meters at the upstream and downstream extremities of the wedge respectively.

In figure 5.3 both joints were assigned the same initial aperture. The potential distribution for the rigid fracture assumption is shown by curve 'H_o', while the final potential distribution following fracture deformation is given by curve 'H_f'. The effect of fracture deformation on the fluid potential in this case has been minimal. Closure of joint 1 while opening of the toe of fracture 2 has led to a slightly more significant potential drop across the downstream portion of joint 2.

Figure 5.4 shows the effect of varying initial fracture aperture for both the rigid and deformed cases. Curve 1 shows the case where fracture aperture 1 is set at about one half fracture aperture 2 and curve two vice-versa. As shown on figure 5.4 the effect of initial aperture on the potential distribution greatly exceeds any deformation effect. In curve 1, where $e_{o,1} \ll e_{o,2}$, almost the total head loss occurs in joint 1 and the effect of fracture deformation on the

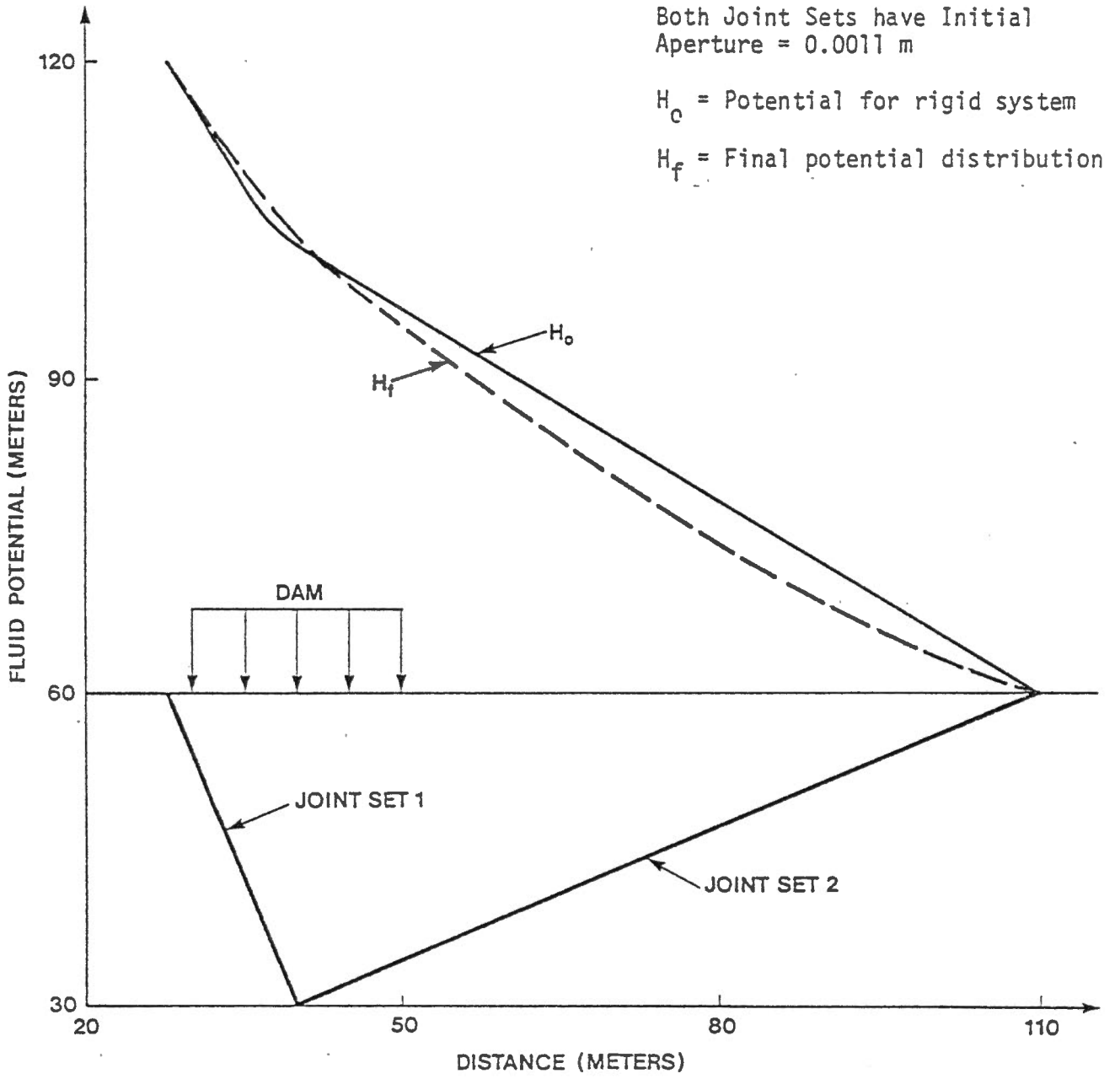

FIGURE 5.3 HYDRAULIC POTENTIAL ALONG JOINT SETS 1 and 2

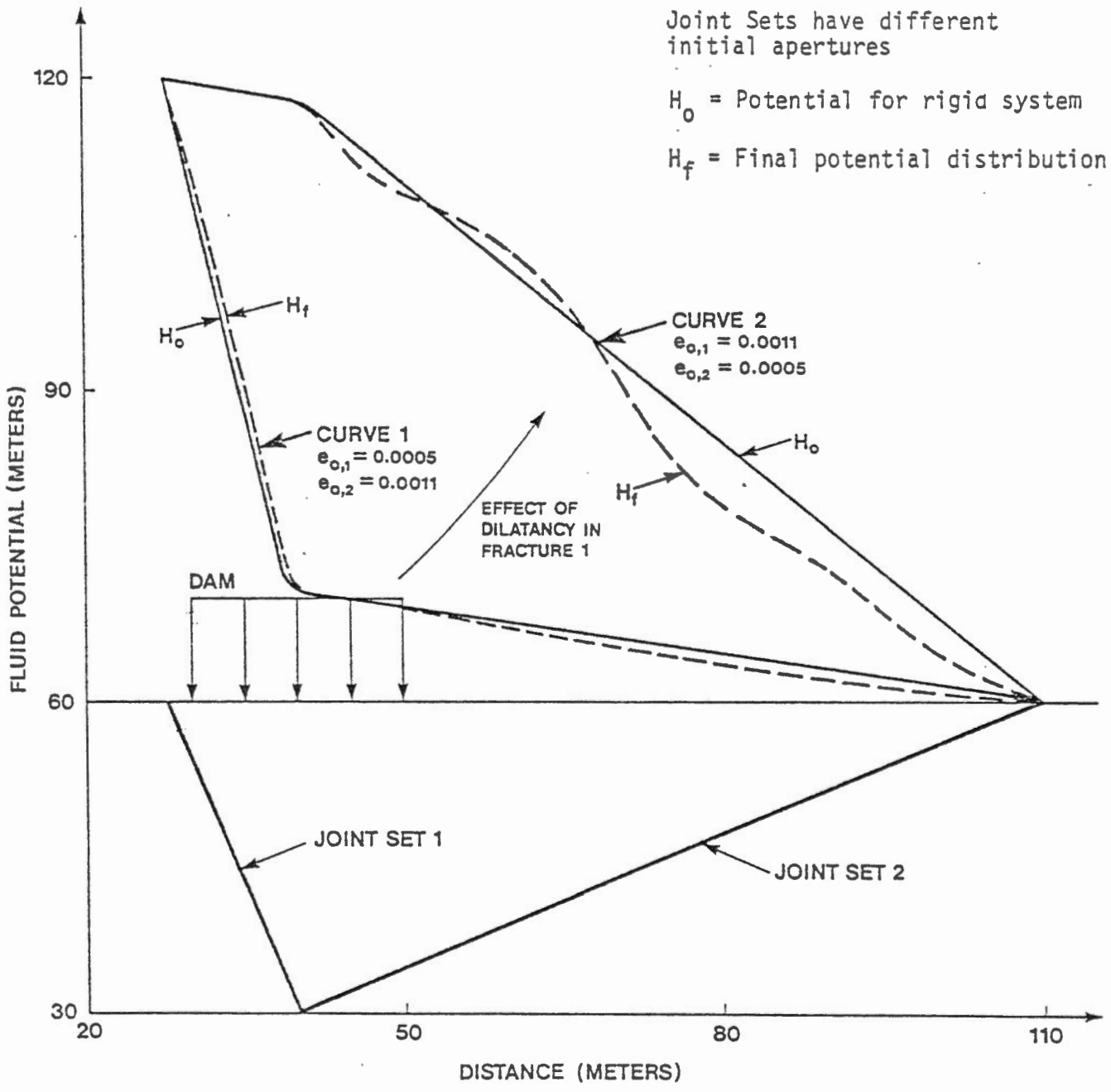

FIGURE 5.4 HYDRAULIC POTENTIAL ALONG JOINT SETS 1 and 2

potential distribution is negligible. The uplift forces on the wedge in this case are very small and hence should have minimal effect on the stability.

In curve 2, $e_{o,1} >> e_{o,2}$, most of the head loss occurs across joint 2, the uplift pressures on the wedge are very high and thus detrimental to overall stability. The rotational motion of the wedge and subsequent opening of joint 2 leads to a small decrease in potential on the downstream portion of the wedge, hence helping to stabilize the structure.

The relatively minor effect of fracture deformation on the fluid potential in this example would be anticipated from the parametric analysis discussed earlier. The initial apertures are both small and hence their normal stiffness is high. This will tend to minimize the normal deformation. Furthermore the highest loading, from the dam, is applied to joint 1 primarily as a shear load, thus having a minimal effect on normal deformation.

It is of interest however to consider the effect of the shear loading discussed previously for the case where joint 1 is dilatant. In this case the shear deformation would tend to open joint 1 causing the pressure distribution given by curve 1 to shift towards curve 2. This effect would, of course, be detrimental to the dam stability.

The total flowrate below the structure is also governed by the fracture aperture distribution. Figure 5.5 shows the variation of the dimensionless flow ratio with variation of the aperture ratio for joints 1 and 2, (e_1/e_2). As shown, the flow quantity increases as e_1 increases with respect to e_2. Referring back to figure 5.4,

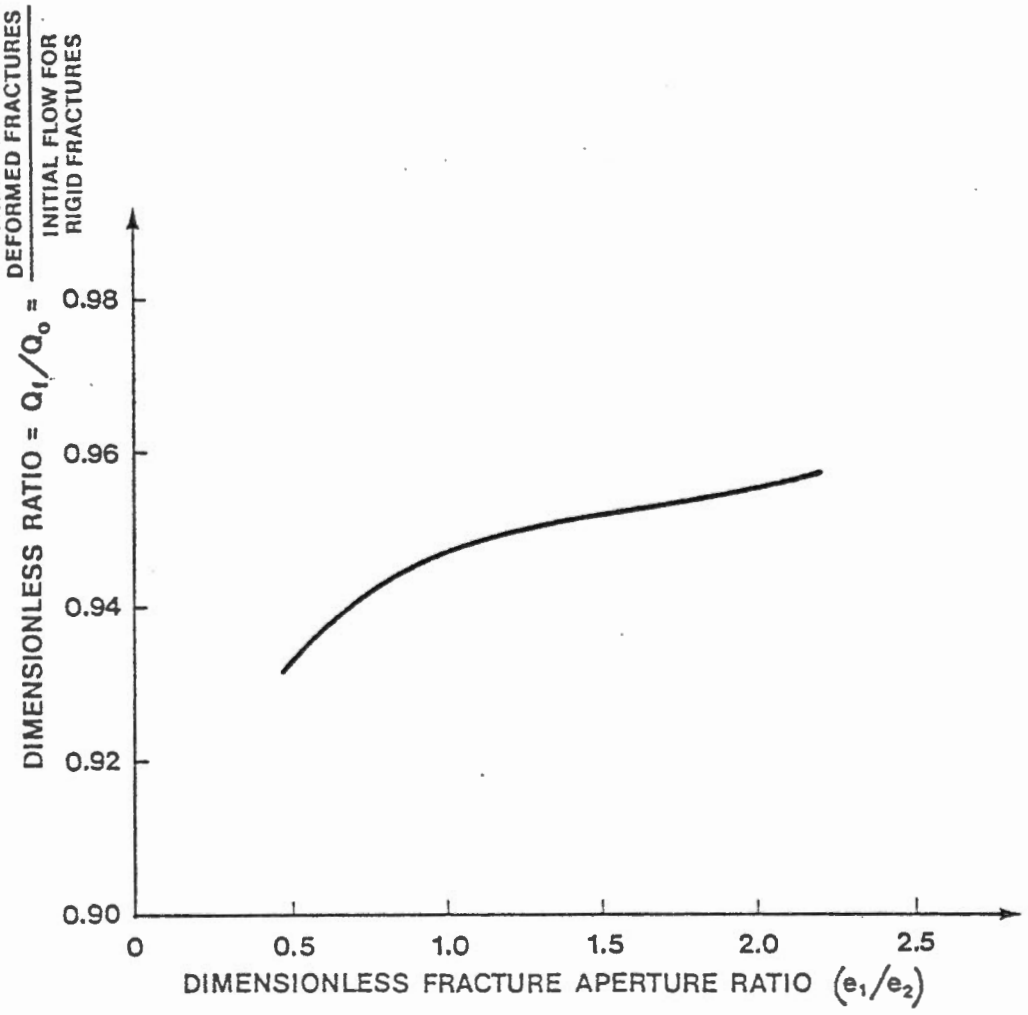

FIGURE 5.5

DIMENSIONLESS FRACTURE APERTURE VERSUS DIMENSIONLESS FLOW RATIO

the reason for this becomes obvious. When $e_1 >> e_2$ very little head loss occurs through joint 1. This increases the effective gradient across joint 2 and hence increases the flowrate following the already established relationship:

$$q_i = K_p \cdot J \quad .$$

The results discussed above indicate a much higher factor of safety for the case corresponding to curve 1 than for the one associated with curve 2. The practical implication of this is that the factor of safety could be significantly increased by grouting joint one and hence shifting the potential distribution curve toward curve 1, assuming both joints had equal aperture originally (figure 5.4). The stability could be further enhanced by providing drainage for joint 2 downstream of the dam which further reduces the uplift pressure in that particular joint. This would essentially annihilate the rotational component applied to the rock wedge.

This example then demonstrates the important effects that fracture aperture and orientation may exert on dam stability. It further shows that standard remedial measures such as grouting and drainage, even when only partially effective, may be a significant aid in stabilization.

As noted however, minor geological details, such as dilatancy in a critical fracture set, may completely alter the analysis. It is hence most critical that very detailed surface, subsurface and laboratory analyses be carried out prior to any comprehensive stability analysis.

5.3 Flow into Tunnel Through Horizontal Fractures

The second example, shown on Figure 5.6, models a 55 meter deep tunnel intersected by a single horizontal fracture. For the initial tests the hydraulic boundary conditions were set as potentials; namely 110 meters remote from the tunnel and at the level of the fracture at 55 meters, at the tunnel wall.

Initially, gravity body loads were applied; the resultant normal stresses and final apertures are shown on Figure 5.7. The normal load across the fracture is, of course, the same as the tangential stress around the tunnel and therefore is affected by the stress concentration due to the tunnel excavation. The resultant fracture deformation follows the same trend as the stresses as would be expected, the maximum fracture closure occurring adjacent to the tunnel wall. Consequently, when the hydraulic boundary conditions are fixed, the fracture conductivity at the tunnel entrance will govern the water inflow. For this particular example the flowrate into the tunnel following deformation of the fracture is only 56% of the flowrate if rigid fractures would be assumed. Although this example includes only one horizontal fracture intersecting the tunnel, basically the same results would be expected for any number of fractures since the stress concentration is uniform around the excavation (i.e. each fracture contributing to identical reduction). Underground structures with shapes other than circular would of course create different stress concentration patterns that might affect fracture deformation quite differently. In light of this, a test was run with the same total load but varying the shape of the stress concentration, e.g. triangular and

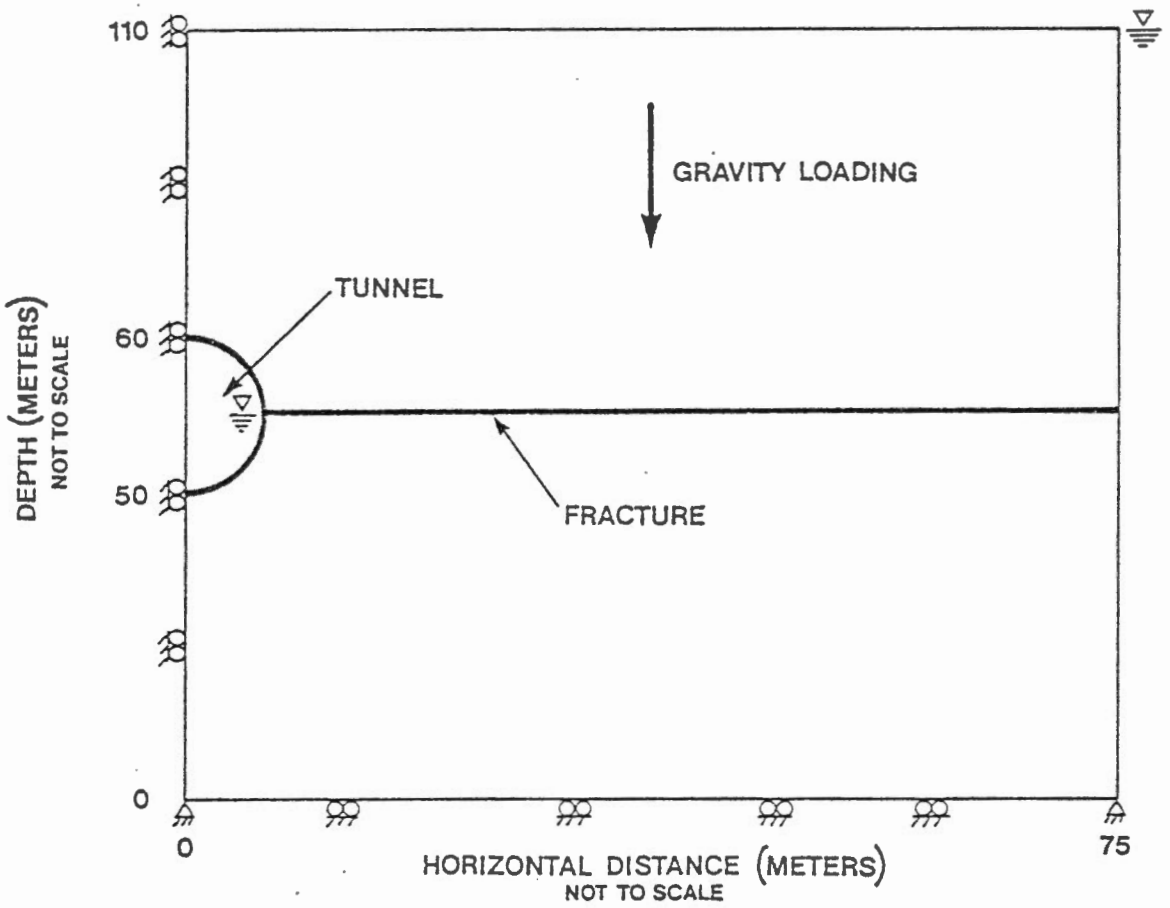

FIGURE 5.6 TUNNEL WITH HORIZONTAL FRACTURE

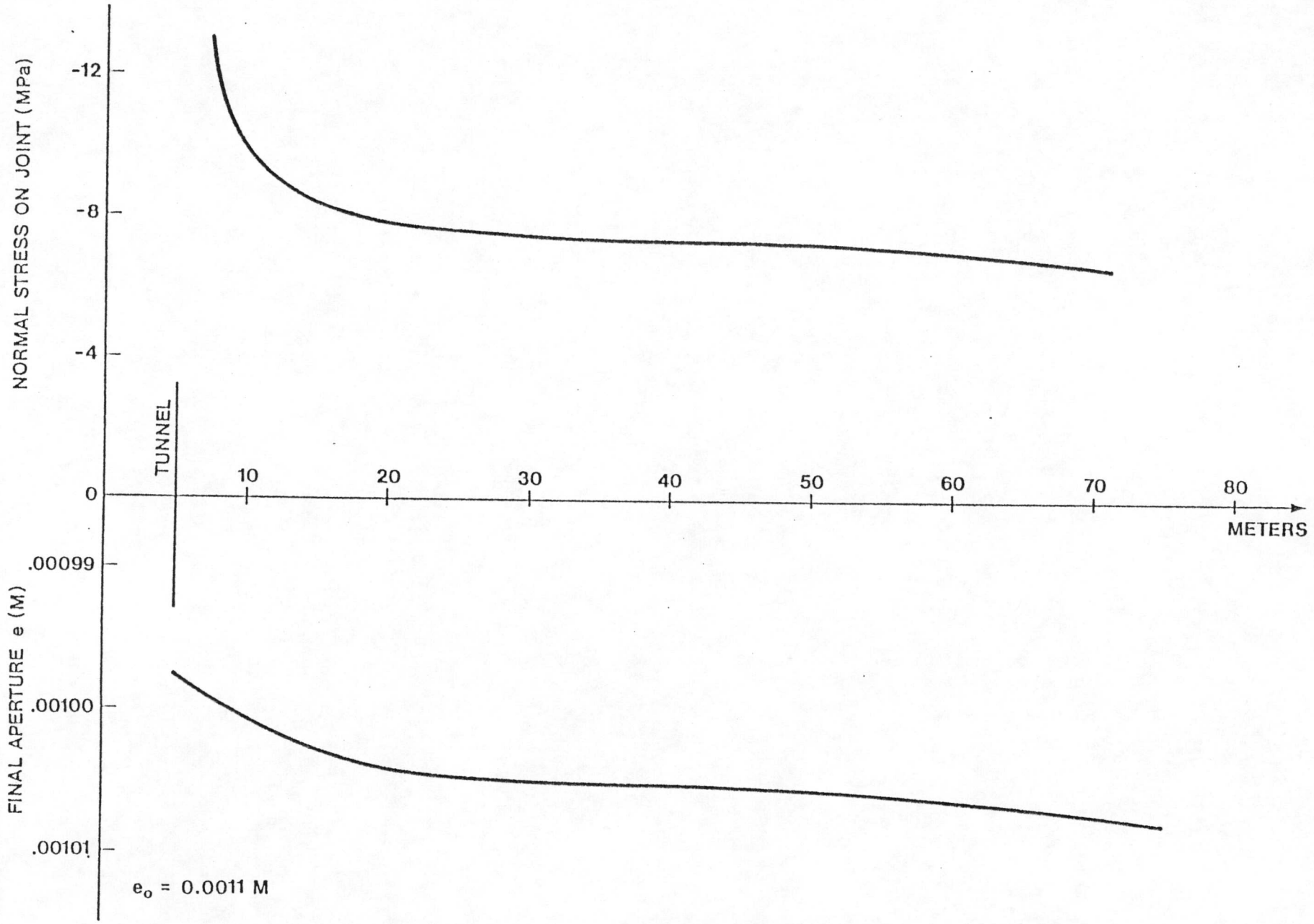

FIGURE 5.7 NORMAL STRESS AND APERTURE CHANGE FOR FIXED BOUNDARY HEADS

parabolic. It was found that these different distributions had a negligible effect (about 1%) on the final flowrate and hence are of little interest.

The zones that would be of more direct interest are the areas of stress concentration compared with areas of stress relief. In such a case, flow in certain areas may be strongly affected while in others little or no change from the initial fracture conductivity might occur.

If boundary conditions are changed such that the flowrate into the fracture and the potential remote from the tunnel are prescribed, then fracture deformation may have a major affect on the potential distribution. The results from such a test case are shown in Figure 5.8. In this test case, although a very stiff fracture (e_o = 0.0001 m) was considered, the fracture deformation caused a change in potential at the tunnel wall as high as 13%. This of course decreases the effective stress across the fracture and hence the final amount of closure.

Figure 5.10 (Wilson 1970), shows the size effect of the tunnel diameter on inflow to the tunnel. Wilsons' model assumes a rigid fracture network and his results show a linear relationship between flowrate and the ratio of tunnel diameter to fracture spacing. These results contradict the work by Maini (1970). As discussed previously, (section 4.3.3), Maini's results appear questionable. A similar test was run using the present approach and varying the number of horizontal fractures intersecting a tunnel. The data generated by this study is summarized on figure 5.11 and shows the existence of a linear relationship similar to the one derived by Wilson. The effect of fracture deformation is simply to slightly adjust the position and slope of this

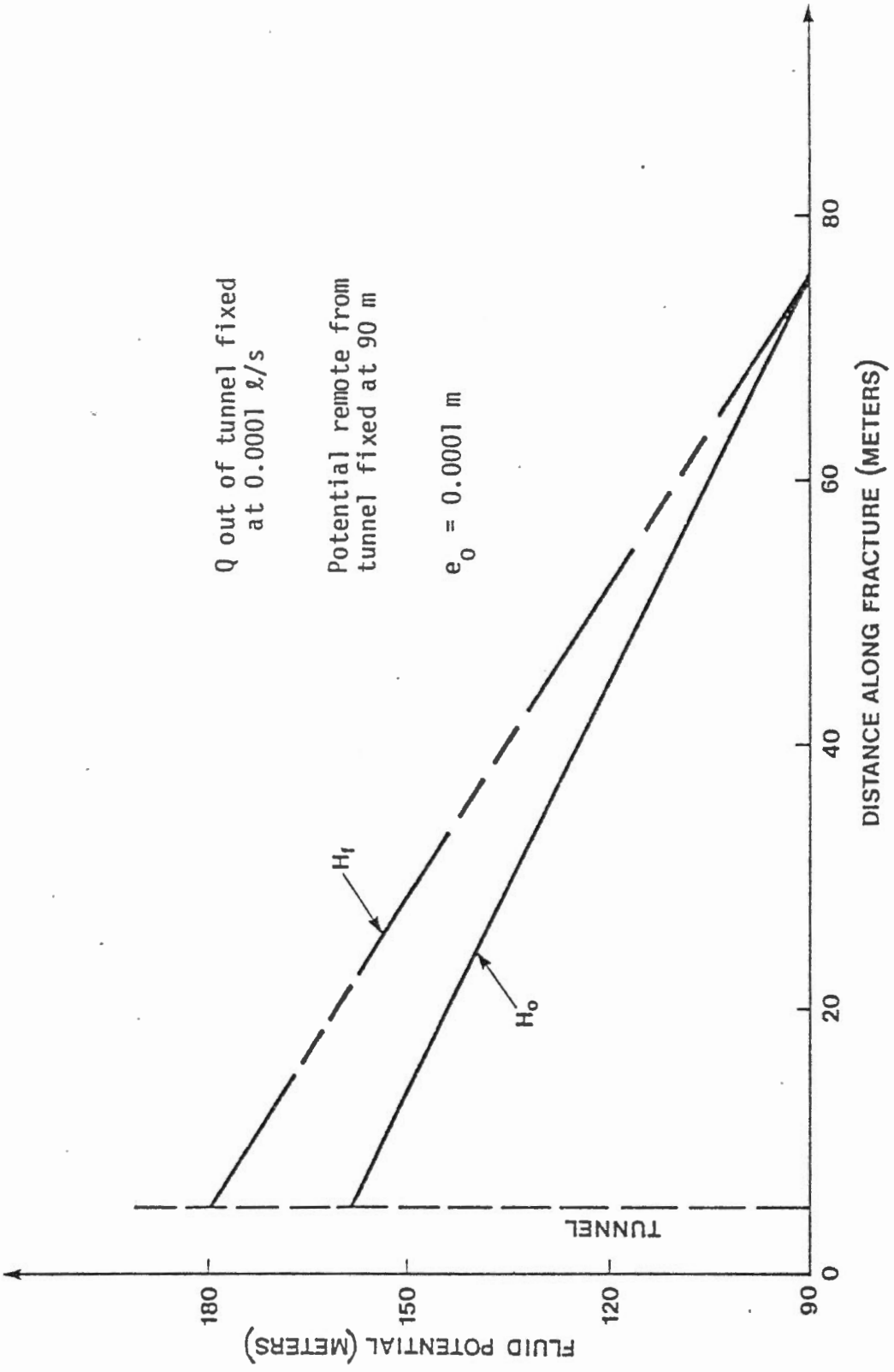

FIGURE 5.8

CHANGE IN POTENTIAL DISTRIBUTION FOR PRESCRIBED FLOWRATE INTO FRACTURE

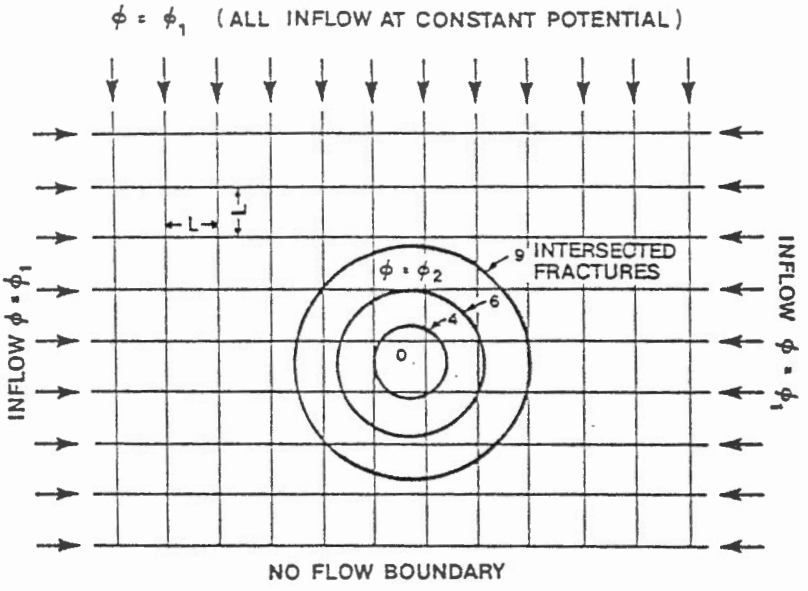

FRACTURE NETWORK FOR TUNNEL PROBLEM

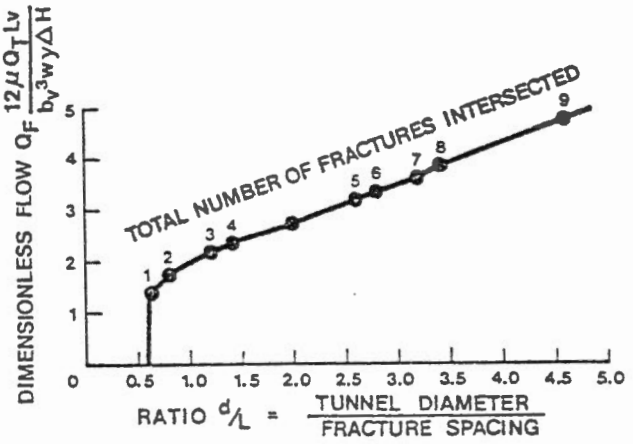

FIGURE 5.9 SIZE EFFECT OF TUNNEL DIAMETER

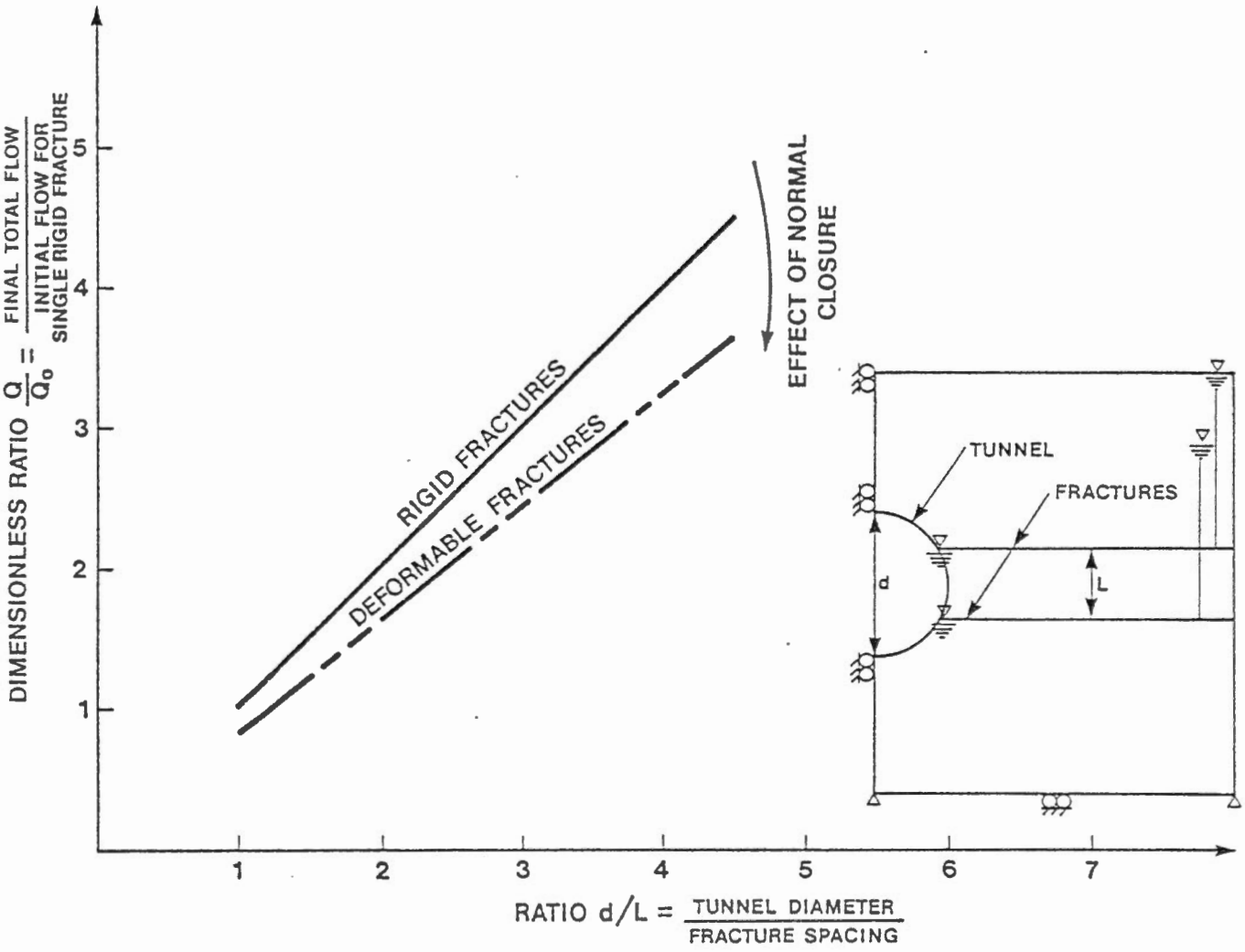

FIGURE 5.10 EFFECT OF FRACTURE DEFORMATION ON SIZE EFFECT OF TUNNEL DIAMETER

relationship. The fracture deformation, in this case normal closure, tends to shift the relation down (i.e. towards less total flow). The introduction of dilatant shear on these fractures would, of course, tend to shift the relation the opposite way.

5.4 Summary

The previous two examples have shown that certain structures may be very sensitive to particular fracture parameters such as orientation, initial aperture, etc. Furthermore fracture deformations under induced or applied loads may exert a significant influence on flowrates and or fluid potentials, depending on the particular structure and boundary conditions involved. Clearly situations such as described in the preceeding chapter may be quite remote from any porous medium analogy.

These examples point out the importance of very detailed surface and subsurface geological investigations for any project in fractured rock. Although the true field conditions can seldom be modelled exactly, deformable fracture flow models at least allow sensitivity analysis of the various field parameters to be performed. The model can further be used to determine if, for a particular case, a statistical approach can give reasonable results.

CHAPTER VI

DISCUSSION

6.1 Statistical Modelling - The Equivalent Porous Medium Analogy

6.1.1 Generalities

The concept of equivalent porous medium modelling involves statistically sampling the properties of the fracture system and using this data to develop a permeability tensor that completely describes the hydraulics of the rock mass. The prime advantage of the model is that no detailed knowledge of the fracture system geometry is required to obtain a quantitative statement of the seepage characteristics of the system.

A number of general assumptions concerning the fracture system(s) are required if a statistical approach is to be used. The most important of these are listed below:

1) each fracture is assumed to be plane and continuous in-plane.

2) the fracture aperture is considered to be consistent.

3) fracture in-filling (if any) is considered to be uniform.

It is obvious that none of the above assumptions model realistic field situations well. The question which arises is at what point the equivalent porous medium model should be discarded.

The two most prevalent statistical models are those by Snow (1965) and Rocha and Franciss (1977). In his work, Snow assumes that all fracture systems form a cubic network, a condition rarely validated in field observations. Rocha and Franciss, in their model apply a correction

factor to force the numerical results to correspond with standard Lugeon field test results. The authors claim that this is required to correct for the assumption of in-plane continuity. However, it could equally well be related to the effect of radial flow in the field tests as discussed later in this chapter.

6.1.2 Scale Effect

A definite limitation to the equivalent porous medium analogy occurs as the fracture spacing increases, (scale effect). That is, each sample volume must contain enough fractures with various orientations, apertures, in-filling, etc., to be representative of the fractured rock mass. Alternately each fracture set may be sampled individually by utilizing careful borehole orientation. However, the same criterion must hold for each sample tested.

The scale effect is hence completely site dependent and thus is extremely difficult to quantify in any general manner. Although numerous attempts at such quantification have been made, none of these have achieved wide recognition.

Rats and Chernyashov (1965) attempted to define the limits for statistical versus discrete modelling based on statistical distributions (reference Figure 2.3). Their work indicates that for standard field sample tests one requires a very small fracture spacing of the order of $\leq$ 10cm for the equivalent porous medium approach to be valid.

Maini (1971) presents data, (refer to Figure 2.4), interpreted from field results that indicate that as the total number of fractures intersecting a test section increases, the flow per fracture decreases

in a non-linear manner to some assymptotic value, after which the author assumes the continuum modelling to be satisfactory.

In his numerical studies Wilson (1970) shows that the total flow into a section should vary linearly as the number of fractures increases. He assumes that if the engineering structure involved is at least fifty times longer than the longest fracture spacing then the equivalent porous medium analogy is satisfactory. Inherent in this assumption however is that each fracture is considered as a fluid conductor.

Barton (1972) found that the spatial frequency of fluid conductors, at his field site in Norway, varied from four to fifteeen times that of the total fracture spacing, based on fractured sections showing zero water take. One of the present authors has also encountered this phenomenon at numerous sites in a variety of rock types. Barton furthermore found that the frequency of fluid conductors tended to decrease with depth. Field observations from deep mines in South Africa, (Cook, personal communications, 1974) and from deep holes (Handin, personal communication, 1974; Hot Dry Rock Geothermal Experiment, Los Alamos Scienfitic Laboratory, 1973) contradict this, indicating that possibly no general trend exists. Including each fracture encountered in a test section as a fluid conductor, may however be very misleading. Barton (1972) states that with the spatial distribution of fluid conductors encountered in his tests the equivalent porous medium analogy must breakdown. This conclusion is further backed up by Gale's (1975) observation that during a packer test certain fractures may preferentially open while others close.

The effect of the above observations is that if Wilson's hypothesis (1970) concerning scale effect is to be used, it must be interpreted as

fifty times the spacing between fluid conductors. The problem inherent in using this in the field is how to determine, accurately, which fractures act as fluid conductors. The authors are not aware of any tests confirming Wilson's hypothesis.

Consequently, although the equivalent porous medium analogy has been used successfully in a number of cases, either petroleum production or regional hydrogeology, these examples deal with extremely large samples for which statistical modelling is adequate.

Baker (1955) succinctly depicts the fundamental problem with use of the equivalent porous medium analogy:

> *The conductivity of a single continuous fracture having an aperture of 0.0254 cm is equivalent to 138 meters of porous medium having a permeability of 10 millidarcys (10^{-6} cm/sec).*

6.1.3 Stress Dependent Permeability

Research into flow through rock fractures has validated the relationship that flow through a fracture is proportional to the cube of the fracture aperture. Furthermore, research over the past fifteen years has shown that fractures subjected to load undergo deformations that are both non-linear and non-recoverable. It is then obvious that fracture apertures and hence conductivities are dependent on both existing stress levels and previous stress history and may be altered by stress changes. This coupling of stress and conductivity holds for any fractured medium and hence must be accounted for in any modelling technique.

However, in equivalent porous medium modelling the coupling of stress and permeability is often ignored. Field tests to determine the

stress-permeability constitutive law for an equivalent porous medium approach must develop the permeability curve for the complete load range to which the rock mass will be subjected because of the non-linear nature of fracture deformation.

As discussed later in this chapter the non-linearity of fracture deformation depends on depth, stress history and stress changes applied or induced in the rock mass under consideration. Thus the problem of determining the coupled stress-permeability tensor for statistical modelling is most complex.

6.2 The Discrete Model

6.2.1 Generalities

In the discrete fracture flow model each discontinuity is modelled individually. For very large rock masses, in order to make the problem tractable, several discontinuities may be incorporated and replaced by a single equivalent discontinuity. The main advantage of this approach is to allow examination of the influence of individual joint parameters on the flow through jointed rock.

6.2.2 Experimental Studies

It was recognized during the earliest fracture-flow research that flow through a single fracture can, in its simplest form, be modelled using a Hele-Shaw apparatus. Some of the earliest fracture-flow experiments, conducted by Lomize (1951) and Louis (1969), utilized a modified version of the Hele-Shaw apparatus to study various parameters such as roughness, tortuosity and turbulence.

Louis found the basic cubic flow law to be valid for both the linear and non-linear laminar flow domains (for one-dimensional flow). Interpretation of Louis' laws (figures 3-15 and 3-16) predict the onset of turbulence for parallel flow at a flowrate of 1.3×10^{-3} m^3/sec, irrespective of fracture aperture. For non-parallel flow however the onset of turbulence could occur at flow rates as low as 0.332×10^{-3} m^3/sec depending on the relative roughness of the fracture. Louis concluded, based on the combination of high gradients and rather wide apertures required, that turbulence was not a major consideration for most rock engineering problems. For example for a fracture aperture of 1 mm a gradient of about 2 is required to initiate turbulence. However, for an aperture of 0.1 mm a gradient of one thousand would be required.

It is not difficult to imagine field situations, especially underground, where gradients well in excess of two might exist. One of the authors has personally measured gradients from 3 to 8.7 above the roof of an abandoned limestone mine in Ohio (Bawden and McCreath, 1978). There was, however, no evidence of turbulence and the fracture apertures, estimated from packer tests to be 0.1 to 0.2 mm, confirm that turbulence should not occur in this case.

Most researchers have agreed with Louis and have ignored turbulent flow. However, Iwai (1977) found that his test data began to deviate significantly (about 20%) from the cubic law for Reynolds numbers greater than 100, even though the apertures tested were very small ($< 250 \times 10^{-4}$ cm). He recommends that testing be extended to include the turbulent regime to determine if the cubic law remains valid. Since Iwai's tests primarily involved radial flow, turbulent effects could be very significant to the

conduct and interpretation of standard packer field tests. The turbulent flow laws presented by Louis are for linear flow and hence the two results are not necessarily comparable. Iwai's exhaustive laboratory and numerical research did, however, tend to validate the cubic flow rate relation for most cases. All of this testing included the effects due to normal load.

Recent research by Ribler (1978) indicates that turbulence may indeed by very significant to the interpretation of standard field injection tests. Using a rigid radial flow model the author demonstrates that narrow fractures ($e \leq 0.13$ mm) are characterized by linear flow at the fracture entrance while fractures with wide apertures ($e \geq 0.4$ mm) are characterized by non-linear flow. In the range between $e = 0.13$ mm to $e = 0.4$ mm a linear relation exists for low head values while a non-linear relation prevails for high bead values.
Ribler shows that the critical energy head at the linear/non-linear transition is mainly dependent on the fracture aperture. The author then uses this result to calculate the fracture aperture and roughness from the flowrate/energy head relation measured in the packer test.

Sharp (1970) challenged the basic cubic flow law relation and proposed that laminar flow was restricted to very low gradients followed by a long transitional period prior to full turbulence. Reinterpretation of this data however (Gale 1975), indicates that the cubic power remains valid.

Laboratory studies on flow through a finely fissured micaschist conducted by Jouanna (1972) also indicated that linear flow was restricted to low gradients. His field tests on the same formation, however,

contradicted the laboratory results. The author's attempt to model his results numerically using a porous medium analogy approach was also unsuccessful, probably due to the very stress dependent nature of the formation conductivity.

Maini (1971) derived radial flow laws for parallel plate flow. His calculations indicate a 58.5 % pressure drop at a distance of a borehole diameter whereas a continuum model would show virtually no pressure drop at this distance. Thus,when interpreting results from standard packer tests one must be very careful in assuming too wide an applicability of the results since it is only those fracture characteristics very close to the borehole that control the pressure-flowrate relation. The recent work by Ribler (1978) discussed previously confirms Maini's hypothesis for radially symmetric flow.

The research as discussed above then indicates that although the cubic flow law may be assumed valid in the modelling of most practical rock engineering problems, one must be aware of the unique situations related to problems with radial flow. In radially symmetrical flow combinations of high Reynolds numbers (Re > 100), moderately wide apertures and high gradients may lead to turbulent flow especially near the entrance from an injection borehole. Ribler (1978) demonstrated that with careful flow and pressure measurements this phenomenon may be used to advantage to determine critical fracture flow parameters (aperture and relative roughness). However, in packer tests where such turbulence either remains unrecognized or non-appreciated due to inaccurate measurements, pressure losses in lines, casing, etc., the calculated conductivity values and/or permeability tensor may bear little resemblance to insitu conditions.

During the early research on fracture flow the fractures were modelled as rigid members. Researchers realized, however, that in reality, fractures deform in response to applied or induced stress changes and that this deformation might be very significant to insitu conductivity determination. Research during the past ten years into the load-deformation character of rock fractures has shown this to be a very complex non-linear phenomenon. More recent experimental work into coupled fracture-flow has indicated that fracture conductivity may be strongly influenced by applied or induced stresses, stress history, etc.

During field studies, Snow (1965) was able to measure surface strains around a wellbore during fluid withdrawal operations. He postulated that these strains were associated with fracture closure related to decreased pore pressures at the well. Gale (1975) measured changes in fracture aperture in an observation well during injection and withdrawal from a nearby well.

The above experimental and field research confirms that the fracture load-deformation character is an important parameter governing fracture conductivity. Thus in any fracture flow study those parameters affecting the load-deformation characters must be studied as well as those affecting conductivity at a fixed aperture.

The main advantage of discrete model studies is their very basic nature. Such tests allow parametric analysis to be performed to determine the importance of different joint characteristics on the fluid flow behaviour. The test results may then be introduced in a numerical technique to analyse large scale cases of interest in rock engineering.

This same very fundamental approach, however, also accounts for most problems encountered in attempting to use this method. This occurs

because for normal field situations, within the limitations of our existing technology it is very difficult, if not impossible, to measure with any degree of confidence all of the required parameters. A further problem associated with obtaining appropriate field data is the high cost of such an exhaustive program. A third problem, although generally of less signficance, especially where a major program is concerned, are the potentially high computational costs involved in running large non-linear programs.

6.2.3 Numerical Studies

Discrete fracture flow modelling techniques first became of practical interest with the development of computers capable of handling large numbers of simultaneous equations. Numerous methods have been used by various researchers. Louis (1969) solved a series of simultaneous equations based on methods used in electrical circuitry. Sharp (1970) and Maini (1971) used the finite difference technique while Wilson (1970) first used the finite element technique. All of this early research ignored the coupling of conductivity and fracture deformation.

Noorishad (1971) first developed a finite element fracture flow model coupling fracture conductivity and fracture deformation. The fracture load-deformation constitutive law was based on the work of Goodman (1970).

Gale (1975) and Iwai (1977) both used Goodman deformable joint elements (Goodman 1976), modified for axisymmetric conditions coupled with radial fracture flow elements for their numerical studies.

The early studies, assuming rigid fractures, indicated that fracture orientation and spacing could radically alter pressure distributions in

structures such as rock slopes, dam foundations, etc., from those assumed from an equivalent porous medium approach. This could, under certain conditions, strongly affect the stability of the structure. Later research, using a coupled deformable fracture flow criterion, indicated that fracture deformation could significantly alter pressure distributions and or flow-rates from those calculated using the rigid fracture assumption.

The present research program used the Goodman joint element (Goodman, 1976) coupled with Wilsons' linear flow element (Wilson, 1970) to model coupled deformable fracture flow. The program, once debugged and modified to handle moderately large amounts of input data, was used for parametric analyses in an attempt to define the range of influence of fracture deformation on conductivity and the limitations of the discrete approach based on existing models. The results of the parametric analysis were given in detail in chapter 3 and the implications are discussed in the following section of this chapter.

Two large scale problems, discussed earlier in this report, were also run to indicate the type of analysis suited to the model.

6.3 Coupled Deformable Fracture Flow

In order to study stress dependent fracture flow, the numerical model must account for both fracture deformation and the coupling between fluid pressures and the stress acting on the fracture. The following assumptions were made:

(i) known fracture geometry.

(ii) permeability is strictly secondary (primary permeability could be added if required).

(iii) intact rock behaves as a linear elastic solid.

(iv) fracture deformation is non-linear,

a) no strength in tension.

b) non-linear normal closure in response to compressive stress

c) simple peak/residual non-linear shear deformation law in response to shear stress.

6.3.1 Fracture Deformation

The fracture/normal load deformation constitutive relation proposed by Goodman (1976) was used for the present research. The model assumes a maximum allowable closure for any fracture under compressive load that may not exceed the initial aperture. The load-deformation curve is highly non-linear, hence with increasing load the normal stiffness increases and consequently there is less deformation for the same load increment.

Experimental studies indicate that fractures are sensitive to their stress history. Cyclic loading produces a wide hysteresis loop, expecially in the first cycle. Hence fractures once subjected to high normal stress and later unloaded may retain a high normal stiffness. Fracture deformation under an imposed load might then be much less than would be anticipated.

The major problem in predicting the response of fractures insitu to normal load lies in obtaining realistic input data for the model. Ideally undisturbed samples of each fracture set should be obtained and tested in the laboratory. Unfortunately it is extremely difficult to

obtain undisturbed samples of fractures. Due to the fact that the sample disturbance cannot be estimated, although the trends shown by the experimental data discussed above appear credible, it is not yet known exactly how these relate to actual insitu behaviour.

As far as shear stress - shear deformation is concerned, Goodman's model (1976) was used. It was found, however, that the detailed input parameters required may lead to difficulties since virtually no existing field studies include all of the necessary data. Problems developed in assigning properties that are both compatible and realistic for parametric studies.

The model handled non-dilatant problems easily and was able to follow the constitutive curve past the peak strength down toward the residual portion. However, since shear deformation by itself does not affect the fracture aperture nor hence conductivity, non-dilatant problems are of little interest to the present study.

The model also includes dilatant effects which may be very significant in fracture conductivity studies. Two limiting boundary conditions were considered:

(i) restrained vertical movement leading to increases in normal stress and peak shear strength.

(ii) constant normal stress leading to increased fracture aperture and conductivity.

Both of the above are of interest in fracture flow. The present study attempted to define under what circumstances dilatancy may be a significant influence.

Barton (1971) indicates that the dilatancy angle that may be expected is a function of the ratio of normal stress to the fracture wall rock strength (reference Figure 3-9). However, the relation between aperture change and shear deformation is not well understood. Goodman (1976) shows this as yet another non-linear curve (Figure 3-10). Thus the introduction of dilatancy means that in solving the problem there are three competing non-linear phenomena that must be accounted for simultaneously.

6.3.2 Fracture Conductivity

The present study has shown that normal fracture deformation is a critical factor governing fracture conductivity. As discussed previously the three parameters controlling the normal deformation are (i) the existing normal stress, (ii) the stress history, and (iii) the normal stiffness. Although the influence of each of these parameters on conductivity can be considered independently, it must be remembered that all three parameters are in fact related and do not act separately.

As discussed earlier in this chapter the higher the applied (compressive) normal load, the greater will be the closure of the fracture aperture. The effect of normal load on conductivity is most clearly seen if the load is taken as a ratio of the applied stress to the compressive strength of the fracture wall rock. A typical example (Figure 3-17) showed that as the load ratio increases toward one, the relative change in conductivity rapidly decreases in a highly non-linear manner. The data then indicated that larger relative conductivity changes would be expected at low normal stress and as the stress level

is increased the conductivity changes become less significant. At some stress level, further conductivity changes can be ignored. This point, however, will depend on the particular fracture in question (e.g. rock type, weathering and alteration on fracture wall, etc.) and hence no global value can be chosen.

It is obvious from this data that the effect of normal stress on conductivity may vary radically depending on the particular site conditions. At sites where existing stresses are small, an additional applied stress might significantly alter fracture conductivities whereas if the existing stress field is quite large the effect of an additional applied or induced stress on conductivity may be negligible.

Also, any increase in the normal stiffness diminishes the relative change in conductivity in a non-linear fashion towards an assymptotic value after which further conductivity change become negligible. It was also shown that very small maximum closures may simply be due to very fine initial apertures or to very fresh strong wall rock such that the asperities or rock bridges transmitting the normal stress are not easily crushed. In the latter case it may be impossible to estimate this parameter insitu.

Hence, as discussed previously, one would generally expect the greatest variation in conductivity with load in areas of low stress or stress relief. The stress history of the fracture can, however, lead to exceptions to this general rule.

Previously loaded fractures (geologically speaking) and subsequently unloaded, could have much higher normal stiffness than would be anticipated from the presently existing level of insitu stress. In this

case further applied load might have minimal effects on conductivity although the near surface location and low insitu stress condition would have suggested that significant changes in conductivity might occur.

Hence each case requires careful geologic interpretation and detailed field study to determine how the loading from a proposed structure may alter the hydraulics of the fractured medium.

As far as the influence of the shear deformation upon the conductivity, two types of shear deformation should be considered. Non-dilatant shear by itself has no effect on conductivity except the possibility of local plugging due to gouge accumulation. Shear strength mobilization, however, is a function of the normal load which may have significant effects on conductivity as discussed in the previous section. Dilatant shear, however, involves a complex coupling between shear and normal deformation and may significantly influence conductivity.

In the first case of restrained normal deformation, such as in the case for most underground situations, the physical conditions are such that the fracture cannot open further. The effect of dilatancy is then to increase the normal load, and hence the shear strength, while at the same time inhibiting normal closure of the fracture in response to this load. The end result of this type of deformation is that the system responds hydraulically as though the fracture system was rigid.

In the other case where the normal deformations are not restrained, such as for open cuts, the fracture is allowed to tolerate the dilatancy while the normal stress remains constant. Because of the cubic fracture

flow relation such deformations might have a very significant influence on fracture conductivity. In reality most cases probably constitute some combination of the above two extremes.

Maini (1971) was first able to demonstrate the feasibility of this concept using a simple laboratory apparatus. The tests, however, are too simplistic to indicate to what degree dilatancy might affect insitu conductivities.

The model used in the present study employs the dilatancy relation of Ladanyi and Archambault (1972). A straight forward coupling of dilatancy and conductivity has been assumed at this time. This relation remains to be confirmed experimentally. As noted previously the model was found to be extremely sensitive to input data for dilatant shear problems. Numerical instabilities commonly occurred although the data was chosen based on published results.

The problems with the conductivity - dilatant shear relation can be evaluated only through extensive and sophisticated laboratory tests which are beyond the scope of the present study. The present results taken from the stable cases, indicate that dilatancy may be critical to fracture conductivity. It is imperative that this relationship be evaluated experimentally so that its affect in practical rock engineering may be accounted for.

In all the examples treated the shear stress was kept below the peak shear strength since it is the conductivity changes prior to failure that are of most interest. Furthermore it is very unlikely that the simple direct coupling of conductivity and dilatancy assumed in this work is valid beyond the peak shear displacement.

It was also established that at low normal stress, very large changes in conductivity may occur under dilatant shear conditions. The conductivity change for any shear displacement is also very dependent on the dilatancy angle for that fracture.

Decreasing shear stiffness and increasing normal stiffness both tend to increase the fracture conductivity. The normal stress level, however, appears to be the most predominant parameter. As the normal stress increases it rapidly overcomes the dilatant effects, irrespective of the other parameters.

The change in relative conductivity decreases with increasing shear stiffness. For any applied shear stress a larger shear stiffness gives a lower shear displacement and hence less dilatancy.

The data from the present model then indicates that the normal load is the primary parameter controlling dilatancy, with shear and normal stiffness as secondary parameters. The relative conductivity curves generated are all non-linear and show that for any one or combination of the above parameters there is a discrete value at which the effect of dilatancy is completely subdued. It is expected that this particular value will be unique to each fracture set and will depend on parameters such as lithology, fracture wall rock properties, weathering and alteration, stress history and dilatency angle. Again many of these parameters are interdependent and determination of their relative importance can only be done experimentally.

Fracture stiffness is not yet well understood. Intuitively both normal and shear stiffness must be related to parameters such as fracture wall rock strength, degree of weathering and/or alteration, area

of contact, roughness and interlocking of asperities, etc. Again detailed experimental investigations will be required in order to evaluate the relative importance of the various parameters and to indicate what type of field measurements are required for numerical input.

To summarize, the results for conductivity with dilatant shear show the following:

(i) at low normal stress dilatancy may cause radical changes in conductivity,

(ii) increasing normal stress and/or normal stiffness will decrease the change in relative conductivity,

(iii) increasing shear stiffness will decrease the change in relative conductivity.

CHAPTER VII

CONCLUSIONS AND RECOMMENDATIONS

The present study has compared the statistical versus the discrete approaches as applied to fluid flow through a fractured medium.

In the statistical approach, the major drawback is the scale effect, whereby the results of a standard packer test are definitely a function of the fracture density. Unfortunately the required functional is site-dependent and is consequently undetermined in most cases.

The second drawback relates to the fact that both the primary and secondary permeabilities are dependent on the existing and induced stress fields. Although this restriction could be taken into account, (i.e. through laboratory and field tests), the scale effect always remains a stumbling-block.

The authors, therefore, believe that when considering fractured rock masses, the statistical approach is valid only in the cases of heavily fractured and/or weathered formations that behave in a manner similar to a porous medium. It should be noted in this context that fracture density is a relative notion and that a better parameter is probably the ratio between the size of the "affected region" to the fracture spacing. One must further beware that only the spacing between those fractures that act as fluid conductors should be used.

Previous experimentalists have established, to the authors' satisfaction, the validity of the cubic flow law for laminar flow in

a fracture. The problems associated with the interpretation of standard packer test data has also been pointed out by numerous researchers. Due to the fact that the fracture conductivity is a function of the effective stress, injection and withdrawal tests may give very different results, the difference being more accute the more highly sensitive the formation. It is, therefore, essential that insitu permeability determinations be made under the smallest possible differential pressure, a procedure which requires accurate and sensitive downhole equipment.

The previous arguments have established the necessity, in any realistic numerical approach, to couple both the flow and stress problems. This problem was fully realized by earlier researchers. Initially, they considered the fractures to be rigid and demonstrated the importance of fracture orientation and spacing. However, discontinuities act as soft inclusions and their deformability can drastically influence both the pressure distribution and the overall permeability of the fractured rock mass. Although all of the conclusions reached using rigid fractures can qualitatively be applied to deformable fractures, the importance of the latter will be a function of the fracture properties as discussed below.

Fracture closure under applied or induced normal stress may, under certain circumstances, exert a significant influence on fracture conductivity. The study has shown that the magnitude of this effect depends on a complex interaction between the normal load itself, the maximum fracture closure, the normal stiffness and the geological (stress) history. Fracture closure and normal stiffness must, at the same time, be related to the particular lithology and degree of weathering

and/or alteration. The only method at present to isolate most of these critical parameters is through laboratory testing, and as yet very little data of this nature is available.

By far the most important property affecting the fluid conductivity is the joint dilatancy and its influence on fracture closure. The authors have further shown the influence of increasing dilatancy angle in increasing the peak shear strength for a particular joint which, in turn, will affect its conductivity.

It should be emphasized that this characteristic will have a different effect for "surface" structures than for buried facilities. In the first case the dilatant movement of the rock mass is essentially unrestrained and conductivity properties are most strongly affected by the rock movement. Conductivity changes in such cases can exceed an order of magnitude. As depth increases restraint becomes more and more important, which increases the strength and hence decreases the probability of movement. The fractures then act in a more rigid manner and dilatancy becomes a second order parameter.

It should also be noted that the influence exerted by the fractures and their properties is always a function of the *relative stiffness* of joints as compared to the intact rock. In this context the importance of the geologic stress history cannot be overstated. Although similar stress conditions and fracture geometry may prevail at one location as another, the overall behaviour will be quite different if prior unloading has occurred.

The authors have shown that the secondary permeability variations due to insitu stress conditions may often be explained by considering

the behaviour of pre-existing fractures. This is backed up by field and laboratory data which revealed the drastic influence of the fractures prevailing adjacent to the borehole wall.

Where remedial measures are to be considered with respect to seepage, one must take careful account of both the fracture geometry and the detailed fracture characteristics.

This research has clearly established the importance of the properties of discontinuities upon the fluid conductivity of fractured rock masses. In order to obtain a full understanding of any field packer test data it is, therefore, of the utter most importance to know both the geometric relations as well as the physical properties with a high degree of confidence. It is further important, due to the very limited area of influence controlling radial flow, that a large number of tests be conducted such that representative limits on the controlling parameters may be determined.

It should also be realized that the work and research on shear dilatancy is in its infancy. A strong effort should be made to obtain a better grasp on the constitutive equations governing this phenomenon in order to avoid numerical instabilities. Further research is also required to delineate the compatibility limits between parameters such as wallrock strength, normal and shear stiffness and dilatancy angle.

One of the important limitations with respect to this research program was the tacit assumption that any differential movement in the fracture could not alter, chemically or physically, the contact surfaces. In reality crushing of the asperities will occur and/or pre-existing gouge will be affected. Realistically speaking, the relationship between fluid conductivity and joint displacement should be obtained experimentally.

The authors also recommend that a special effort be made to extend this work to include transient and turbulent flow regimes for both radial and linear conditions. This will require extensive laboratory testing to establish the proper equations of state.

The work reported here could also be extended to include seepage within the rock matrix, a situation that may prevail in fractured porous media.

Finally, in order to make the numerical approach more attractive for applications to very large engineering situations, the computer programmes should be optimized and other numerical approaches or combinations thereof investigated.

REFERENCES

BAKER, W.J. "Flow in Fissured Formations", 4th World Petroleum Congress, Rome, 1955. Section II, paper 7.

BARENBLATT, G., ZHELTOV, I. and KOCHINA, I. "Basic Concepts in the Theory of Seepage of Homogeneous Liquids in Fissured Rocks", 1960. PPM, 24,pp. 852-864.

BARTON, N.R. "A Model Study of Air Transport from Underground Openings Situated Below Groundwater Level", N.G.I., 1972.

BAWDEN, W.F. and McCREATH, D.R. "Geotechnical Study of an Abandoned Limestone Mine for Crude Oil Storage", 31st Canadian Geotechnical Conference, Winnipeg, Manitoba, October 1978.

BIANCHI,L., & SNOW, D.T. "Permeability of Crystalline Rock Interpreted from Measured Orientations and Apertures of Fractures",1968. Annals of Arid Zone, Vol.8, No.2, pp. 231-245.

CALDWELL, J.A. " The Theoretical Determination of the Fluid-Potential Distribution in Jointed Rocks", 1971. M.Sc. Thesis, University of Witswatersraand.

DUFFAUT, P. and LOUIS, C. "L'eau Souterraine et l'équilibre des pentes naturelles", 1972. 24th I.G.C.

DUGUID, J.O. "Flow in Fractured Porous Media", 1973. Ph.D. Thesis, Princeton University.

DUGUID, J.O. and ABEL,J.F. "Finite Element Galerkin Method for Analysis of Flow in Fractured Porous Media", 1974. In Finite Element Methods in Flow Problems, Ed.by Oden, J., Zienkiewicz, O.C., Gallagher, R.H. and Taylor, C. U.A.H. Press, Huntsville, Alabama, pp. 599-616.

GALE,J.E. "A Numerical, Field and Laboratory Study of Flow in Rocks with Deformable Fractures", 1975. Ph.D. Thesis, University of California, Berkeley.

GALE,J.E., TAYLOR,R.L., WITHERSPOON,P.A. and AYATOLLAHI, M.S. "Flow in Rocks with Deformable Fractures", 1974. In Finite Element Methods in Flow Problems, Ed.by Oden,J.T., Zienkiewicz,O.C., Gallagher, R.H. and Taylor, C. U.A.H. Press, Huntsville, Alabama, pp. 583-598.

GOODMAN, R.E. "The Mechanical Properties of Joints", 1974. Proceedings 3rd Congress Int.Soc.Rock Mechanics, V.1, pp. 127-140.

GOODMAN,R.E. HEUZE,F.E., and OHNISHI,Y. "Research on Strength - Deformability - Water Pressure Relationships for Faults in Direct Shear", 1972. Geotech.Engr.Report, University of California, Berkeley.

GOODMAN, R, TAYLOR, R. and BREKKE, T. "A Model For the Mechanics of Jointed Rock", 1968. J. of Soil Mech. and Foundation Div. Proceedings ASCE.

GOODMAN,R.E. "Methods of Geological Engineering", West Publishing Company, 1976.

IWAI,K. "Fundamental Studies of Fluid Flow Through a Single Fracture", Ph.D. Thesis, U.of California, Berkeley, 1976.

JOUANNA, P. "Effet des Sollicitations Mecaniques sur les Ecoulements dans Certains Milieux Fissurés", 1972. Docteur ES - Sciences Physiques These, U.de Toulouse, Fr.

KATZ, D.L. and COATS, K.H. "Underground Storage of Fluids", 1968. Ulrich's Books, Ann Arbor, Michigan, U.S.A.

LEWIS,D.C. & BURGY, R.H. "Hydraulic Characteristics of Fractured and Jointed Rx", 1964. Ground Water, V.2, No.3, pp. 4-9.

LOMIZE,G. "Filtratsiia v treshchinovatykh porodakh", (Water Flow in Jointed Rock), 1951. Gosenergoizdat, Moscow.

LOUIS,C. "A Study of Groundwater Flow in Jointed Rock and its Influence on the Stability of Rock Masses", 1969. Rock Mechanics Research Report No.10, Imperial College, University of London, September.

LOUIS,C. "Rock Hydraulics", 1974. Course-Int. Centre for Mech. Sciences - Udine, Italy. (Reprinted from "Rock Mechanics", 1974, CISM 165, Edited by L.Müller.

LOUIS,C. "De L'Hydraulique des Roches", Introduction, 1974. Publication, Bureau de Recherches Géologiques et Minières, Orléans, Fr.

LOUIS,C. "Les Caractéristiques hydrauliques du massif de Fondation du barrage de Grand-Maison (Isère)", 1972. Bulletin du BRGM.

LOUIS,C. and PERNOT,M. "Three-Dimensional Investigation of Flow Conditions of Grand Maison Damsite", 1972. Proc.Symp.Int.Soc. Rock Mecs., Perc. Through Fiss.Rock,Stuttgart.

LOUIS, C. and Maini, Y.N., "Determination of In-Situ Hydraulic Parameters in Jointed Rocks, 1970. Imperial College of Science and Technol., Rock Mechanics Research Report, No. D10, 24 p.

LOUIS,C. "Les Drainages dans les Roches Fissurées", 1972. Bulletin BRGM,

LOUIS,C. "Ecoulement à trois Dimensions dans les roches Fissurées". Rev. Ind. Minér. Fr., No. spéc., 15 juillet 1970. pp 73-93.

LOUIS,C. "Etude des écoulements d'eau dans les roches fissurées et de leurs influences sur la stabilité des massifs rocheux", E.D.F., Bulletin de la Direction des Etudes et Recherches, Série A Nucléaire, Hydraulique Thermique, No.3, 1968, pp.5-132.

LOUIS,C. and WITTKE,W. "Etude Experimentale des Ecoulements d'eau dans un Massif Fissuré, Tachien projet, Formose", 1971. Geotechnique, 21, No.1,pp.29-42.

LOUIS,M. "Influence de L'Etat de Contrainte Sur Les Ecoulements Dans Les Roches", Revue de L'Industrie Minerale, Juillet 1971, pp. 152 - 154.

MAINI, Y.N.T., "In Situ Hydraulic Parameters in Jointed Rock - Their Measurement and Interpretation", 1971. Ph.D. Thesis, Imperial College, U.of London.

MORGENSTERN, R.R., and GUTHER, H. "Seepage into an Excavation in a Medium Possessing Stress - Dependent Permeability", 1972. Proc.Symp. of Int.Soc. of Rock Mechanics, Stuttgart, p. T2-C.

NAG,D.K. "Model Analysis of Fractured and Jointed Rock Masses", 1971. M.Sc. Thesis, University of London, Imperial College.

NOURISHAD,J., WITHERSPOON, P.A., and BREKKE, T.L. "A Method For Coupled Stress and Flow Analysis of Fractured Rock Masses", 1971. Geotech. Engr. Pub. No. 71-6, University of California, Berkeley.

OHNISHI, Y. "Laboratory Measurement of Induced Water Pressure in Jointed Rocks", 1973. Ph.D. Thesis, University of California,Berkeley.

PARSONS, M.L. "Determination of Hydrogeological Properties of Fissured Rocks," 1972. Proc. 24th Geological Congress, Montreal, Section II, Hydrogeology, pp. 89-99.

RAYNEAU,C. "Contribution a L'Etude des Ecoulements Autour D'un Forage en Milieu Fissuré", 1972. These, Docteur-Ingenieur Université des Sciences et Technique du Languedoc, Académie de Montpellier, Fr.

RATS, M.V. and CHERNYASHOV, S.N. "Statistical aspect of the problem on the permeability of jointed rocks", 1965. Paper no. 73, Symposium on the Hydrology of Fractured Rocks, Dubrovnik,Yugoslavia, UNESCO.

Ri BLER, P. "Determination of the Water Permeability of Jointed Rock", English edition of Volume 5, Publications of the Institute for Foundation Engineering, Mechanics, Rock Mechanics and Water Ways Construction, RWU (University) Aachen, Federal Republic of Germany, 1978.

RODATZ,N. and WITTKE, W. "Wechselwirkung Zwischen Deformation und Durchströmung un Klüffigen, Anisotropen Gebirge", 1972. Proc. Symp. of International Society of Rock Mechanics, Percolation Through Fissured Rock, Stuttgart, p. T2-1.

ROMM, E.S. "Flow Phenomena in Fissured Rocks", 1966.
Moscow, 284 pp., (In Russian).

SHARP,J.C. "Fluid Flow Through Fissured Media", 1970.
Ph.D. Thesis, Imperial College of Science and Technology, London.

SNOW,D.T. "A Parallel Plate Model of Fractured Permeable Media", 1965.
Ph.D. Thesis, University of California, Berkeley.

SNOW,D.T. "Three hold Pressure Test for Anisotropic Foundation Permeability", 1966. Fels.U.Ing.Geol., V.4, p. 298.

SNOW,D.T. "Fracture Deformation and Changes in Permeability and Storage Upon Changes of Fluid Pressure", 1968a.
Colorado School of Mines Quarterly, V. 63, no.1, p.201.

SNOW, D.T. "Hydraulic Character of Fractured Metamorphic Rocks of the Front Range and Implications to the Rocky Mountain Arsenal Well", 1968b. Colorado School of Mines Quarterly, 63.

SNOW,D.T. "The Frequency and Apertures of Fractures in Rocks", 1969.
International J. of Rock Mechanics and Mining Sci., V.7, no. 1, pp.23-40.

STERNBERG, Y.M. and SCOTT, V.H. "The Hele-Shaw Model -- A Research Device in Groundwater Studies"

WILSON,C. "An Investigation of Laminar Flow in Fractured Porous Rocks", 1970. Ph.D. Thesis, University of California, Berkeley.

WILSON,C.R., and WITHERSPOON, P.A. "An Investigation of Laminar Flow in Fractured Rocks", 1970. Geotechnical Report No. 70-6, University of California, Berkeley.

WITHERSPOON,P.A., GALE, J.E. TAYLOR,R.L. and AYATOLLAHI,M.S.
"Investigation of Fluid Injection in Fractured Rock and Effect on Stress Distribution", 1974. U.of California, Report TE-74-4.

WITHERSPOON,P.A. and GALE, J.E. "Mechanical and Hydraulic Properties of Rocks Related to Induced Seismicity", 1975. First International Symposium Ind. Seis., Banff, September 1975.

ZHELTOV,U.P. "On Single-Phase Liquid Flow Through Deformed Fractured Non-porous Rocks", 1961. Appl. Math and Technical Physics, No.6, USSR.

BIBLIOGRAPHY

AIYER, A.K. "An Analytical Study of the Time-Dependent Behaviour of Undergound Openings", 1969. Ph.D. Thesis, U. of Illinois .

AMMURI, I.S.Y. "Correlation of Joint Roughness with Geology", 1972. M.Sc. Thesis, Imperial College, University of London.

ARIS,R. "Vectors, Tensors and the Equations of Fluid Mechanics", 1962. Prentice-Hall Inc., Englewood Cliffs, N.J.

BACHMAT, Y. "Basic Transport Coefficients as Aquifer Characteristics", 1965. Proceedings of Dubrovnik Symposium, Hydrology of Fractured Rocks, UNESCO.

BEAR, J. "Dynamics of Fluids in Porous Media", 1972. Am Elsevier.

BERZAL, J.L. "Groundwater Flow in Slopes -- Computer Analysis", 1972. M.Sc. Thesis, Univ. of London, Imperial College.

BIOT, M. "General Theory of Three-Dimensional Consolidation", 1940. J.App.Phys, 12, 155-164.

BIOT,M. "Theory of Deformation of a Porous Viscoelastic Anisotropic Solid", 1956. J. Appl. Phys., 27, 459-467.

BIOT,M. "Theory of Elasticity and Consolidation for a Porous Anisotropic Solid", 1956. J.Appl. Phys., 26, 182-185.

BIRKS, J. "A Theoretical Investigation into the Recovery of Oil From Fissured Limestone Formations by Water-Drive and Gas-Cup Drive", 1955. Fourth World Petroleum Congress, Rome, Section II/F, Paper 2.

COOPER,H. "The Equation of Groundwater Flow in Fixed and Deforming Coordinates", 1966. J.Geophys.Res., 71, 4783-4790.

ERGUN,I. "Stability of Underground Openings in Jointed Media", 1970. Ph.D. Thesis, Imperial College, University of London.

EVANS,D.M. "The Denver Area Earthquakes and the Rocky Mountain Arsenal Well", 1966. The Mountain Geologists, V.3, No. 1.

GRINGARTEN,A.C., and WITHERSPOON,P.A. "A Method of Analyzing Pump Test Data From Fractured Aquifers". Proceedings of the Symposium Int. Society of Rock Mechanics, Percolation Through Fissured Rock, p. T2-C, Stuttgart, 1972.

HAN,C.Y. "The Technique of Obtaining Equipotential Lines of Groundwater Flow in Slopes, Using Electrically Conductive Paper", 1972. Imperial College, University of London.

HANTUSH,M.S. "Wells in Homogeneous Anisotropic Aquifers", 1966. Water Resources Research, V.2, No.2, pp. 273-279.

HANTUSH,M.S., and THOMAS,R.G. "A Method for Analyzing a Drawdown Test in Anisotropic Aquifers", 1966. Water Resources Research, V.2, No.2, pp. 281-286.

HODGSON,R.A. "Regional Study of Jointing in Comb.Ridge, Navajo Mountain Area, Arizona and Utah", 1961a. Am.Assoc.Pet. Geol.Bull., V.45, p.1.

HODGSON,R.A. "Classification of Structures on Joint Surfaces",1961b. Am.Jour.Sci., V.259, pp. 493-502.

KAZEMI,H., SETH, M.S., and THOMAS,G.W. "The Interpretation of Interference Tests in Naturally Fractured Reservoirs with Uniform Fracture Distribution", 1969. Soc.Pet.Engr.J., V.9, No.4, p. 463.

KAZEMI,H. "Pressure Transient Analysis of Naturally Fractured Reservoirs with Uniform Fracture Distribution", 1969. Soc. Pet. Engr. J., V.9, No.4, pp. 451-462.

MAHTAB,M.A., BOLSTAD,D.D., ALLDREDGE,J.R., and SHANLEY,R.J. "Analysis of Fractured Orientations for Input to Structural Models of Discontinuous Rock", 1972. U.S.Dept.Int., Bur.Mines Rept. Invest., N. 7669.

NELSON, R.W. "Solution of Very Large Groundwater Flow Problems; Digital Methods versus Analog Simulation", February 1964. Hanfor Laboratories Report.

NOREN,D., L.O.EMMELIN, and S.PAULSON. "Compressed Air Power Plants - Airstore", 1970. V.B.B. Sweden.

OZKAHRAMAN,H.T. "A Model Investigation of Circular Openings in Discontinuous Rock", 1971. M.Sc. Thesis, Imperial College, University of London.

PAPADOPIULOS, I.S. "Nonsteady Flow to a Well in an Infinite Anisotropic Aquifer", 1967. Proceedings of the Dubrovnik Symposium on the Hydrology of Fractured Rocks, V.1, pub.no. 73, IASH (AIMS - UNESCO).

ROEGIERS, J.C. "The Development and Evaluation of a Field Method for In-situ Stress Determination Using Hydraulic Fracturing", Technical Report MRD-1-75, Missouri River Division, Corps of Engineers, Omaha, Nebraska, March 1975.

ROFAIL, N. "Analysis of Pumping Test in Fractured Rocks", 1965. Proceedings of the Dubrovnik Symposium, Hydrology of Fractured Rocks, UNESCO.

SCHEIDEGGER, A.E. "The Physics of Flow Through Porous Media", 1960. University of Toronto Press.

SHANLEY,R.J. and MAHTAB, M.A. "Delineation and Analysis of Clusters in Orientation Data", 1976. In Math.Geology.

SHEHATA,W.M. "Geohydrology of Mount Vernon Canyon Area, Jefferson Co., Colorado", 1971. Ph.D. Thesis, Colorado School of Mines, Golden, Colorado.

SLOAN, S.W. "Numerical Modelling of Selected Axisymmetric Problems in Geomechanics", M.A.Sc. Thesis (unpublished), Monash University, Australia, April 1978.

WARREN, J.E., and PRICE, H.S. "The Behaviour of Naturally Fractured Reservoirs", 1961. Journal Soc. Pet.Engr., V.3, no.3, pp. 245-255.

WARREN, J.E. and ROOT, P.J. "The Behaviour of Naturally Fractured Reservoirs", 1963. Trans AIME, V. 228, p. 245.